THE OCEAN-AIR EXCHANGE OF CARBONYL SULFIDE (OCS) AND HALOCARBONS

Steven Dow Hoyt
B.S., University of California, Irvine, 1972
M.S., Oregon State University, Corvallis, 1976

A dissertation submitted to the faculty
of the Oregon Graduate Center
in partial fulfillment of the
requirements for the degree
Doctor of Philosophy
in
Environmental Science

July 1982

The dissertation "The Ocean-Air Exchange of Carbonyl Sulfide (OCS) and Halocarbons" by Steven Dow Hoyt has been examined and approved by the following Examination Committee:

Reinhold A. Rasmussen, Thesis Advisor
Professor

M. A. K. Khalil, Thesis Advisor
Associate Professor

Douglas F. Barofsky
Associate Professor

John A. Cooper
Professor

Thomas M. Loehr
Professor

ACKNOWLEDGMENTS

I thank all of the people who have made this dissertation possible. This includes all of my friends, fellow students, and faculty who have seen me through this project.

In particular, I thank my parents who helped me get started on this endeavor and who encouraged me along the way. I especially thank Lisa for being with me and sharing in this experience and for keeping me on track when the going got slow.

I thank Dr. Barofsky and Dr. Beeson for their help in providing direction toward my final topic and their guidance and encouragement along the way.

Finally, I thank Dr. Rasmussen for providing ideas, financial support, and the experimental equipment that were responsible for the work, and Dr. Khalil for the many stimulating discussions about the models and how to make them work properly. Also I thank them for their encouragement and faith in my abilities. I thank my examining committee for their efforts to improve the dissertation, and Edie Taylor for her thoughtful and cheerful typing of the manuscript.

TABLE OF CONTENTS

LIST OF TABLES

List of Tables (continued)

LIST OF FIGURES

List of Figures (continued)

List of Figures (continued)

Abstract

THE OCEAN-AIR EXCHANGE OF CARBONYL SULFIDE (OCS)

AND HALOCARBONS

Steven D. Hoyt

Oregon Graduate Center

Beaverton, Oregon

Dissertation Advisors: Reinhold A. Rasmussen & M. A. K. Khalil

The measurement of the ocean-air flux of trace gases is important to understand their global budgets since the ocean can act as a source, reservoir, or sink of atmospheric gases. Many topics on ocean-air exchange are discussed in this dissertation, but the objectives were to evaluate the two-film model in its application to ocean-air exchange problems, develop a measurement protocol for carbonyl sulfide (OCS) in air and water samples, and apply the two-film model to calculate the ocean flux for OCS, CH_3I, $CHCl_3$, CH_3CCl_3, F-11 ($CFCl_3$), F-12 (CF_2Cl_2), CCl_4, and PCE ($CCl_2=CCl_2$).

The two-film model, which is widely used to calculate the flux of gases from the ocean, was compared to another more complicated model. But because of the large uncertainty in the experimental measurement of the transfer coefficients, the two-film model gave comparable results to the other model and was chosen for use in the flux calculations because of its simplicity.

A propagation of error analysis of the two-film model showed that the major sources of uncertainty in flux results depend on the Henry's constant of the gas studied and the saturation value of the gas in the

ocean. For gases produced in the ocean, the major source of uncertainty is in the transfer coefficient and the seawater concentration. For gases for which the ocean acts only as a reservoir, the major source of uncertainty is in the measurement of the Henry's constant (H).

For OCS no measurements of H have been made in seawater, so an experimental procedure was developed to determine H for OCS as a function of temperature using atmospheric partial pressures of the gas. The results for H varied from 1.2 at 5°C to 2.7 at 25°C, and were about 20% higher than the distilled water measurements using the pure gas.

For analysis of the seawater samples a method was developed for collecting, storing, and analyzing the samples in a single gas-tight bottle. This procedure allows the multiple analyses to be performed on each sample in the laboratory rather than taking equipment on board a ship. OCS was found to be stable in the sample bottles for storage periods of up to one month and was free of contamination for the fluorocarbons. The OCS samples were analyzed by a GC/MS technique which gave positive identification of the OCS peak and has a detection limit of about 35 pptv.

The two-film model with the updated values for K_ℓ and H was used with the seawater data to calculate the OCS ocean flux and the flux of some halocarbon gases from seawater and air samples collected on oceanographic cruises in the Atlantic and Pacific Oceans. The ocean was found to be a significant source of OCS (0.8 Tg/yr), CH_3I (0.2 Tg/yr), and $CHCl_3$ (0.7 Tg/yr). The results for CH_3CCl_3, F-11, F-12,

CCl_4, and $CCl_2{=}CCl_2$ indicate that the uncertainty in the flux is large since the saturation is close to zero, and the ocean acts as a reservoir for these compounds, storing an amount close to equilibrium with the atmospheric concentrations.

CHAPTER 1

INTRODUCTION

For many years the immense reservoirs of the global environment seemed capable of handling all of the by-products of man's activities without noticeable perturbation. Since the late 1940's, population increases coupled with increases in energy and synthetic chemical production have resulted in large quantities of gases being released to the environment. Many of these gases react rapidly and are effectively removed, but others such as carbon dioxide (CO_2), the chlorofluorocarbons, methane (CH_4), and some other trace gases are increasing in atmospheric concentration (Rasmussen and Khalil, 1981a, 1981c; Khalil and Rasmussen, 1981a; Weiss, 1981; Keeling et al., 1976) and have led scientists to study what potential effects these increases might have on the global environment.

At the present time there are two areas of concern for the global increase in the concentration of gases due to man's activities. The first is the so-called "greenhouse effect," where increased atmospheric gases would trap more of the outgoing infrared radiation emitted by the earth, causing the earth's surface temperature to increase (Kellogg and Schware, 1981; Hileman, 1982; NAS, 1975a). The second is a decrease in stratospheric ozone caused by the increased reaction with chlorine from chlorofluorocarbons (Bauer, 1979; Crutzen et al., 1978; Molina and Rowland, 1974; Cicerone et al., 1975). The ozone decrease could result in an increase in skin cancer caused by ultraviolet radiation (NAS, 1982).

In order to predict whether a gas will fall into one of these two categories, models are constructed to describe the atmospheric behavior of the gas, by balancing the various sources of a gas with its atmospheric reactions and sinks. In studying the sources and sinks of gases, the ocean, because of its size and biological productivity, can be a major source for some gases and act as a sink for others.

Early attempts at modeling the ocean-atmosphere distribution of a gas were the result of interest in finding sinks for the increasing atmospheric carbon dioxide (CO_2). CO_2 belongs to the group of gases that exhibit the "greenhouse effect" described earlier. Bolin (1960) applied a modified version of the two-film model (Whitman, 1923) to determine the flux of atmospheric CO_2 to the ocean. In the application of this model to ocean-air exchange problems, in situ measurements of the mass transfer coefficients were also made, which became useful for the study of other gases (Broecker and Peng, 1974).

Since its application to CO_2, some version of the two-film model has been used to study the ocean as a source or sink for other natural gases such as N_2O (Pierotti and Rasmussen, 1980; Singh et al., 1979), CH_4, CO (Swinnerton and Lamontagne, 1974; Lamontagne et al., 1973), dimethyl sulfide (DMS) (Lovelock et al., 1972; Nguyen et al., 1978; Barnard et al., 1982), and CH_3I (Liss and Slater, 1974; Rasmussen et al., 1982d). With the interest in the chlorofluorocarbons and their potential impact on the ozone layer, the two-film model has also been applied to the calculation of the ocean as a potential sink for F-11, F-12 (Junge, 1976), and CCl_4 (Liss and Slater, 1974).

The use of F-11 and F-12 as tracers of ocean water masses has also been explored (Gammon, 1982). Thus, ocean-atmospheric exchange has played an important role in studying the cycles of gases in relation to the two major global environmental problems described earlier.

The objectives of this dissertation are to evaluate the two-film model in its application to ocean-atmosphere exchange problems, develop a measurement protocol for carbonyl sulfide, OCS, in air and water samples, and apply the two-film model to calculate the ocean flux for OCS, methyl iodide (CH_3I), chloroform ($CHCl_3$), methylchloroform (CH_3CCl_3), F-11 ($CFCl_3$), F-12 (CF_2Cl_2), carbon tetrachloride (CCl_4), and perchloroethylene (C_2Cl_4, abbreviated PCE).

In Part 1 the objectives are to compare the two-film model to other gas-liquid exchange models. The literature values for the physico-chemical parameters used in this model will be compiled for use in the flux calculations. These data will then be used for an analysis of the sources of uncertainty in the application of the two-film model to ocean-atmosphere exchange of trace gases. In Part 2 the objectives are to develop an instrumental measurement system for OCS using gas chromatography-mass spectrometry (GC/MS). A sample collection method based on headspace analysis will be developed for the analysis of trace gases in seawater. This methodology will be evaluated for OCS and will also be used for measuring the Henry's constant for OCS in seawater. In Part 3 the objectives are to use the models and experimental techniques developed to calculate the ocean-atmosphere flux of OCS, CH_3I, and other halocarbons, and to compare these

flux values with other sources to determine the importance of the ocean in the global cycles of these gases.

Chapter 2 starts with a brief review of the two-film model, the surface renewal models, and the box model. An example of how the box model can be used to calculate the ocean-atmospheric distribution of OCS is shown. The biological and physical structure of the ocean relevant to flux models is discussed at the end of the chapter. The application of the models relies on obtaining accurate values for two physico-chemical constants, the Henry's constant (H) and the liquid transfer coefficient (K_ℓ). Chapter 3 describes these important parameters. The thermodynamic theory relating the air-water partitioning to H and the temperature and salinity dependence of H are presented. The measured value of H for the gases studied are tabulated, and by comparing the values of different research groups an estimate of the uncertainties in H can be obtained. The measurement of K_ℓ is also described along with the dependence of K_ℓ on the diffusion coefficient and the windspeed.

In the application of a model, a realistic appraisal of the uncertainties should be made. Even though the ocean flux has been calculated previously for some of the gases in the study, there has been no attempt to quantitatively estimate the uncertainty in using the two-film model. Chapter 4 describes the types of uncertainties in ocean-atmosphere flux calculations, and a propagation of error procedure is applied to the two-film model to determine which terms contribute the most to the total uncertainty for each gas.

Chapters 5 and 6 describe the basic instrumentation used to identify and measure the concentrations of the selected gases along with a detailed study of the OCS analytical procedure, including linearity, detection limit, and verification of the identified peak. Chapter 7 describes a new procedure for seawater gas analysis where the sample is collected in a gas-tight container and the headspace analyzed directly, eliminating potential sources of contamination. An important part of any sampling and analysis program is determining what the stability of the collected samples is. In Chapter 8 the stability of air and seawater in the sample bottles is tested for OCS to understand how storage may affect the measured concentration. Chapter 9 describes the experimental measurement apparatus developed for the determination of the Henry's constant for OCS.

In Chapter 10 the models and measurement techniques developed in Part 1 and Part 2 are used along with the data from samples collected on three oceanographic cruises to calculate the flux of OCS, CH_3I, $CHCl_3$, and other halocarbons. Air and seawater samples were collected on one trip in the Atlantic Ocean and two trips in the Pacific Ocean. In addition, some samples from the moderately biologically productive Pacific coast were collected from fishing boats. The data from these samples were used in the two-film model to calculate the ocean flux of the gases studied. These fluxes are compared with other sources for the gases, and their importance to potential global environmental problems is discussed.

This dissertation was written to provide the reader with a complete account of ocean-atmosphere trace gas exchange, in addition to describing the research on several important topics. Only recently has the full importance of trace gas flux measurements been realized, and up to this point only a limited number of seawater and atmospheric measurements suitable for ocean flux modeling have been made. The measurements presented here show for the first time that the ocean is a major source of OCS and $CHCl_3$ in the global environment, and confirm that the anthropogenic gases such as F-11, F-12, and CH_3CCl_3 are in equilibrium in the surface waters. A methodology for the collection of seawater samples for subsequent analysis of the trace gas content in the laboratory has been developed and successfully applied. While many questions have been answered, there are still many others that have been generated. The methodology and data provided here can serve as a starting point for research into these new areas.

PART I

A STUDY OF OCEAN-AIR GAS EXCHANGE MODELS

CHAPTER 2

MODELS FOR CALCULATING THE OCEAN-AIR FLUX OF TRACE GASES

2.1 Introduction

Modeling the exchange of gases across the air-sea interface began with studies of the transfer of oxygen between the atmosphere and the ocean (Redfield, 1947), and with efforts to estimate the potential of the ocean as a sink for increasing carbon dioxide (CO_2) from fossil fuel burning (Revelle and Suess, 1957; Bolin, 1957). The models used in these calculations were originally developed for chemical engineering applications to measure the adsorption of gases by liquid, and were adapted for use in chemical oceanography. Following the CO_2 studies and with the improvement of analytical techniques for gases, these models were used to determine the ocean flux of trace gases such as methane (CH_4), carbon monoxide (CO) (Swinnerton and Linnenbom, 1966), nitrous oxide (N_2O) (Weiss, 1982; Rasmussen and Pierotti, 1979), and the chlorofluorocarbons (Junge, 1976).

The models used for calculating gas exchange are based on the movement of a gas to the air-water interface followed by transfer across the interface. The transfer of the gas through the bulk air or water phase can take place by either convective mixing, diffusion, or a combination of the two. The transfer across the interface is assumed to be instantaneous, and proceeds as a result of a difference in the partial pressures of the gas in the two phases (see Chapter 3). Using

these basic features several models have been proposed for calculating gas exchange, differing in the mechanism for the transfer of the gas to the interface region. The most commonly used models are the two-film model, the surface renewal model, and the box model.

The modeling of gas exchange in the ocean presents some problems not found in engineering applications. The ocean is often heterogeneous due to currents and thermal gradients and cannot always be considered well mixed. For gases produced in the ocean by biological activity, the concentration can vary considerably due to the productivity of the area sampled or the season (Lovelock et al., 1976; Rasmussen et al., 1982d). For this reason calculations of ocean fluxes of gases need to take into account the ocean structure and the biological productivity.

The two-film model and the surface renewal models will be compared, and it will be shown that they produce similar flux values for ocean-atmosphere exchange problems if the mass transfer coefficients are measured in situ. An example of a box model calculation for carbonyl sulfide (OCS) is shown where the ocean source and atmospheric lifetime can be calculated using data on the flux, sources, and sinks. In the final section, the physical and biological processes that affect gas exchange are discussed along with how this information can be incorporated into the flux calculations to give more realistic results.

2.2 Two-Film Model

The two-film model, also called the stagnant film model, is the most commonly used method for calculating the flux of gases across the ocean-air interface. The model was first described by Whitman (1923) and is based on diffusion through a thin surface film where the partial pressure difference between the atmosphere and the ocean is the driving force for transfer.

The advantages of the model are that it is simple to use, the parameters in the model can be related to physical processes which can be measured, and the results agree with the more complicated models (Danckwerts, 1970). The main disadvantage is that the model is based on the concept of a stagnant film of uniform thickness at the surface of the ocean. In reality, the film thickness can vary considerably due to wind speed and the breaking action of waves (Kanwisher, 1963), making the stagnant film thickness a parameter that cannot be directly measured or theoretically determined.

The two-film model is shown schematically in Figure 2.1 and is derived with the following assumptions. The bulk air and water phase are well mixed and have a uniform composition, C_g and C_ℓ. There is a thin layer at the interface of each phase δ_g and δ_ℓ through which mass transfer takes place by diffusion. At the interface the gas concentration C_{gs} and liquid concentration $C_{\ell s}$ are in equilibrium and are related to each other by Henry's Law (Chapter 3). The rate of transfer

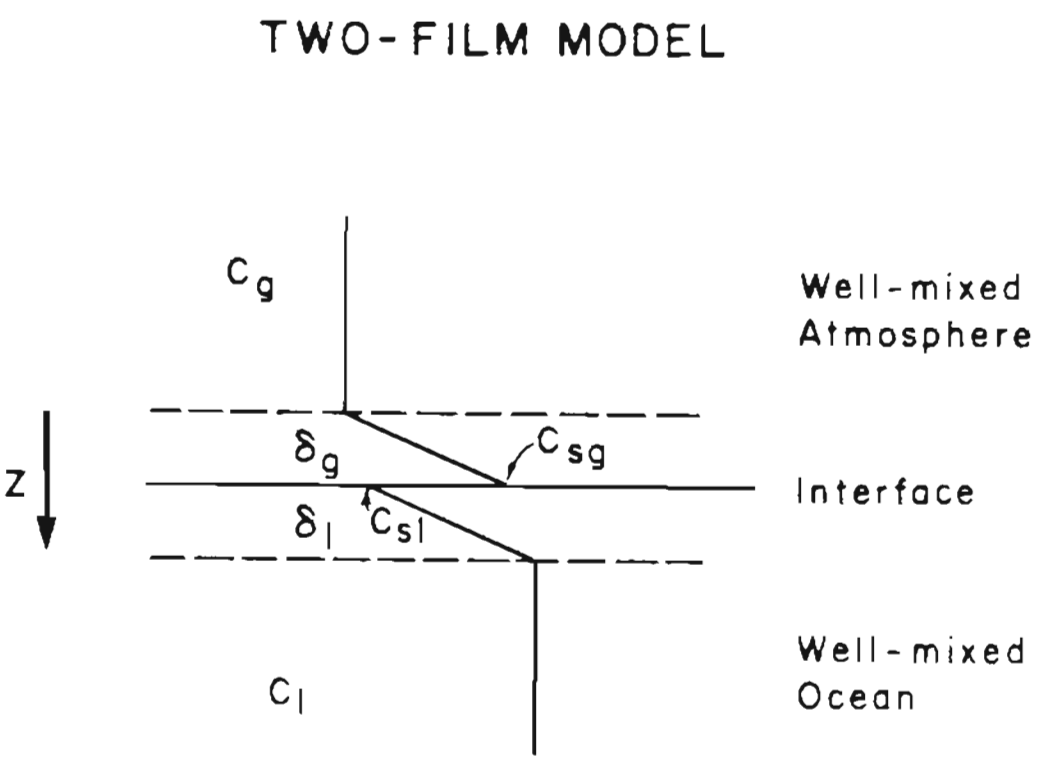

Figure 2.1. Schematic of two-film flux model. C_g is the atmospheric concentration, C_l is the bulk liquid concentration, C_{sl} is the liquid concentration at the interface, and C_{sg} is the atmospheric concentration at the interface. δ_g is the gas phase film thickness, and δ_l is the liquid phase film thickness.

through the interface is assumed to be rapid, so the rate limiting step for gas exchange is diffusion through the stagnant film.

The mathematical development of the model has been reviewed in several articles and books (Whitman, 1923; Liss and Slater, 1974; Neely, 1980) and will be presented here as a basis for comparison with other models to be discussed.

The transport through the stationary films at the interface is assumed to take place by diffusion and is described by Fick's first law, where the flux through each film is equal to a diffusion coefficient times the concentration gradient.

$$F_g = D_g \left(\frac{\partial C_g}{\partial z} \right) \qquad (2.2\text{-}1a)$$

$$F_\ell = D_\ell \left(\frac{\partial C_\ell}{\partial z} \right) \qquad (2.2\text{-}1b)$$

F_g and F_ℓ are the flux through the gas and liquid interfacial region respectively. D_g and D_ℓ are the diffusion coefficient in the gas and liquid, and C_g is the gas concentration and C_ℓ is the liquid concentration. For actual applications, each of the films is assumed to be a layer of thickness δ so equations (2.2-1) can be approximated as:

$$F_g = k_g (C_g - C_{sg}) \qquad (2.2\text{-}2a)$$

$$F_\ell = k_\ell (C_{s\ell} - C_\ell) \qquad (2.2\text{-}2b)$$

C_{sg} and $C_{s\ell}$ are the gas and liquid concentrations at the liquid interface, and k_g and k_ℓ are the gas and liquid mass transfer coefficients defined as:

$$k_g = \frac{D_g}{\delta_g} \tag{2.2-3a}$$

$$k_\ell = \frac{D_\ell}{\delta_\ell} \tag{2.2-3b}$$

δ_g and δ_ℓ are the gas and liquid phase film thicknesses. k has the dimensions of velocity and describes the rate of transfer through each interfacial region.

Assuming the transport between the two phases to be a steady state process, equations (2.2-2a) and (2.2-2b) can be set equal to each other:

$$F_g = F_\ell = k_g(C_g - C_{sg}) = k_\ell(C_{s\ell} - C_\ell) \tag{2.2-4}$$

The equations are difficult to use in this form since it is hard to measure the interface concentrations, C_{sg} and $C_{s\ell}$. By assuming the interface is in equilibrium (Scriven and Pigford, 1958), Henry's law can be used to relate the two interface concentrations, C_{sg} and $C_{s\ell}$ (see Chapter 3 for a detailed discussion of Henry's law):

$$C_{sg} = HC_{s\ell} \tag{2.2-5}$$

where H is the Henry's Constant. Equation (2.2-5) can be substituted into equation (2.2-4), and with some rearrangement can be written in a form that does not depend on the surface concentrations:

$$F\left(\frac{H}{k_\ell}+\frac{1}{k_g}\right) = C_g - HC_\ell \tag{2.2-6a}$$

$$F\left(\frac{1}{k_\ell}+\frac{1}{Hk_g}\right) = \frac{C_g}{H} - C_\ell \tag{2.2-6b}$$

These equations can be simplified by defining an overall mass transfer coefficient K_g or K_ℓ that has contributions from both k_g and k_ℓ.

$$\frac{1}{K_g} = \frac{H}{k_\ell}+\frac{1}{k_g} \tag{2.2-7a}$$

$$\frac{1}{K_\ell} = \frac{1}{k_\ell}+\frac{1}{Hk_g} \tag{2.2-7b}$$

$$K_g = \frac{K_\ell}{H} \tag{2.2-8}$$

Substituting K_g and K_ℓ into equation (2.2-6), the final form of the flux equations is obtained.

$$F = K_g(C_g - HC_\ell) = K_\ell\left(\frac{C_g}{H} - C_\ell\right) \tag{2.2-9}$$

Equation (2.2-9) gives the total flux of a gas across the air-water interface. To evaluate the flux for a particular gas, the concentra-

tion in the atmosphere (C_g) and the ocean (C_ℓ) must be measured, the Henry's constant must be known, and the value of K must be determined. The bulk gas and liquid concentrations can be measured using techniques described in Chapters 5, 6, 7, and 8. The values for H and K are different for each compound and depend on the pnysical parameters at the ocean-air interface. In Chapter 3 the methods that have been used to determine H and K for OCS and the halocarbons listed in the introduction will be discussed.

2.3 Penetration Theory and Surface Renewal Theory

One of the limitations of the two-film model is that when a liquid and a gas are first brought together, equilibrium is not immediately established because of the time for diffusion (penetration) into the water parcel. Penetration theory (Higbie, 1935) and later surface renewal theory (Danckwerts, 1951, 1955) were developed to provide a more realistic assessment of occurrences at the interface. The interpretation of penetration theory has since been expanded to the idea of a turbulent eddy of water that continually brings new parcels to the surface for a time period where gas exchange can take place. One exposure of the water at the surface would not require complete equilibrium to be established.

Instead of assuming a constant flux through the surface, penetration theory describes the gas diffusing through the liquid near the surface according to Fick's second law, which gives the change in concentration with surface exposure time:

$$\frac{\partial C}{\partial t} = D \frac{\partial^2 C}{\partial z^2} \qquad (2.3\text{-}1)$$

This equation can be solved using the boundary conditions described below (Danckwerts, 1951; Higbie, 1935). C_g/H is the water concentration in equilibrium with the air concentration, and C_ℓ is the initial or bulk concentration in the water.

1)	$C = C_g/H$	$z = 0$	$t > 0$
2)	$C = C_\ell$	$z > 0$	$t = 0$
3)	$C = C_\ell$	$z = \infty$	$t > 0$

The solution to equation (2.3-1) in terms of the error function, erfc:

$$C = C_\ell + \left(\frac{C_g}{H} - C_\ell \right) \operatorname{erfc} \left[\frac{z}{2\sqrt{D_\ell t}} \right] \qquad (2.3\text{-}2)$$

The flux at the ocean surface ($z = 0$) can be calculated using Fick's first law, which is the derivative of equation (2.3-2) with respect to z, at $z = 0$.

$$F = D \left(\frac{\partial C}{\partial z} \right)_{z=0} = \left(\frac{C_g}{H} - C_\ell \right) \sqrt{\frac{D_\ell}{\pi t}} \qquad (2.3\text{-}3)$$

where t is the length of time the water spends at the interface. Higbe (1935) called this the exposure time, t_e, and assumed that it is the same for all parcels of water reaching the surface. The

exposure time can be calculated from the overall transfer coefficient K:

$$K = \sqrt{\frac{D_\ell}{\pi t_e}} \qquad (2.3\text{-}4)$$

A difficulty with penetration theory is that the exposure time, t_e, is never really known, nor can it be theoretically calculated (Danckwerts, 1970). Consequently, K has to be experimentally determined in order to get t_e to use in subsequent calculations.

Surface renewal theory is a modification of penetration theory, which assumes that the exposure time is not constant for all parcels of water but can vary from 0 to infinity (Danckwerts, 1951, 1955, 1970). Danckwerts suggested that a more realistic approach would be to assume that there is no correlation between the age of a parcel of water at the surface and its chance of being replaced, and defined a surface age distribution function which describes the fraction of surface area belonging to different age groups t + dt. Regardless of the age of the water parcel, its fractional rate of replacement with fresh water is equal to s. So if the surface area of an age group is ϕdt at time t, it will be $\phi dt - s\phi dt$ at time t + dt, where $s\phi dt$ represents the fraction replaced with fresh water. This can be described as a first order loss process.

$$\frac{d\phi}{dt} = -s\phi \qquad (2.3\text{-}5)$$

Equation (2.3-5) can be integrated to get the surface area distribution function, which gives the surface area, ϕ, as a function of exposure time, t.

$$\phi = se^{-st} \tag{2.3-6}$$

Since equation (2.3-3) gives the flux per unit area, it can be multiplied by ϕ to get the flux for each exposure time.

$$F(t) = \left(\frac{C_g}{H} - C_\ell \right) \sqrt{\frac{D_\ell}{\pi t}}\, se^{-st} \tag{2.3-7}$$

This equation can be integrated over all exposure times (0 to ∞) to give the average flux.

$$F = \left(\frac{C_g}{H} - C_\ell \right) \sqrt{D_\ell s} \tag{2.3-8}$$

The result is similar to penetration theory with K given by:

$$K = \sqrt{D_\ell s} \tag{2.3-9}$$

The value for s, the fractional rate of replacement, must be determined experimentally since it cannot be theoretically evaluated.

The major difference between the surface renewal theories and the two-film model is that the two-film model predicts that K is

proportional to D, where the surface renewal models predict that K is proportional to $D^{\frac{1}{2}}$. The two theories will give the same results when K is measured for a tracer gas with a diffusion coefficient similar to the gas of interest, but can give substantially different flux values for gases with diffusion coefficients different from those of the tracer (see Chapter 3).

Conceptually surface renewal theory is more appealing since it seems to be a better model of what is really happening at the surface. It is very useful for chemical engineering applications where exposure times between the chemical and the water surface are short and can often be estimated. For environmental applications the exposure times cannot be estimated any better than the surface film thickness, so the simpler two-film model is usually used.

2.4 Box Models Applied to Ocean-Atmosphere Exchange

The box model is a powerful tool for calculating the distribution of chemicals in the environment, and can be used for ocean-atmosphere flux calculations. The model is based on the conservation of mass equation applied to any number of desired boxes of various sizes. For oceanographic modeling the box model is often more desirable than a continuous model since the ocean is composed of layers of water internally well mixed but substantially different from the surrounding water. Depending on the choice of boxes, models can be set up to calculate the distribution of chemicals between the atmosphere and the

mixed layer of the ocean, describe the movement to and from the deep ocean, and calculate the ocean flux of a gas from depth profile data. Box models have been used with tracer gases such as $^{14}CO_2$ and Radon to measure the transfer coefficient, K, for use in the two-film model (Craig, 1957; Broecker and Peng, 1974).

An ocean-atmosphere box model can be formulated by dividing the system into one or more well mixed boxes. The conservation of mass equation can be applied to each box.

Mass Change = Flow into box - Flow out of box +

Production in box - Loss in box

For a system of N boxes the conservation of mass equation can be written as a series of equations for the boxes (Khalil, 1979).

$$\frac{d}{dt}\begin{bmatrix} C_1 \\ C_2 \\ \cdot \\ \cdot \\ \cdot \\ C_N \end{bmatrix} = \begin{bmatrix} K_{11} & K_{12} & \ldots & K_{1N} \\ K_{21} & K_{22} & \ldots & K_{2N} \\ & & & \\ & & & \\ & & & \\ K_{N1} & K_{N2} & \ldots & K_{NN} \end{bmatrix} \begin{bmatrix} C_1 \\ C_2 \\ \\ \\ \\ C_N \end{bmatrix} + \begin{bmatrix} S_1 \\ S_2 \\ \\ \\ \\ S_N \end{bmatrix} - \begin{bmatrix} L_1 \\ L_2 \\ \\ \\ \\ L_N \end{bmatrix} \qquad (2.4\text{-}1)$$

where K_{ii} represents the overall transport term between the boxes and can be written as a sum of the diffusion terms, D_{NN}, and the velocity terms, k_{ii}, for the boxes. If the loss terms are written as first order processes, $L_i = k_i C_i$, they can be combined with the K terms, and equation (2.4-1) can be simplified to:

$$\frac{dC}{dt} = - \begin{bmatrix} K_{11} & K_{12} & \ldots & K_{1N} \\ K_{21} & K_{22} & \ldots & K_{2N} \\ & & & \\ K_{N1} & K_{N}2 & \ldots & K_{NN} \end{bmatrix} \underline{C} + \underline{S} \qquad (2.4\text{-}2)$$

where $\underline{C}$ and $\underline{S}$ are defined as the column vectors from equation (2.4-1). The solution to this differential equation is (Khalil, 1979):

$$\underline{C} = \exp(-\Omega t)\underline{C}o + \exp(-\Omega t) \int_o^t \exp(\Omega t') . \underline{S}(t')dt' \qquad (2.4\text{-}3)$$

where the matrix, Ω, contains both the transport and sink terms. For many naturally produced gases, S(t) is a constant in time, so $\underline{C}$ is equal to:

$$\underline{C} = \Omega^{-1} \underline{S} \qquad (2.4\text{-}4)$$

To demonstrate how the box model can be used in ocean-atmosphere calculations, the carbonyl sulfide distribution will be calculated in

the next section using a two-box model. If depth profile data are available, more boxes can easily be added to the model, and the flux from the ocean can be calculated. In Chapter 3 the methods used to calculate K from a box model will be discussed.

2.5 Atmospheric OCS Distribution Calculated Using a Two-Box Model

The global OCS budget can be calculated using the box model shown in Figure 2.2 In this model the atmosphere is divided into a stratospheric box and a tropospheric box. One box can be used for the troposphere since the concentration of OCS is uniform (Torres et al., 1980). The ocean is divided into two boxes, one representing the mixed layer and the other the deep ocean. The mixed layer concentration is assumed to be constant, and is equal to the average concentration weighted to the different productivity areas (see Chapter 10).

The transport terms, (k_i), the rate constants for hydrolysis, K_m, and for tropospheric loss mechanisms, K_T, are shown in Table 2-1, along with the concentrations of OCS in the four boxes. k_1 and k_4 are small compared with the other terms, so the stratospheric box and the deep ocean box can be eliminated from the calculation since their contribution is small. This simplifies the model to two main boxes: the troposphere and the ocean mixed layer. The mass balance equation can be written for the global sources and sinks of OCS as shown in equation (2.4-2).

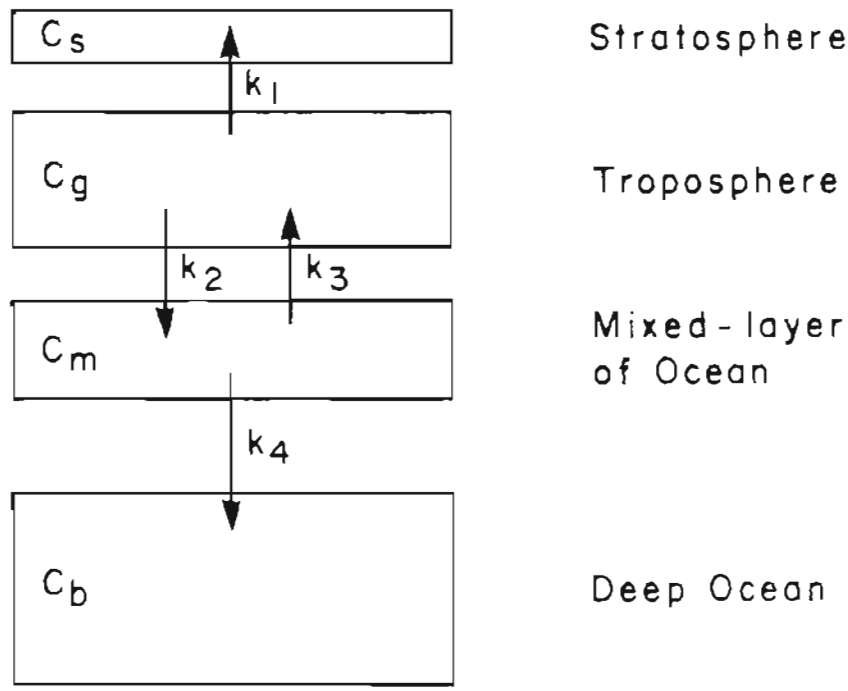

Figure 2.2. Box model for the distribution and mass balance of OCS between the atmosphere and the ocean.

TABLE 2-1

Data for OCS Box Model

Tropospheric concentration $\equiv \bar{C}_T = 500$ pptv

Ocean mixed layer concentration $\equiv \bar{C}_m = 800$ pptv

Deep ocean concentration $\equiv \bar{C}_D = 0$ pptv

Atmospheric burden $\equiv m_T = 4.3 \times 10^{12}$ g OCS

Ocean mixed layer burden $\equiv m_m = 7.3 \times 10^{10}$ g OCS

Tropospheric source (Table 10-4) $\equiv S_T = 3.2 \times 10^{12}$ g/yr

Hydrolysis rate constant $\equiv K_m = 71\ yr^{-1}$

Henry's constant $\equiv H = 1.7$

Volume mixed layer $\equiv V_m = 3.6 \times 10^{22}\ cm^3$
(100 m deep)

Area of ocean $\equiv A_o = 3.6 \times 10^{18}\ cm^2$

Avogadro's number $\equiv N^o = 6.02 \times 10^{23}$

Number of molecules in troposphere $\equiv N^{\infty} = 8.7 \times 10^{43}$
(Khalil, 1979)

Transport to the stratosphere* $\equiv k_1 = 0.12\ yr^{-1}$

Transport to the deep ocean $\equiv k_4 = 0.002\ yr^{-1}$

* Khalil, 1979

To avoid corrections due to the different volumes in the boxes, the equations can be written in terms of the total mass in each box (m_i), so the flux of OCS is also given in terms of the mass per unit time. Starting with equation (2.2-9), the concentrations are expressed as m_i and the flux is calculated as mass per year for the total ocean.

$$F = \text{Flux} = A_o \circ K_\ell \left(\frac{m_g \, N^\circ}{HN^\infty \, RT} - \frac{m_m}{V_m} \right) \tag{2.5-1}$$

The mass in each box can be calculated using equation (2.4-4) since the sources for OCS are assumed to be constant with time.

$$\underline{S} = \begin{bmatrix} -\left(K_T + \dfrac{A_o K_\ell N^\circ}{HN^\infty RT} \right) & \dfrac{A_o K_\ell}{V_m} \\ \dfrac{A_o K_\ell N^\circ}{HN^\infty RT} & -\left(K_m + \dfrac{A_o K_\ell}{V_m} \right) \end{bmatrix} \underline{m} \tag{2.5-2}$$

Since these are two equations, one for each box, equation (2.5-2) can be solved for any two unknowns. For OCS the two unknowns are the tropospheric lifetime, K_T, and the ocean source, S_m. The tropospheric sources of OCS, S_T, are given in Table 10-4 and have been independently estimated to be 2.5 Tg/yr. The ocean sink term, K_m, was calculated using the hydrolysis rate constant of Thompson (1935) at the average ocean pH. Both S_T and K_m could be uncertain by a factor of two, but currently are the best available values.

Substituting in the data from Table 2-1 and performing the matrix multiplication, the ocean mixed layer source and atmospheric lifetime are found to be:

$$S_m = 5.9 \times 10^{12} \text{ g/yr}$$
$$1/K_T = 1.4 \text{ years}$$

While the lifetime can be calculated from only the tropospheric data and the ocean mixed layer source can be determined from the ocean data, the use of a simple box model as shown allows both of these quantities to be calculated at once, and, more importantly, assures that all of the values found from the model are consistent. This has not always been the case in the literature when separate calculations are done and the results combined into a global budget.

2.6 Physical and Biological Processes in the Ocean

To use the two-film or box model to maximum advantage in ocean-atmosphere exchange calculations, the physical structure and biological make-up of the ocean must be understood so that the correct selection of sampling sites or arrangement of boxes can be made. As with the atmosphere, temperature and salinity gradients divide the ocean into density layers which do not readily exchange with each other, but unlike the atmosphere the mixing within each of these layers is much slower. For gases of biological origin, concentrations can vary greatly due to the productivity and nutrient availability in

different regions of the ocean. In this section the physical and biological structure of the ocean will be described to provide guidelines for formulating ocean-atmosphere exchange models.

The vertical structure of the ocean is shown in Figure 2.3. The upper layer, called the mixed layer, extends down to approximately 100 meters and is of uniform composition since the water is mixed at a rapid rate by the surface winds (Neumann, 1965). This layer can be identified by a constant temperature profile shown in Figure 2.3, line C. The temperature of the mixed layer varies with latitude from about 0° to 26°C as shown in Figures 2.4 and 2.5 (Defant, 1961), and is an important parameter in gas exchange studies since the solubility of a gas is a function of temperature (see Chapter 3). The mixed layer is primarily responsible for ocean-atmosphere exchange because the gas concentration within this layer is readily available for exchange with the atmosphere since the residence time of an inert gas in this layer is about 20 days (Peng et al., 1979).

Below the mixed layer there are the intermediate waters and the deep ocean. The intermediate waters act to separate the deep ocean from the mixed layer since the low temperature and high density of the deep waters keep them from mixing with the surface waters. The exchange of water between the deep ocean and the mixed layer is on the order of about 500 to 1000 years (Craig, 1957), so the loss of a gas to the deep ocean is not considered significant for most gases. However, recent evidence (Gammon et al., 1982) suggests that cold ocean currents originating near the poles may bring fresh water into the

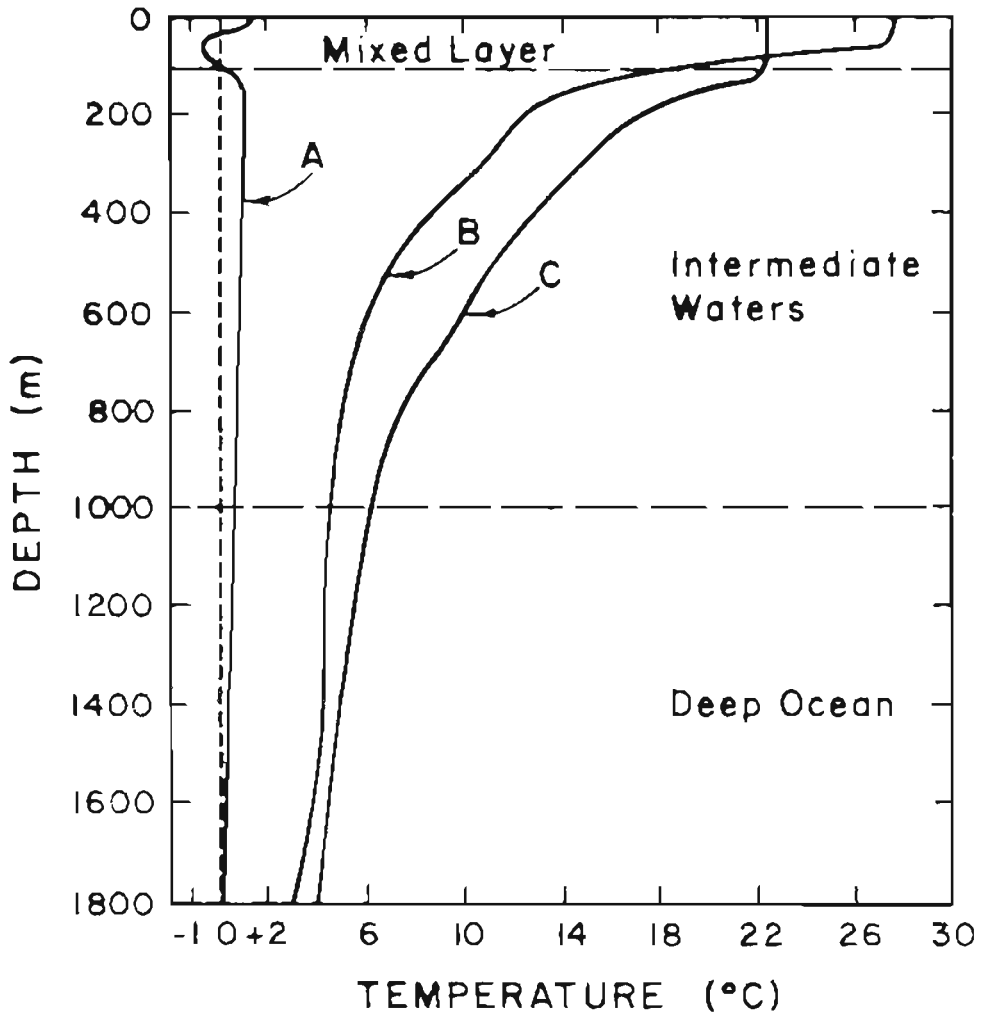

Figure 2.3. Major vertical divisions of the ocean, showing how they are related to the ocean temperature at different latitudes. A is the profile at 60°S, B is the profile at the equator, and C is the profile at 20°N.

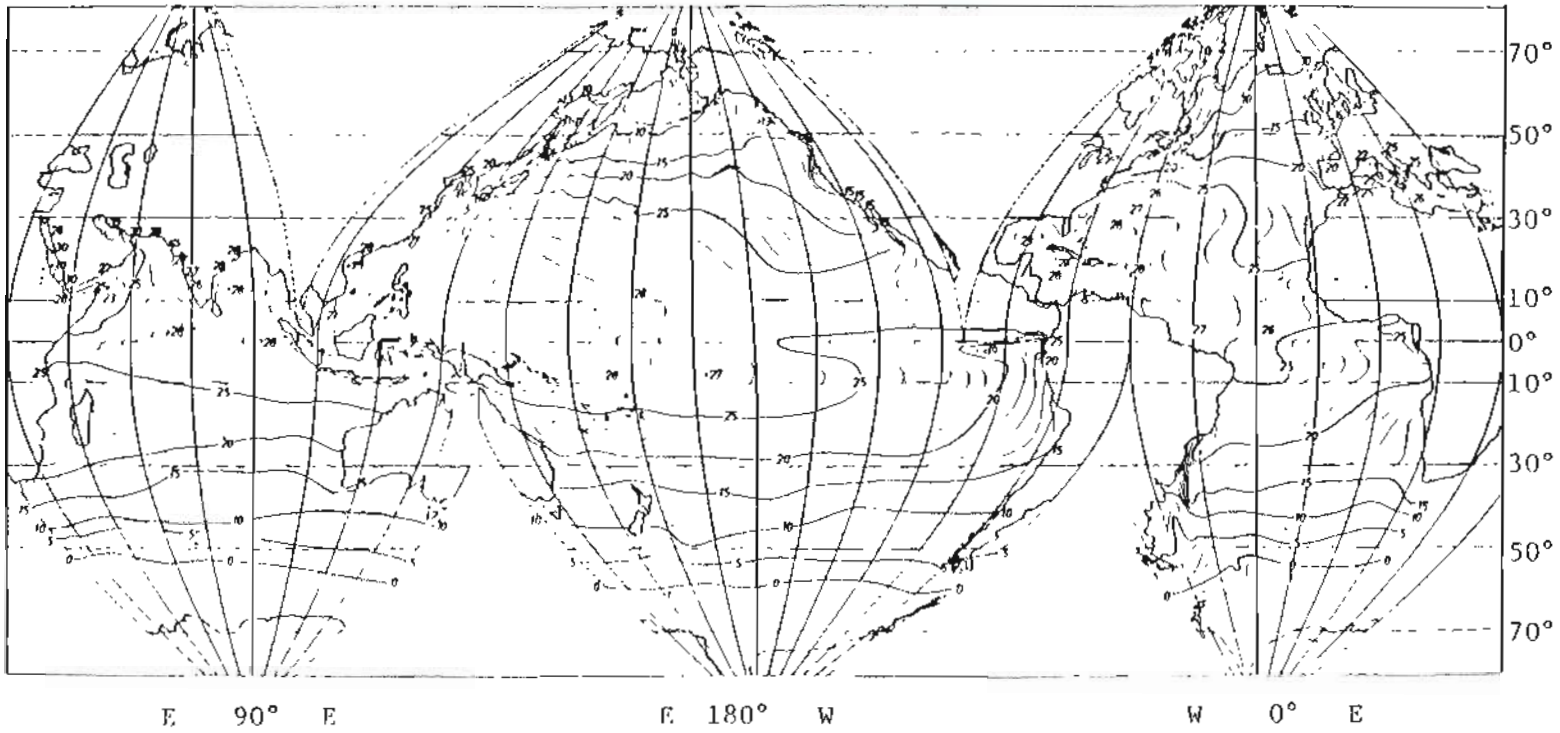

Figure 2.4. Surface temperature (°C) of the world oceans for August (Defant, 1961).

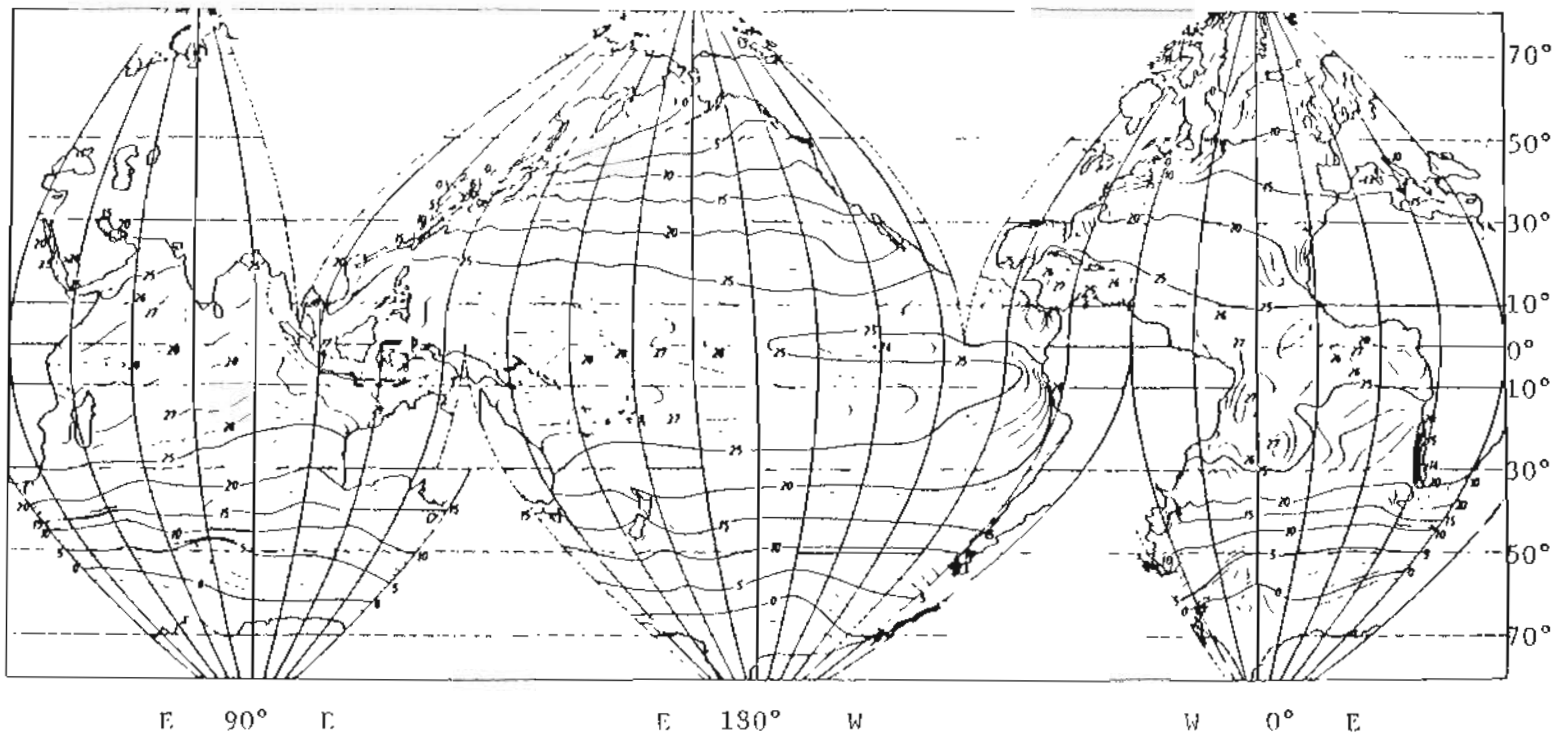

Figure 2.5. Surface temperature (°C) of the world oceans for February (Defant, 1961).

deep ocean in less than 20 years, but the volume of this water is not known.

Ocean currents are driven by energy from the wind and sun and are responsible for the horizontal and vertical mixing of water masses. The physical mixing processes are a result of energy exchange at the ocean-atmosphere boundary in the form of heat and momentum. The upper layer of the ocean is mixed primarily by wind-driven oceanic currents, which are shown in Figure 2.6 (Defant, 1961). Mixing in the intermediate and deep waters can take place by slope currents, so named because they originate at the surface and slope downward through the ocean, and by thermohaline currents (Neumann, 1965). The thermohaline currents are caused by the differences in evaporation and precipitation rates at the ocean surface which result in salinity and temperature changes. The changes in temperature and salinity cause the water mass to either rise or fall because of its change in density, resulting in the movement of surface water masses to the keep ocean. This process is responsible for the sinking of cold water masses in the North Atlantic and Antarctic regions, and the weak bottom currents from the high latitudes towards the equator as shown in Figure 2.7 (Neumann, 1965).

Another important physical process affecting the ocean-atmosphere exchange of biologically produced gases are the upwellings of deep, nutrient-rich waters. These areas occur off the western coast of continents in the low latitudes, and are caused by the trade winds blowing along the coast combined with the geostrophic effect to move the surface water away from the coast allowing cold water to rise and take its place (Riley and Chester, 1971). These upwellings are important since

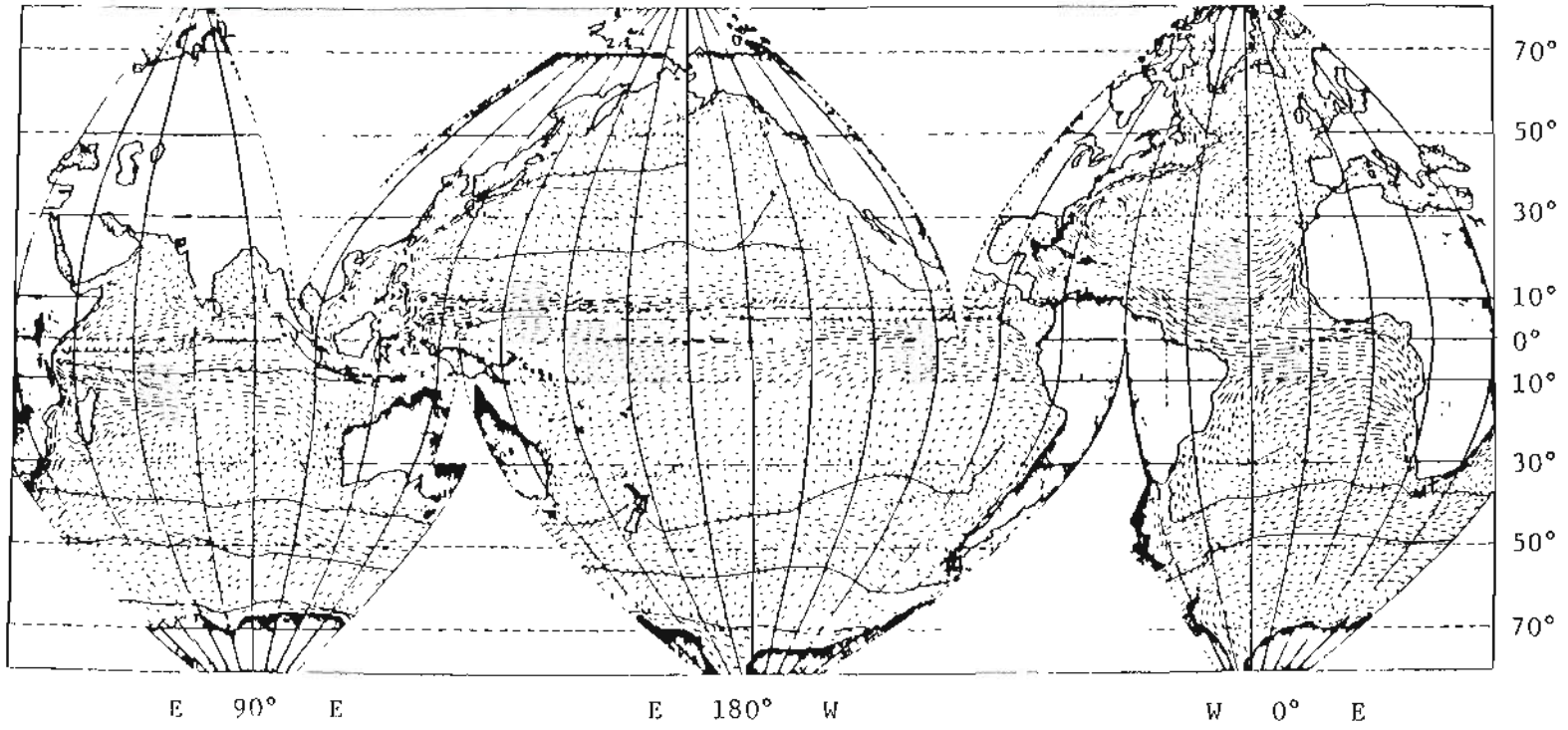

Figure 2.6. Ocean surface currents for northern hemisphere winter (Defant, 1961).

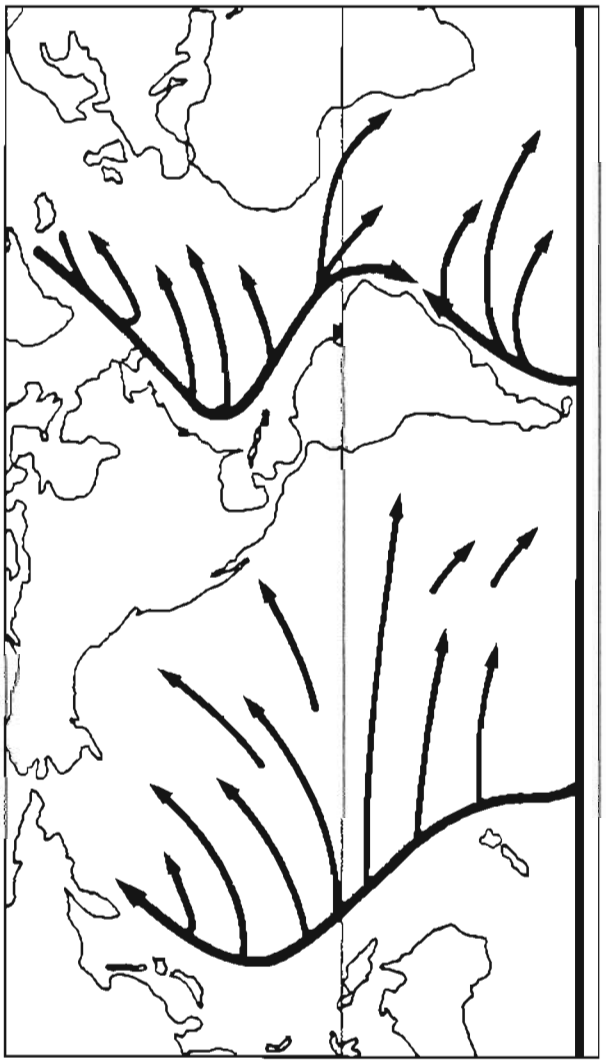

Figure 2.7. Flow of the deep ocean waters.

the biological productivity in these regions is high because of nutrients brought in by the cold water.

The seawater concentrations of gases produced by biological activity can vary depending on the productivity of the area, the season, and the time of day. When modeling the ocean flux of trace gases, it is important to design a comprehensive sampling program to sample the various productivity areas, and also to take into account the wide range of concentrations that might be found.

Depending on the input of sunlight and nutrients, the biological productivity of the ocean varies widely. Regions of nutrient upwellings or continental runoff would be expected to have more biological activity than the open ocean areas with low nutrient concentrations. A map of the primary productivity areas of the world's oceans has been compiled by Koblentz-Mishke et al. (1970) and is shown in Figure 2.8. The original five areas have been combined and divided into three major areas, low, moderate, and high. Table 2-2 shows the percentage of the total ocean area of each productivity type, along with the carbon production rate. The productivity is determined by measuring the intensity of photosynthesis by marine algae at a given location. The standard method of measurement is the radiocarbon method of Neilsen (1951), which measures the amount of ^{14}C uptake by algae per day. Care must be taken in application of the primary productivity areas based on algae measurements to the production of a specific gas, since gases are often produced by specific organisms which may vary from location to location (Lovelock et al., 1972).

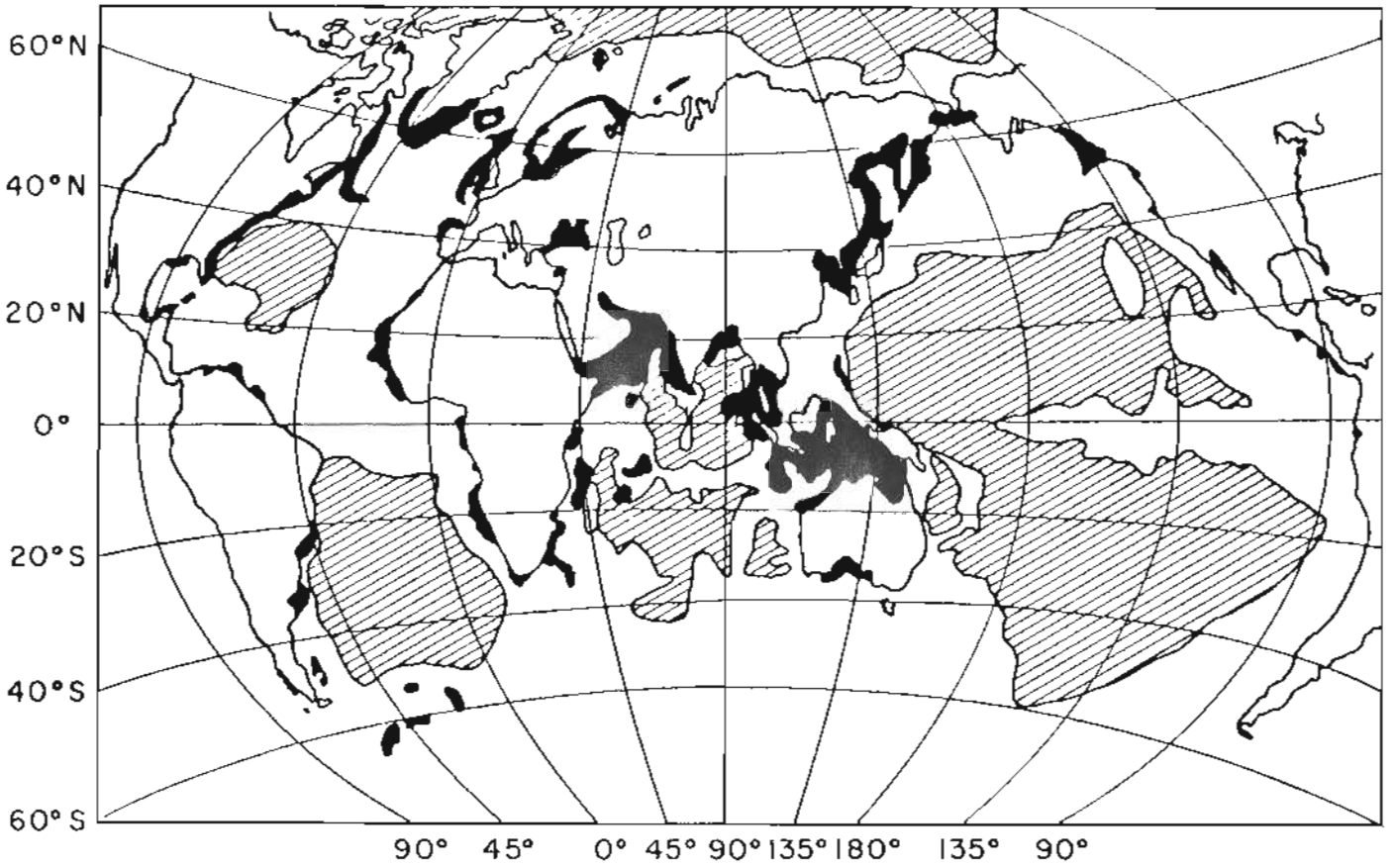

Figure 2.8. Map of the primary productivity areas of the world's oceans. The black area represents the high productivity, the white area represents moderate productivity, and the shaded area represents low productivity.

TABLE 2-2

Biological Primary Productivity Regions

of the Oceans

Productivity Area	% Total Ocean	Total Area (cm^2)	mg C/m^2 per day
High	3	1.1×10^{17}	>500
Moderate	57	2.1×10^{18}	100 - 500
Low	40	1.4×10^{18}	<100

The heterogeneity of the ocean, especially for gases of biological origin, can be expected to give large variations in the gas concentrations in seawater. For gases produced in the ocean, samples need to be collected from many types of productivity areas to get an accurate estimate of the flux.

2.7 Conclusions

The transfer of a gas across the ocean-atmosphere interface can be thought of as the process of convective transport of the gas, in a well mixed layer, to the interface where it moves by diffusion through a thin surface film in the direction from high partial pressure to low partial pressure. This can be described by either a stagnant film model or a surface renewal model. While conceptually the models are very different, in actual application both models predict that the flux is equal to a transfer coefficient, K, times an air-water concentration difference, as given by equations (2.2-9) and (2.3-8). The models differ in that K for the two-film model is proportional to D, and for the surface renewal model K is proportional to $D^{\frac{1}{2}}$. Chapter 3 will show that for gases with diffusion coefficients similar to the tracer gas the difference in the flux calculated using the two models is small compared to other uncertainties. However, there are fundamental differences in the models because they predict a different dependence on the diffusion coefficient, D.

The box model can be used to get a more comprehensive understanding of the distribution of a gas between the atmosphere and the ocean. This was shown for OCS where the atmospheric lifetime and ocean source were calculated from the concentration distribution. The box model can also be used with ocean profile data to calculate the flux. This will be shown in Chapter 3 where this procedure is used on tracer gases to determine K.

To select the appropriate locations to collect samples for use with the two-film model or to set up the optimum number of boxes for the box model, the physical and biological structure of the ocean is an important consideration. Ocean productivity can have a tremendous effect on the concentrations of gases produced by biological mechanisms, which will be shown for the case of methyl iodide and OCS in Chapter 10. It is often convenient to divide the ocean into productivity areas and calculate the flux for each area. Significant differences in the flux values is a good indication that biological production may be taking place.

CHAPTER 3

DETERMINATION OF THE HENRY'S CONSTANT, H, AND MASS TRANSFER COEFFICIENT, K

3.1 Introduction

The Henry's constant, H, and the transfer coefficient, K, are important parameters in the study of gas exchange at the ocean-atmosphere interface. In Chapter 2, gas exchange models were presented which required H and K in addition to the air and seawater concentrations. The value of H relates the liquid concentration to the gas concentration by means of Henry's law and along with C_g and C_ℓ determine whether gas transfer is to or from the ocean. K is a measure of the rate of gas transfer and does not affect the direction of the flux.

In this chapter the experimental measurement of H and K will be described, and tables listing the literature values for these constants have been compiled. Since H is a function of temperature and salinity and K is a function of the gas molar volume and windspeed, the dependence of H and K on these parameters will be discussed along with the theoretical basis for this dependence. Excellent reviews for the measurement of the Henry's constant and gas solubility exist (Markham and Kobe, 1981; Battino and Clever, 1966), and several papers on the measurement of the transfer coefficient have been written (Broecker and Peng, 1974; Peng et al., 1979).

3.2 Henry's Law

An empirical relationship was formulated in 1803 by Sir William Henry, who experimentally found that the quantity of a gas dissolved in a given mass of water is proportional to the pressure of the gas. Henry's law in its best known formulation is given in terms of the partial pressure and mole fraction of a gas (Hildebrand and Scott, 1964):

$$p = H\,X \tag{3.2-1}$$

where p is the partial pressure of gas, H is the Henry's constant for that gas and X is the mole fraction in solution. Henry's law is valid in dilute solutions of non-ideal gases where the molecules of solute are so few that the solvent can separate them enough to form a uniform environment (Hildebrand and Scott, 1964).

For a gas that exhibits ideal behavior, the Henry's constant is equal to the equilibrium vapor pressure of the gas (p^o), and the gas is said to follow Raoult's law (Moore, 1972).

$$p = p^o\,X \tag{3.2-2}$$

Figure 3.1 illustrates the relationship between the two laws. Line A shows the Raoult's law description of the ideal behavior of a gas. Line B shows the actual gas behavior, which is non-ideal at intermediate mole fractions. Line C shows the Henry's law fit to the actual gas

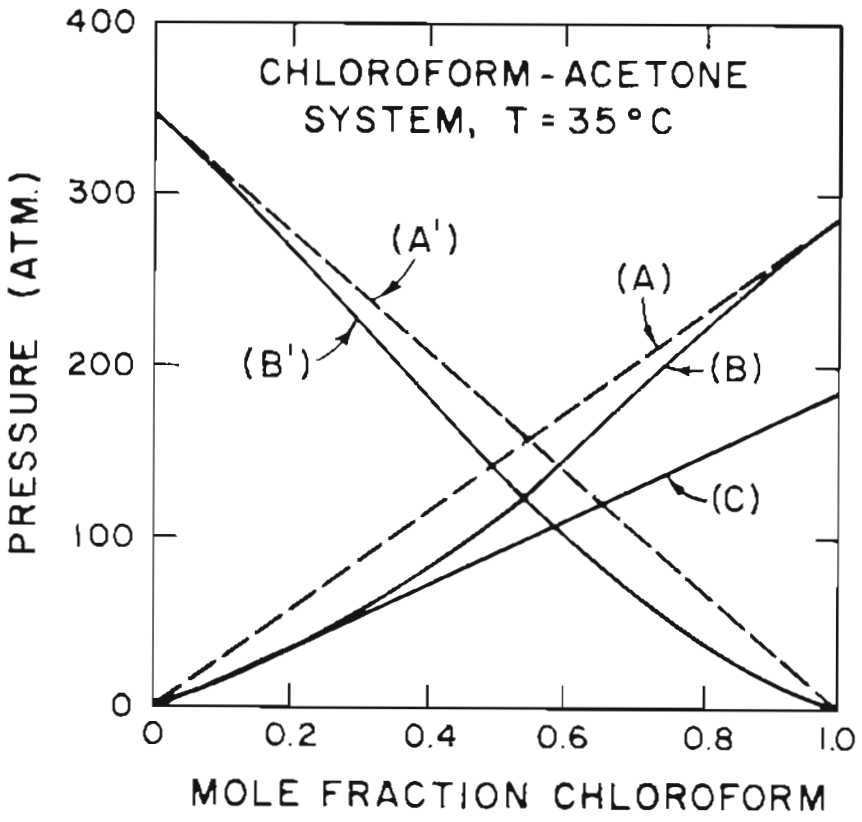

Figure 3.1. Variation of partial pressure with composition for the chloroform-acetone system. The dotted line represents ideal behavior, and the solid line, B, shows the actual behavior. A' and B' are the corresponding curves for acetone. Line C shows the Henry's law fit at low pressures (concentrations).

behavior at low concentrations. This figure demonstrates that even though the gas is non-ideal and deviates from Raoult's law, a Henry's constant can be found to empirically describe the gas behavior at low mole fractions (Denbigh, 1971). For many gases, Henry's law is valid up to a pressure of one atmosphere with only about a 1 to 3% deviation (Daniels and Alberty, 1970).

Henry's law and Raoult's law were first established from experimental data, but it is also possible to derive them from thermodynamic criteria for equilibrium between two phases. For two phases to be in equilibrium the chemical potentials (μ) of the components in each phase must be equal (Denbigh, 1971).

$$\mu^{gas} = \mu^{solu} \tag{3.2-3}$$

In order that the derivation be valid for both ideal and non-ideal solutions, the chemical potentials can be written in terms of the fugacity, f (Mackay et al., 1979):

$$\mu^{gas} = \mu^*(T) + RT \ln f^{gas} \tag{3.2-4}$$

$$\mu^{solu} = \mu^*(T) + RT \ln f^{solu} \tag{3.2-5}$$

μ^* is the reference state chemical potential. The fugacity is an idealized vapor pressure which makes it possible to use the ideal expression for the chemical potential and correct it for non-ideal effects (Mackay, 1979; Mackay and Paterson, 1981). The fugacity of a component in each phase can be related to its partial pressure (Mackay et al., 1979):

$$f^{gas} = \phi\ p^{gas} = \phi\ Y\ P \tag{3.2-6}$$

$$f^{solu} = \gamma\ p^{solu} = \gamma\ X\ p^{o} \tag{3.2-7}$$

where ϕ and γ are the fugacity coefficients, p is the partial pressure, P is the total pressure, and p^{o} is the equilibrium vapor pressure of the pure liquid at some temperature (T).

Substituting equations (3.2-4) and (3.2-5) into equation (3.2-3) and simplifying:

$$f^{gas} = f^{solu} \tag{3.2-8}$$

Substituting in the fugacity of each phase from equations (3.2-6) and (3.2-7):

$$\phi\ p^{gas} = \gamma\ X\ p^{o} \tag{3.2-9}$$

This can be rearranged:

$$\frac{p^{gas}}{X} = \frac{\gamma p^{o}}{\phi} = K \tag{3.2-10}$$

For ideal behavior γ and ϕ will both equal 1, so the constant K is equal to the vapor pressure of the pure component p^{o}. This is the Raoult's law expression. For non-ideal behavior γ and ϕ do not have to be equal to 1, so the constant K is equal to the Henry's Constant, H, and the gas follows Henry's law. For the region over which Henry's law is obeyed the ratio of γ to ϕ must not change.

The ideal solubility of a gas can be calculated using equation (3.2-10) (Hildebrand and Scott, 1964). For ideal solutions γ and ϕ are equal to 1 and for a pure gas present at 1 atmosphere pressure:

$$X = \frac{1}{p^o} \tag{3.2-11}$$

Thus, the solubility can be calculated from the vapor pressure of the pure component. This is true only if the gas behaves ideally over its whole composition range, i.e., it follows line A in Figure 3.1. For calculating the solubility of most gases in water this turns out to be a poor approximation.

For applications of Henry's law to environmental calculations in dilute solutions equation (3.2-10) can be rewritten in a more convenient form (Markham and Kobe, 1941), using the liquid concentration, C_ℓ.

$$p = H' C_\ell \tag{3.2-12}$$

Using the ideal gas law, the pressure can be expressed as a gas phase concentration (C_g):

$$\frac{p}{RT} = \frac{n}{V} = C_g \tag{3.2-13}$$

R is the gas constant, T is the absolute temperature, n is the number of moles and V is the volume. Using equations (3.2-12) and 3.2-13), Henry's law can be written as:

$$C_g = H\ C_\ell \tag{3.2-14}$$

or

$$H = \frac{C_g}{C_\ell}$$

The constant H is expressed with C_g and C_ℓ in the same units so H is unitless (Neeley, 1980) which distinguishes it from the H in equation (3.2-1). Notice that the value of H will be different if the concentrations are expressed as masses rather than in moles.

For substances which have vapor pressures above 1 atm at the temperature of measurement, the Henry's constant can be determined from gas solubility measurements made at 1 atm with pure gas (Douglas, 1967; Weiss, 1970).

$$H = 1/C_{\ell s} \tag{3.2-15}$$

where $C_{\ell s}$ is the solubility of the gas. In the literature the Henry's constant for gases is often expressed as the gas solubility. The two common ways of expressing gas solubility are the solubility coefficient, α, and the Bunsen absorption coefficient, β.

The solubility coefficient, α, was defined by Ostwald in 1894 as "the ratio of the volume of the absorbed gas to that of the absorbing liquid." If these are V_ℓ^* and V_s, then α is given as:

$$\alpha = \frac{V_\ell^*}{V_s} \tag{3.2-16}$$

The volume of gas, V_ℓ^*, is reported at 760 mmHg and at the specified temperature of the measurement. Since α is measured at a gas partial pressure of 760 mmHg, equation (3.2-16) is really a simplification of equation (3.2-14) (Battino, 1966).

$$\frac{V_\ell^*}{V_s} = \frac{C_\ell}{C_g} \tag{3.2-17}$$

The relation between α and K_H is given by:

$$\alpha = 1/K_H \tag{3.2-18}$$

α has also been called the distribution coefficient, K_D (Stumm and Morgan, 1970).

The Bunsen absorption coefficient, β, was proposed by Bunsen in 1855 and is defined as "the volume of gas reduced to 0°C and 760 mm pressure of mercury, which is absorbed by the unit volume of liquid under the pressure of 760 mm." β is similar to α except the volume of gas is reduced to 0°C and 760 mmHg using the ideal gas laws (Markham and Kobe, 1941):

$$\beta = \frac{V_\ell^*}{V_s} \tag{3.2-19}$$

$$\alpha = \beta \left(\frac{T}{273^\circ\ K}\right) \left(\frac{760}{760-p_s}\right) \tag{3.2-20}$$

The conversions among the different forms of solubility expressions and the Henry's constant are given in Table 3-1.

TABLE 3-1

Equations for Converting Between the Different Forms of the Henry's Constant and Solubility

$$H = \frac{C_g}{C_\ell} \qquad \text{(unitless)}$$

$$H = \frac{p}{C_\ell} \qquad H_1 \equiv \frac{\text{mmHg} \cdot \text{L}}{\text{mole}} \qquad H_2 = \frac{\text{atm} \cdot \text{L}}{\text{mole}}$$

$$\alpha = 1/H \qquad \text{(unitless)}$$

$$\alpha = \beta \quad \frac{T(^\circ K)}{273} \quad \frac{760}{760 - p_S(\text{mmHg})} \qquad \beta \text{ @ STP}$$

$$H = \frac{H_1}{62.4} \quad \frac{1}{T(^\circ K)}$$

$$H = \frac{H_2}{0.0821} \quad \frac{1}{T(^\circ K)}$$

For substances below their critical temperature that have vapor pressures greater than their partial pressures at the temperature of the experiment, the Henry's constant can be calculated from the solubility data if the equilibrium vapor pressure is known (Mackay et al., 1979; Neeley, 1980). This can be demonstrated by going back to equation (3.2-9) which describes the equilibrium between the vapor and liquid. Equations (3.2-6) and 3.2-7) can be substituted into (3.2-9):

$$\phi \; Y \; P \; = \gamma \; X \; p^{o} \qquad (3.2\text{-}21)$$

For environmental calculations, P is about 1 atmosphere, which means that ideal gas behavior can be assumed, so $\phi = 1$ and $p = Y \; P$.

$$p = \gamma \; X \; p^{o} \qquad (3.2\text{-}22)$$

This can be rearranged:

$$\frac{p}{X} = \gamma \; p^{o} = H \qquad (3.2\text{-}23)$$

Considering a pure component in water, its vapor pressure, p, will be equal to p^{o}, the equilibrium vapor pressure of the pure component, and its concentration in water, X, will equal its solubility, X^{s}.

$$\frac{p^{o}}{X^{s}} = \gamma \; p^{o} \qquad (3.2\text{-}24)$$

Substituting this value of $\gamma \; p^{o}$ into equation (3.2-23), gives the Henry's constant in terms of the vapor pressure and water solubility:

$$H = \frac{p^o}{x^s} \qquad (3.2\text{-}25)$$

This can be put into a form to give the Henry's constant from the water solubility, C_ℓ^s, in mg/L (Neeley, 1980; Thibodeaux, 1979):

$$H = 16.04 \frac{p^o M}{TC_\ell^s} \qquad (3.2\text{-}26)$$

p^o is in mmHg, T is in degrees Kelvin, and M is the molecular weight. When using this method to calculate the Henry's constant, the equilibrium vapor pressure and the solubility must be for the same state (Mackay et al., 1979). If the solubility of the solid in water is used, the vapor pressure of the solid at that temperature must also be used. Often extrapolation through the critical point is necessary.

Table 3-1 summarizes the expressions of the Henry's constant and the conversion from one form to another. Since the symbols often vary depending on the application and the authors, it is important to be sure the correct form of the Henry's constant along with the correct units are being used. In keeping with the standard terminology used for flux calculations in the literature and in Chapter 2, the Henry's constant will be referred to as H, regardless of the actual form used.

3.3 Temperature Dependence of the Henry's Constant

The temperature dependence of the Henry's constant can be explained thermodynamically by examining the temperature dependence of the chemical potential for each phase. The chemical potentials for the solution and gas phases in their ideal form are given by:

$$\mu^{solu} = \mu^* + RT\ln X \tag{3.3-1}$$

$$\mu^{vap} = \mu^o + RT\ln p \tag{3.3-2}$$

These can be rewritten in the form:

$$\frac{\mu^{solu}}{T} = \frac{\mu^*}{T} + R\ln X \tag{3.3-3}$$

$$\frac{\mu^{vap}}{T} = \frac{\mu^o}{T} + R\ln p \tag{3.3-4}$$

Equilibrium is described by equating the chemical potentials for the two phases divided by the temperature of that phase.

$$\frac{\mu^{solu}}{T} = \frac{\mu^{vap}}{T} \tag{3.3-5}$$

Any change in the chemical potential in one phase must be compensated by a comparable change in the chemical potential of the other phase. This can be expressed as the differential of equation (3.3-5) (Denbigh, 1971):

$$d\left(\frac{\mu^{solu}}{T}\right) = d\left(\frac{\mu^{vap}}{T}\right) \tag{3.3-6}$$

For ideal gas behavior μ^{vap} is a function of temperature and pressure, while for the ideal solution μ^{solu} is a function of temperature, pressure, and composition. Consequently, equation (3.3-5) can be expressed in its functional form:

$$\frac{\mu^{solu}}{T} = f(P,T,X)$$

$$\frac{\mu^{vap}}{T} = f(T,p) \qquad (3.3\text{-}7)$$

The differential in equation (3.3-6) can be expanded in terms of the variables described above:

$$\frac{d\mu^{solu}}{dT} = \frac{\partial}{\partial T}\left(\frac{\mu^{solu}}{T}\right) dT + \frac{\partial}{\partial p}\left(\frac{\mu^{solu}}{T}\right) dp + \frac{\partial}{\partial X}\left(\frac{\mu^{solu}}{T}\right) dX \qquad (3.3\text{-}8)$$

$$\frac{d\mu^{vap}}{dT} = \frac{\partial}{\partial T}\left(\frac{\mu^{vap}}{T}\right) dT + \frac{\partial}{\partial p}\left(\frac{\mu^{vap}}{T}\right) dp$$

Substituting (3.3-8) into (3.3-6):

$$\frac{\partial}{\partial T}\left(\frac{\mu^{solu}}{T}\right)_{P,X} dT + \frac{1}{T}\left(\frac{\partial \mu^{solu}}{\partial P}\right)_{T,X} dp + \frac{1}{T}\left(\frac{\partial \mu^{solu}}{\partial X}\right)_{T,P} dX$$

$$= \frac{\partial}{\partial T}\left(\frac{\mu^{vap}}{T}\right)_{P} dT + \frac{1}{T}\left(\frac{\partial \mu^{vap}}{\partial P}\right)_{T} \qquad (3.3\text{-}9)$$

This equation can be simplified by substituting the definitions of the change in chemical potential with temperature at constant pressure and the change in chemical potential with pressure at constant temperature (Denbigh, 1971; Lewis and Randall, 1961):

$$\left(\frac{\partial \mu^{solu}/T}{\partial T}\right)_{P,X} = -\frac{H^{vap}}{T^2} \qquad \left(\frac{\partial \mu^{vap}/T}{\partial T}\right)_{P} = -\frac{H^{solu}}{T^2} \qquad (3.3\text{-}10)$$

and

$$V^{vap} = \left(\frac{\partial \mu^{vap}}{\partial p}\right)_T \qquad \left(\frac{\partial \mu^{solu}}{\partial p}\right)_{T,X} = V^{solu}$$

$$\left(\frac{\partial \mu^{solu}}{\partial X}\right)_{T.P} = \frac{RT}{X} \tag{3.3-11}$$

Equation (3.3-7) becomes:

$$-\left(\frac{H^{solu}}{T^2}\right) dT + \frac{V}{T}\, dp + \frac{R}{X}\, dX = -\left(\frac{H^{vap}}{T^2}\right) dT + \frac{R}{p}\, dp \tag{3.3-12}$$

H^{solu} is the partial molar enthalpy in solution, V is the partial molar volume, H^{vap} is the enthalpy per mole in the vapor phase. Equation (3.3-12) can be rearranged:

$$d \ln \frac{p}{X} = \frac{H^{vap} - H^{solu}}{RT^2}\, dT + \frac{V}{RT}\, dp \tag{3.3-13}$$

From equation (3.2-1), p/X can be set equal to the Henry's constant H. $H^{vap} - H^{solu}$ is the enthalpy of vaporization, ΔH^{vap}. The second term drops out at constant pressure. The resulting equation is known as the van't Hoff equation (Lewis and Randall, 1961):

$$\frac{d}{dT} \ln H = \frac{\Delta H^{vap}}{RT} \tag{3.3-14}$$

The integrated form of the equation can be used to determine the temperature dependence of H.

$$\ln H = \frac{\Delta H^{vap}}{RT} + \text{Constant} = A_1 + A_2\left(\frac{1}{T}\right) \tag{3.3-15}$$

Equation (3.3-15) can be used as a first approximation for relating H to T, but a better fit can be obtained by using the dependence of ΔH^{vap} on the temperature as described by the Kirchoff equation (Lewis and Randall, 1961; Weiss, 1970):

$$\frac{d\Delta H}{dt} = \Delta Cp \tag{3.3-16}$$

where ΔCp is the difference in the heat capacity of the gas between two temperatures and ΔCp can be written as a power series in temperature:

$$\Delta Cp = a + bT + cT^2 \tag{3.3-17}$$

From equation (3.3-17):

$$\Delta H = \Delta H^{o} + \int \Delta Cp dT \tag{3.3-18}$$

where ΔH^{o} is a constant. Therefore, substituting equation (3.3-18) into (3.3-14) and integrating gives:

$$\ln H = A_1 + A_2\left(\frac{1}{T}\right) + A_3 \ln T + A_4 T + A_5(T^2) \tag{3.3-19}$$

This equation has been used by several authors (Weiss, 1970; Glew and Moelwyn-Hughes, 1953; Morrison, 1954; Douglas, 1967). In actual use the coefficients A_i ($i = 1, \ldots, 5$) of equation (3.3-19) are determined by an empirical least squares fit of the data. Application of

such a procedure has shown that it is generally unnecessary to include A_4 and A_5 (Weiss, 1970). The simplified equation (3.3-19) being:

$$\text{Ln } H = A_1 + A_2 \left(\frac{1}{T}\right) + A_3 \text{ lnT} \qquad (3.3\text{-}20)$$

is sufficient for most environmental applications. Other specialized equations have been proposed (Benson and Krause, 1976) but do not improve the results. Not only are most environmental data described well by equation (3.3-20), but it is also derivable from theory as shown above.

In Chapter 9 equation (3.3-20) is used to calculate the temperature dependence of some recently obtained data on the solubility of carbonyl sulfide, OCS, in seawater.

3.4 Literature Values of the Henry's Constant

Table 3-2 is a list of Henry's constant values extracted from the literature. All values have been recalculated into the units of H as defined in equation (3.2-14) so that they can be used in equation (2.2-9) for calculation of ocean-atmosphere flux of chemicals. The results of several workers are shown for comparison to give some idea of the uncertainties involved.

The variation of the Henry's constant with temperature is shown when the data are available. When data are available for only a limited number of points, then actual data points are indicated by a (+) and a temperature dependence is calculated by either equation (3.3-15) or equation (3.3-20). Data for both distilled water and seawater are

TABLE 3-2

Henry's Constants (H)

COMPOUND	S o/oo	TEMPERATURE, °C 0	5	10	15	20	25	30	35	40	REFERENCE
OCS	D			1.16	1.40	1.66	1.95	2.24			Seidell (1940) Winkler (1903)
OCS	S			1.4*	1.7*	2.0*	2.3*	2.7*			
OCS	S	1.0†	1.2†	1.5	1.9	2.3	2.7	3.2†			Rasmussen et al. (1982c)(Chapter 9)
CH_3I	D	0.072*	0.091*	0.11	0.14*	0.17*	0.21	0.26*	0.31*	0.38*	Hunter-Smith et al. (1982)
	S	0.086*	0.011*	0.13	0.17	0.20	0.25	0.31*	0.37*	0.46*	
CH_3I	D	0.075	0.097	0.127	0.160	0.198	0.238	0.278			Glew & Moelwyn-Hughes (1953)
CH_3I	S	0.09*	0.12*	0.15*	0.19*	0.24*	0.29*	0.33*			
CH_3I	D							0.25		0.35	Swain & Thornton (1961) (2)
CH_3I	S							0.30*		0.42*	
$CHCl_3$	D						0.16				Calculated from data of McGovern

Salinity
S ≡ seawater; D ≡ distilled water

TABLE 3-2 (continued)

COMPOUND	S o/oo	TEMPERATURE, °C 0	5	10	15	20	25	30	35	40	REFERENCE
$CHCl_3$	S						0.19				Calculated from Data of McGovern
$CHCl_3$	D					0.11[a]	0.13[b]				McConnell (1975) (a); Dilling (1977) (b)
$CHCl_3$	S					0.13*	0.16*				
$CHCl_3$	D	0.065*	0.082*	0.10*	0.13*	0.16	0.20	0.24*	0.30*	0.36*	Hunter-Smith et al. (1982)
$CHCl_3$	S	0.078*	0.098*	0.12	0.16	0.19	0.24	0.29*	0.36*	0.43*	
F-11	D	1.8*	2.0	2.4	2.8	3.2	3.6	4.1	4.7*		Hunter-Smith et al. (1982)
F-11	S	2.2*	2.6	3.1	3.6	4.3	5.0	5.7	6.6*		
F-11	D	2.8		4.3		6.6					Data from Zeninger (Junge, 1976)
F-11	S		5.6			11				20	
F-12	D		11.9	14.3		20.0					Data from Zeninger (Junge, 1976)
F-12	S	20.8		23.3		25.0				29.4	
F-12	S		5.6			11				20	Data from Zeninger (Junge, 1976)

TABLE 3-2 (continued)

COMPOUND	S o/oo	TEMPERATURE, °C 0	5	10	15	20	25	30	35	40	REFERENCE
N_2O	D	0.752	0.903	1.07	1.29	1.44	1.70	1.86	2.12		Weiss & Price (1979)
N_2O	35	0.93	1.11	1.30	1.56	1.73	2.02	2.21	2.52		
N_2O	35	0.71	1.10	1.27	1.47	1.72	1.78	1.82			Seiler & Schmitt
N_2O	35	0.766					1.65			2.26	Markham & Kobe (1941)
CH_3CCl_3	D					1.41[a]	1.2[b]				McConnell (1975)(a) Dilling (1974)(b)
CH_3CCl_3	S					1.7[a*]	1.4[b*]				
CH_3CCl_3	D	0.22*	0.26	0.32	0.38	0.45	0.53	0.62	0.73*		Hunter-Smith et al. (1982)
CH_3CCl_3	S	0.28*	0.36	0.47	0.60	0.75	0.94	1.2	1.4*		
CH_3Cl	D		0.189	0.241	0.284	0.335	0.386				Glew & Moelwyn-Hughes (1953)
CH_3Cl	S		0.23*	0.29*	0.34*	0.40*	0.46*				
SF_6	D	68.0			131.6		181.8				Friedman (1954)
SF_6	S	82*			158*		218*				

TABLE 3-2 (continued)

COMPOUND	S o/oo	TEMPERATURE, °C 0	5	10	15	20	25	30	35	40	REFERENCE
$Cl_2C=CClH$ (TCE)	D					0.36[a]	0.49[b]				McConnell (1975) (a); Dilling (1977) (b)
Cl_2C-CCl_2 (PCE)	D					0.82[a]	0.49[b]				McConnell (1975 (a); Dilling (1977) (b)
CCl_4	D						0.87				Dilling (1977)
	S						1.0*				
CCl_4	D	0.40*	0.48	0.58	0.60	0.83	0.98	1.15	1.34*		Hunter-Smith et al. (1982)
CCl_4	S	0.57*	0.58	0.87	1.05	1.3	1.5	1.8	2.2*		

* extrapolated values using: $\ln H = A_1 + A_2 \frac{1}{T}$

* taken as 1.2 times distilled water values

† extrapolated values using: $\ln H = A_1 + A_2 \frac{1}{T} + A_3 \ln(T)$

shown. The variation of H with salinity is not shown since over the range normally found this effect is only 1-2%. Where data are not available for seawater, it was estimated as being approximately 20% higher than distilled water values. This is a reasonable approximation which can be verified by comparing seawater and distilled water values where both have been measured.

3.5 Determination of the Mass Transfer Coefficients

In Chapter 2 it was shown that the rate of exchange of a gas between the atmosphere and the ocean is proportional to the transfer coefficient, K. In the case of the two-film model, K is made up of contributions from k_g, the transfer coefficient for the gas phase, and k_ℓ, the transfer coefficient for the liquid phase. This relationship is given by equation (2.2-8). It does not matter whether K_g or K_ℓ (to be jointly referred to as K) is calculated, but the appropriate form of the flux equation (2.2-9) must be used. The advantage of using K_ℓ is that for most gases k_g is large, so $K_\ell = k_\ell$ and does not require the use of the Henry's constant, H, as the calculation of K_g does ($K_g = k_\ell/H$).

Because the value of K is made up of contributions from many terms, which cannot be easily evaluated (stagnant film thickness, organic surface film resistance, wind, bubbles, etc.), K cannot be measured under controlled laboratory conditions and applied to field measurements as H was. To get an accurate estimate of K, measurements should be made at the actual sampling location under prevailing

conditions. This is usually done by using a trace gas such as $^{14}CO_2$, H_2O, or radon. These values of K can be adjusted for the diffusivity of the gas being studied. Since there are different theories on how this adjustment should be made (i.e., two-film theory or stagnant film theory), the best results are obtained for gases which have molar volumes similar to the tracer. The measurement of K each time a sample is collected for a flux calculation is a difficult and expensive task, so, as a compromise, the value of K has been measured at many sites in the ocean and the data averaged to get a value of K for average ocean conditions. By looking at the variability in K, the uncertainty in using this procedure can be estimated.

The measurement of the gas phase mass transfer coefficient, k_g, is not as difficult as it is for the liquid phase. Estimates of k_g have been made by studying the evaporation of water (Liss and Slater, 1974; Liss, 1973; Schooley, 1961). For the case of evaporation of a pure liquid, the liquid phase resistance will be negligible, so:

$$\frac{1}{K_g} = \frac{1}{Hk_g}$$

With the appropriate value for the Henry's constant, H, (see section 3), k_g can be calculated from measured evaporation rates.

Using the data obtained from Schooley, Liss calculated $k_g(H_2O)$ to be equal to 3,000 cm/hr. k_g for other gases can be calculated by correcting for the different diffusion rates. Since this value is usually much larger than k_ℓ, it is not necessary to use k_g in the calculation of the overall transfer coefficient, K.

Early measurements of k_ℓ were made using the natural distribution of $^{14}CO_2$ before bomb testing in 1954 (Craig, 1957; Revelle and Suess, 1957; Broecker, 1963). Atmospheric $^{14}CO_2$ is produced by the interaction of $^{12}CO_2$ and cosmic rays, and is exchanged with the ocean where it decays. By assuming the $^{14}C/^{12}C$ ratio in the atmosphere and the ocean has remained constant over the last 2000 years, a steady state will be reached between the ocean and the atmosphere (Craig, 1957). Thus, the flux of $^{14}CO_2$ into the ocean must equal the amount lost by radioactive decay. This can be represented by the mass balance equation (Broecker and Peng, 1974):

$$A \frac{D}{\delta} \left[\frac{C_{mix} \times H_{^{12}CO_2}}{H_{^{14}CO_2}} \left(\frac{^{14}C}{^{12}C} \right)_{atm} - C_{mix} \left(\frac{^{14}C}{^{12}C} \right)_{mix} \right]$$

$$= V \left[\Sigma C_{ocean} \left(\frac{^{14}C}{^{12}C} \right)_{ocean} \right] \lambda \qquad (3.5\text{-}1)$$

A is the ocean surface area, V is the volume, and λ is the radioactive decay constant for ^{14}C $(1/8250\ yr^{-1})$. $H_{^{12}CO_2}/H_{^{14}CO_2}$ is the ratio of the Henry's constants for the CO_2 isotopes, which is equal to 0.96. $\left(\frac{^{14}C}{^{12}C} \right)_i$ is the isotope ratio for the ith layer, and C_i is the concentration of CO_2. The equation can be solved for D/δ, which is equal to the transfer coefficient, K_ℓ. By assuming that k_g is negligible, K_ℓ will be equal to k_ℓ. Table 3-3 summarizes the values of K_ℓ and δ_ℓ found using the natural $^{14}CO_2$ distribution.

TABLE 3-3

Field Measurements of Liquid Mass Transfer Coefficients

A. Transfer coefficient measured using pre-bomb $^{14}CO_2$

K_1 (CO_2) cm/hr	δ (microns)	Reference
17-44	13-33	Craig (1957)
25	23	Revelle and Suess (1957)
23	25	Broecker (1963)
9-33	33-67	Craig (1963)
$\bar{K}_1$ = 19 cm/hr	$\bar{\delta}$ = 30 microns	

B. Transfer coefficient measuring using bomb testing $^{14}CO_2$

K_1 (CO_2) cm/hr	δ (microns)	Reference
29-44	13-20	Young and Fairhall (1968)
17-34	17-33	Nydal (1968)
$\bar{K}_1$ = 21 cm/hr	$\bar{\delta}$ = 27 microns	

C. Transfer coefficients measured from radon profiles

† K_1 (CO_2) cm/hr	δ (microns)	Reference
16	47±29 (n = 110)	Peng et al. (1979)
12.2	63±30 (n = 31)	Broecker and Peng (1974)
39	20± 4 (n = 12)	Peng et al. (1974)
K_1 = 16* cm/hr	$\bar{\delta}$ = 48 microns	

* weighted average

† converted to CO_2 base using equation (3.6-1)

The measurement of the $^{14}C/^{12}C$ ratios produced as a result of nuclear bomb testing can also be used to determine k_ℓ. Essentially the same procedure that was described above can be used except samples were taken after 1954. The values for k_ℓ and δ_ℓ determined by various authors are shown in Table 3-3. One difficulty with this method is the potential for errors due to the horizontal transport of material in the oceans (Broecker and Peng, 1974).

Another method for determining k_ℓ that is independent of $^{14}CO_2$ is the distribution of radon gas in the ocean (Broecker and Peng, 1974; Peng et al., 1974; Peng et al., 1979). Dissolved radium (^{226}Ra) is uniformly distributed in the ocean and undergoes radioactive decay along the following pathway:

$$^{226}Ra \rightarrow {}^{222}Rn + \alpha \qquad \lambda = 3.85 \text{ days}$$

If there were no fluxes of radon gas across the air-ocean interface, then the concentration of radon would be in equilibrium with the radium and there would be a uniform concentration in the ocean. Since a concentration gradient exists between the mixed layer of the ocean and the deep, this information can be used to calculate the film thickness using a one-box model.

The conservation of mass equation can be written for the box of interest, which is the mixed layer of the ocean:

$$\frac{dC}{dt} = \lambda \left(C_E - C_z \right) - \frac{k_\ell}{h} \left(C_\ell - \frac{C_g}{H} \right) \qquad (3.5\text{-}2)$$

C_E is the radium concentration in equilibrium with dissolved radon, determined from deep ocean concentrations of radon or by direct measurement of radium. C_z is the radon concentration at depth z, C_ℓ is the mixed layer concentration, and C_g is the atmospheric concentration. C_z is usually taken to be uniform in the mixed layer, h, so it is equal to C_ℓ. Assuming the system is at steady state (dC/dt = 0), equation (3.5-2) can be solved for K_ℓ or δ_ℓ.

$$K_\ell = \frac{h\lambda \ (C_E - C_\ell)}{(C_\ell - C_g/H)}$$

$$\delta_\ell = D/k_\ell$$

Radon concentration profiles were obtained by Broecker (Broecker and Peng, 1974; Peng et al., 1974; Peng et al., 1979) at many locations around the world during the GEOSECS program. Measurements were made in the Atlantic and Pacific Oceans in both the northern and southern hemispheres. The film thickness, δ_ℓ, was found to vary between 20 microns and 120 microns, with an average of 47 microns (Peng et al., 1979). The variability is thought to be caused by different wind speeds, but plots of film thickness against wind speed showed poor correlation. Values for K_ℓ and δ_ℓ for the radon measurements are shown in Table 3-3 for comparison with the CO_2 data.

In the review paper on air-sea exchange by Liss and Slater (1974), all of the available data (except Peng et al., 1979) were averaged to get a value of K_ℓ (or k_ℓ) for CO_2 of 20 cm/hr. Since then Peng et al. (1979) have reported an additional 110 stations in the Atlantic, Pacific, and Antarctic Oceans with an average value for k_ℓ of 12 cm/hr (Rn). Considering the uncertainty, there is no significant difference ($\alpha = 0.1$) between these two numbers, but due to the large number of locations sampled, the value of 12 cm/hr (Rn) will be used as an average value of K_ℓ under average ocean conditions.

3.6 Dependence of K on Diffusion Coefficient and Wind Speed

The values for k_g obtained from the CO_2 and the radon measurements and for k_ℓ from the water evaporation experiments can be used to calculate an approximate value of k_g and k_ℓ for other gases by correcting for the differences in the rate of diffusion of the gases. By combining equation (3.2-3) for two gases, the transfer coefficient of one gas can be calculated from the second using the two-film approach.

$$k_2 = k_1 \left(\frac{D_2}{D_1} \right) \tag{3.6-1}$$

For surface renewal and penetration theory the correction is calculated using equations (3.3-5) and (3.3-7):

$$k_2 = k_1 \left(\frac{D_2}{D_1} \right)^{1/2} \tag{3.6-2}$$

In the case of liquid transfer coefficients, k_ℓ, equation (3.6-2) seemed to give the best approximation to available laboratory experimental results (Danckwerts, 1970). Recently a paper by Torgerson et al. (1982) compared the transfer coefficients, k_ℓ, for ^{3}He and ^{222}Rn in a small lake and concluded that equation (3.6-1) provided the best representation of the data. At this time there is no firm evidence to select one approach over the other.

To use either equation (3.6-1) or equation (3.6-2) the diffusion coefficients for the gases must be determined. For many gases the diffusion coefficients in air and water have been measured experimentally. For other gases the diffusion coefficients in water have been calculated using empirical equations.

The calculation of the gas phase diffusion coefficients used to determine k_g can be made by applying Graham's law:

$$\frac{D_{1g}}{D_{2g}} = \left(\frac{M_2}{M_1} \right)^{\frac{1}{2}} \qquad (3.6\text{-}3)$$

The diffusion coefficients in the liquid phase are more difficult to determine since there is no simple theory for their calculation. Several empirical methods for calculating liquid diffusion coefficients have been reviewed by Reid and Sherwood (1966). One recommended method, often used, was proposed by Wilke and Chang (1955).

$$D_\ell = 7.4 \times 10^{-8} \frac{T \, (\alpha M_{H_2O})^{\frac{1}{2}}}{\nu_2 \, V^{0.6}} \qquad (3.6\text{-}4)$$

M_{H_2O} is the molecular weight of water, T is the absolute temperature, α is an association factor (α = 2.6 for water), ν is the viscosity, and V is the molecular volume of the solute at its normal boiling point (cm^3/mole). When this equation is used for the comparison of two gases, all of the constant terms cancel. The resulting ratio is:

$$\frac{D_{\ell 1}}{D_{\ell 2}} = \left(\frac{V_2}{V_1} \right)^{0.6} \qquad (3.6\text{-}5)$$

A listing of molar volumes of some gases is given in Appendix B. Often the molar volume relationship is approximated by the molecular weight ratio shown below (Liss and Slater, 1974); however, there is no theoretical or experimental basis for using this equation in the liquid phase.

$$\frac{D_{\ell 1}}{D_{\ell 2}} = \left(\frac{M_2}{M_1} \right)^{\frac{1}{2}} \qquad (3.6\text{-}6)$$

Table 3-4 lists the transfer coefficients, k_ℓ, for selected gases from the radon value of 12 cm/hr, and adjusted for diffusion rates using equations (3.6-1) and (3.6-2). Table 3-5 gives the values of k calculated from the average CO_2 value for k_ℓ of 20 cm/hr. These values can be compared with those reported by Liss and Slater (1974), listed in Table 3-5 or calculated using their methodology (equation (3.6-6))

TABLE 3-4

Transfer Coefficients Calculated from Radon Measurements

@ 20°C and average global windspeed, 15 knots

Compound	M	V_l * cm³/mole	D_l cm²/sec	$\frac{D_l}{D_{Rn}}$	$k_\ell = k_{Rn}\left(\frac{D_l}{D_{Rn}}\right)$	$k_\ell = k_{Rn}\left(\frac{D_l}{D_{Rn}}\right)^{1/2}$	$\left(\frac{M_{Rn}}{M_l}\right)^{1/2}$	$k_\ell = k_{Rn}\left(\frac{M_{Rn}}{M_l}\right)^{1/2}$
CO_2	44	34.0 +	1.64×10^{-5}	1.37	16	16	2.24	27
OCS	60	51.5 +	1.24×10^{-5}	1.03	12	14	1.92	23
CH_3I	142	62.9	1.13×10^{-5}	0.94	11	13	1.25	15
$CHCl_3$	121	82.8	0.96×10^{-5}	0.80	9	12	1.35	16
CH_3Cl	51	47.5	1.34×10^{-5}	1.12	13	15	2.09	25
CH_3CCl_3	134	115	0.72×10^{-5}	0.60	7	11	1.29	15
$(CH_3)_2S$	62	77.4	1.00×10^{-5}	0.83	10	13	1.89	23
CCl_4	154	101.2	0.85×10^{-5}	0.71	8	12	1.20	14
N_2O	46	36.4 +	1.57×10^{-5}	1.31	15	16	1.20	14
F-11	138	110	0.81×10^{-5}	0.68	8	11	1.27	15
F-12	121	108	0.82×10^{-5}	0.68	8	11	1.35	16
TCE	132	107	0.82×10^{-5}	0.68	8	11	1.30	16
PCE	166	128	0.74×10^{-5}	0.62	7	11	1.16	14
					cm/hr	cm/hr		cm/hr

$$D_l = D_{Rn}\left(\frac{V_{Rn}}{V_l}\right)^{0.6}$$

$D_{Rn} = 1.2 \times 10^{-5}$ cm/hr @ 20°C (Broecker and Peng, 1974)

* Estimated from atomic volumes

\+ Measured

TABLE 3-5

Transfer Coefficients Calculated from $^{14}CO_2$ Measurements

@ 20°C and average global windspeed, 15 knots

Compound	M	V_I * cm^3/mole	D_I cm^2/sec	$\frac{D_I}{D_{CO_2}}$	$k_\ell = k_{CO_2}\left(\frac{D_I}{D_{CO_2}}\right)$	$k_\ell = k_{CO_2}\left(\frac{D_I}{D_{CO_2}}\right)^{1/2}$	$\left(\frac{M_{CO_2}}{M_I}\right)^{1/2}$	$k_\ell = k_{CO_2}\left(\frac{M_{CO_2}}{M_I}\right)^{1/2}$
CO_2	44	34.0 †	1.64×10^{-5}	1	20	20	1	20
OCS	60	51.5 †	1.24×10^{-5}	0.76	15	17	0.86	17
CH_3I	142	62.9	1.13×10^{-5}	0.69	13	17	0.56	11
$CHCl_3$	171	82.8	0.96×10^{-5}	0.59	12	15	0.60	12
CH_3Cl	51	47.5	1.34×10^{-5}	0.82	16	18	0.93	19
CH_3CCl_3	134	115	0.72×10^{-5}	0.43	9	13	0.57	11
$(CH_3)_2S$	62	77.4	1.00×10^{-5}	0.61	12	16	0.84	17
CCl_4	154	101.2	0.85×10^{-5}	0.52	10	14	0.53	11
N_2O	46	36.4 †	1.57×10^{-5}	0.96	19	20	0.98	20
F-11	138	110	0.81×10^{-5}	0.49	10	14	0.56	11
F-12	121	108	0.82×10^{-5}	0.50	10	14	0.60	12
TCE	132	107	0.82×10^{-5}	0.50	10	14	0.58	12
PCE	166	128	0.74×10^{-5}	0.45	9	13	0.51	10
					cm/hr	cm/hr		cm/hr

$D_I = D_{CO_2}\left(\frac{V_{CO_2}}{V_I}\right)^{0.6}$

$D_{CO_2} = 1.64 \times 10^{-5}$ cm/hr @20°C (Broecker and Peng, 1974)

* Estimated from atomic volumes

† Measured

At the beginning of this section, the transfer coefficient, K, was shown to be a function of the diffusion coefficient of the gas. Laboratory experiments in wind tunnels have shown that K is also dependent on the windspeed over the water surface (Kanwisher, 1963; Broecker et al., 1978; Liss, 1973). For this reason it has been postulated that the value of K used in ocean-atmosphere exchange calculations may also be dependent on the average ocean windspeed (Broecker and Peng, 1974; Liss and Slater, 1974).

Wind tunnel experiments on the exchange of O_2 and CO_2 (Kanwisher, 1963; Hoover and Berkshire, 1969; Liss, 1963) were interpreted to mean the liquid transfer coefficient, K_ℓ, was proportional to the square of the wind speed. This relationship was soon adopted and used for ocean data also. Two problems arise with relating K_ℓ to v^2. First, there is no rationale based on mass transport theory for this model (Deacon, 1977; Cohen et al., 1978; Wu, 1969), and, second, actual field data for K_ℓ do not appear to have any correlation with the wind speed (Peng et al., 1979; Hasse and Liss, 1980). For these reasons the effects of wind speed on the oceanic values of K_ℓ are still being evaluated.

Cohen et al. (1978) presented a more rigorous approach by relating K_ℓ to the friction velocity, U^*, effective roughness height, Z_o, and the air kinematic viscosity, ν_a. These variables can be combined to describe a unitless Reynolds roughness number, R_e^* (Wu, 1969).

$$R_e^* = \frac{Z_o U^*}{\nu_a} \qquad (3.6\text{-}6)$$

They were able to get good correlation between K_ℓ and R_e^* for wind tunnel data, but found that the correlation was also dependent on the mixing speed in the bulk water phase. This suggests that the actual amount of water mixing due to currents or waves at a particular location may have an effect on K_ℓ. This would explain why laboratory data correlate well with wind speed while field data do not.

Wu (1969) suggested that the wind stress on the ocean could be divided into three regimes, which may also be applicable to the measurement of K_ℓ (Cohen et al., 1978). The first is for wind speeds between 0 and 3 m/sec, where the flow is aerodynamically smooth and the wind stress is low. The value of K_ℓ in this region is approximately constant and does not vary with wind speed. This is consistent with the wind tunnel data that show little change in K_ℓ with wind speeds below 3 m/sec. The second region is between 3 m/sec and 15 m/sec, where the wind stress coefficient and surface roughness increase with velocity. This region is characterized by an almost linear increase in K_ℓ with wind speed as related by equation (3.3-6). The third region is wind speed above 15 m/sec, where the wind stress coefficient becomes constant and does not change with wind speed. Since there are no wind tunnel data at these values, it is difficult to say what happens in this region, but considering that the field radon measurements do not show significantly higher values for K_ℓ at wind speeds greater than 15 m/sec (Peng et al., 1979), the value of K_ℓ may also level off.

This type of approach would seem to explain the data of Peng et al. (1979) which are highly variable and do not correlate with wind speed. At low wind velocities (≤ 3 m/sec) most of the values of K_ℓ are low; at wind speeds above 3 m/sec the values are highly variable and may result from a combination of wind speed and ocean mixing (for which there is no good measurement). It is hard to deduce any relationship above 15 m/sec since only a few data points are available. Most disturbing is the lack of correlation in the $3 \rightarrow 15$ m/sec range. One reason for this may be that the measured radon profiles really represent conditions that existed several days before the actual measurements took place (half-life of radon is 3.8 days). However, preliminary data using a continuous measurement process to scan the radon-deficient layer every two hours (Roether and Kramer, 1978) and provide resolution of transient effects (i.e., wind velocity changes) also show no relationship between the transfer coefficient and wind velocity (Hasse and Liss, 1980). At the moment the problem remains unresolved.

The current consensus is that there is no firm relationship between K_ℓ and wind speed, and the best procedure for determining K_ℓ is to average the radon data by Peng et al. (1979) or use the average of the $^{14}CO_2$ measurements to get an average value of K_ℓ over the whole ocean (Hasse and Liss, 1980). Meanwhile, more experiments are needed to establish the relationship between wind speed, ocean mixing, and K_ℓ.

CHAPTER 4

ANALYSIS OF UNCERTAINTY IN THE TWO-FILM FLUX MODEL

4.1 Introduction

The two-film model or some version of it has been used for nearly all calculations of the flux of trace gases to or from the ocean. The origin of the model and the methods used to measure K and H were described in Chapters 2 and 3, along with the factors which affect K (wind speed, bubble formation, etc.). While this model has been widely applied to oceanographic measurements, there has been no work to quantitatively evaluate the uncertainties involved in using the model. By doing a propagation of error analysis on the model for various gases, the parameters contributing the most uncertainty to the final result can be identified. This can provide information to design more efficient air-sea exchange experiments.

To estimate the uncertainties associated with calculating a total oceanic flux using the two-film model one can ask three basic questions: 1) Does the two-film model really describe what happens at the ocean-air interface? 2) What are the major uncertainties in using the two-film model for a particular gas? 3) Based on a limited number of samples, how well does the calculated flux represent the whole ocean? For questions 1) and 3) quantitative answers are hard to find, but the qualitative aspects of these questions were discussed in Chapter 2. The answer to question 2) can be formulated

in a quantitative manner, using a propagation of error procedure on the flux equation. This chapter describes this procedure for the two-film model with one sample and this same model with multiple samples at one location. The results will then be used to determine what factors contribute most to the total uncertainty for specific gases.

4.2 Error Propagation Analysis of the Two-Film Model

For one sample collected at one location the flux of a gas across the air-ocean interface can be calculated using equation (2.2-9):

$$F = K_\ell \left(\frac{C_g}{H} - C_\ell \right) \tag{2.2-9}$$

From this equation the flux can be defined in terms of the four independent variables, K_ℓ, C_g, C_ℓ, and H. The uncertainty in determining F described by the standard deviation of F, σ_F, can then be written as:

$$\sigma_F^2 = \Sigma \left(\frac{\partial F}{\partial x_i} \right)^2 \sigma_{x_i}^2 \tag{4.2-1}$$

Substituting into this expression the partial derivatives of F with respect to each of the independent variables in equation (2.2-9) gives:

$$\sigma_F = \left[\left(\frac{C_g}{H} - C_\ell \right)^2 \sigma_{K_\ell}^2 + \left(\frac{K_\ell}{H} \right)^2 \sigma_{C_g}^2 + \left(\frac{K_\ell C_g}{H^2} \right)^2 \sigma_H^2 + K_\ell^2 \sigma_{C_\ell}^2 \right]^{1/2} \tag{4.2-2}$$

The relative error, σ_F/F, can be found by dividing (4.2-2) by F. The water saturation, S, can be defined as:

$$S = (1 - \beta) \tag{4.2-3}$$

where β is HC_ℓ/C_g. The relative error terms for the independent variables, σ_{x_i}/x_i, can be expressed as $\tilde{\sigma}_{x_i}$, so $\tilde{\sigma}_F$ can be written as:

$$\tilde{\sigma}_F = \left[\tilde{\sigma}_{K_\ell}{}^2 + \frac{1}{S^2} \tilde{\sigma}_{C_g}{}^2 + \frac{1}{S^2} \tilde{\sigma}_H{}^2 + \frac{(S+1)^2}{S^2} \tilde{\sigma}_{C_\ell}{}^2 \right]^{\frac{1}{2}} \tag{4.2-4}$$

where

$$\frac{1}{S^2} = B^2 \text{ and } \frac{(S+1)^2}{S^2} = C^2 \tag{4.2-5}$$

Equation (4.2-5) can be written in the form of an error equation where the contribution to the total relative error, ε_T, for each independent variable is given as ε_i:

$$\varepsilon_T = \left(\varepsilon_{K_\ell}{}^2 + \varepsilon_{C_g}{}^2 + \varepsilon_H{}^2 + \varepsilon_{C_\ell}{}^2 \right)^{\frac{1}{2}} \tag{4.2-6}$$

A plot of B and C versus the saturation, S, is shown in Figure 4.1, where B and C represent the multiplier terms for $\tilde{\sigma}_{C_g}{}^2$, $\tilde{\sigma}_H{}^2$, and $\tilde{\sigma}_{C_\ell}{}^2$. When B or C is greater than 1, it enhances the contribution to the relative error in the flux $\tilde{\sigma}_F$ for the associated terms. A value of S = 0 corresponds to equilibrium between the air and the seawater, while a value of S > 0 indicates the water concentration is above the equilibrium value. Since different gases have different saturation values, S, they will also have different values for the ε_i's. Consequently, the independent variables that contribute the most to ε_T may vary from gas to gas.

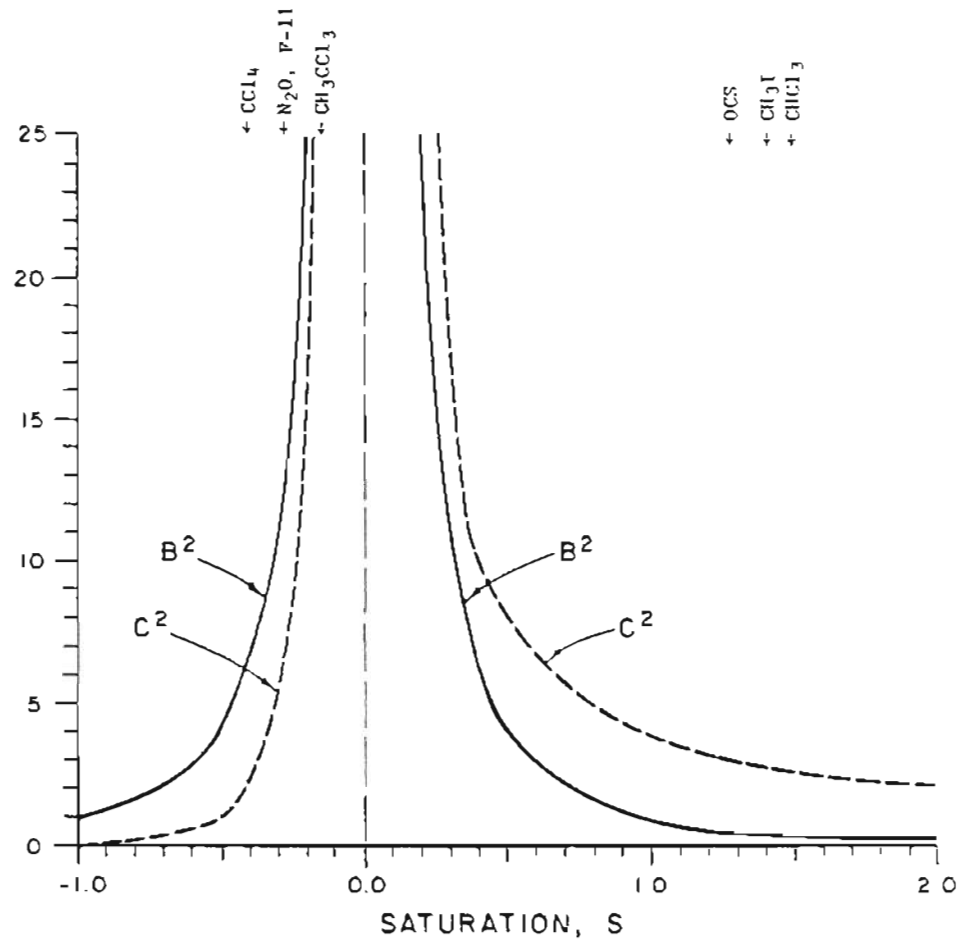

Figure 4.1. Uncertainty coefficients of equation (4.2-1) as a function of saturation, S. Saturation values of specific gases are shown at the top of the figure.

Figure 4.1 shows where the gases to be studied fall on the saturation curve. From this figure several interesting features of the flux model can be seen. First, for a flux from the air to the water, B^2 will always be larger than the multiplier for K_ℓ, and as equilibrium is approached, this difference becomes greater. The effect of this is that, for gases near equilibrium, ε_H will be greater than ε_{K_ℓ} and possibly be the major source of uncertainty in the total flux. Second, as equilibrium is approached, both B and C go to infinity, so it can never be established with a few measurements whether there is a flux into or out of the ocean. An example of this is methyl chloroform. Third, for a flux from the water to the air, B becomes small as the gas gets further from equilibrium, and the major uncertainties will be in the measurement of C_ℓ and K_ℓ. This is found to be true for CH_3I, OCS, and $CHCl_3$.

Equation (4.2-4) was derived assuming that only one sample was used for calculating the ocean-air flux. For most experiments samples will be collected from many sites, and it is important to see what effect multiple sample collection has on the flux uncertainty.

Consider the case of collecting a group of seawater samples and atmospheric samples at one sample site. It is not necessary to calculate the flux for each air and water sample since the atmospheric concentration should be uniform. The flux can be calculated by averaging the atmospheric C_g values and the ocean C_ℓ values. One value of H is used since the temperature should be constant at one location. The average flux is given by:

$$\bar{F} = K_\ell \left(\frac{\bar{C}_g}{H} + \bar{C}_\ell \right) \tag{4.2-7}$$

The error analysis can be done as before except there are more terms involved since $\bar{F}$ is a function of more variables:

$$\bar{F} = f(K_{1j}\ C_{g1},\ C_{g2}, \ldots C_{gnj}\ C_{\ell 1},\ C_{\ell 2}, \ldots C_{\ell nj}\ H) \tag{4.2-8}$$

Again, equation (4.2-2) can be used to calculate $\sigma_{\bar{F}}$.

The partial derivatives of F can be determined as before except the values for C_g and C_ℓ are replaced by their averages $\bar{C}_g$ and $\bar{C}_\ell$.

$$\frac{\partial \bar{F}}{\partial K_\ell} = \left(\frac{\bar{C}_g}{H} - \bar{C}_\ell \right) \qquad \frac{\partial \bar{F}}{\partial H} = \frac{K\bar{C}_g}{H^2}$$

$$\frac{\partial \bar{F}}{\partial C_{g_i}} = \frac{K_\ell}{H} \left(\frac{1}{n} \right) \qquad \frac{\partial \bar{F}}{\partial C_{\ell_i}} = K_\ell \left(\frac{1}{n} \right) \tag{4.2-9}$$

Substituting equations (4.2-9) into (4.2-1) and using the same procedure to go from equation (4.2-5) to (4.2-6), the expression for the relative error in the average flux $\tilde{\sigma}_{\bar{F}}$ is obtained.

$$\tilde{\sigma}_F = \left[\tilde{\sigma}_{K_\ell}^{\,2} + \frac{1}{\bar{S}^2} \tilde{\sigma}_H^{\,2} + \frac{1}{\bar{S}^2} \left(\frac{1}{n^2} \right) \left(\tilde{\sigma}_{C_{gi}}^{\,2} + \ldots \tilde{\sigma}_{C_{gn}}^{\,2} \right) + \frac{(\bar{S}+1)^2}{\bar{S}^2} \left(\frac{1}{n^2} \right) \left(\tilde{\sigma}_{C_{\ell i}}^{\,2} + \ldots \tilde{\sigma}_{C_{\ell n}}^{\,2} \right) \right]^{\frac{1}{2}} \tag{4.2-10}$$

where $\bar{S} = (1 - H\overline{C_\ell}/\overline{C_g})$.

Since $\sigma_{C_{\ell_1}} = \sigma_{C_{\ell_2}} = \sigma_{C_{\ell_n}}$ and $\sigma_{C_{g_1}} = \sigma_{C_{g_2}} = \sigma_{C_{G_n}}$, equation (4.2-8) can be simplified to:

$$\tilde{\sigma}_F = \left[\tilde{\sigma}_{K_\ell}^2 + \frac{1}{\bar{S}^2} \tilde{\sigma}_H^2 + \frac{1}{\bar{S}^2} \frac{\tilde{\sigma}_{C_g}^2}{n} + \frac{(\bar{S}+1)^2}{\bar{S}^2} \frac{\tilde{\sigma}_{C_\ell}^2}{n} \right]^{1/2} \qquad (4.2\text{-}11)$$

Comparing equation (4.2-11) with (4.2-4) shows that $\tilde{\sigma}_E$ will be smaller than $\tilde{\sigma}_F$ only if the major source of error is due to the measurement of C_ℓ or C_g, since the uncertainties in these terms are now divided by the number of measurements. The errors for C_ℓ and C_g become the standard errors of the mean. If $\tilde{\sigma}_F$ is limited by K_ℓ or H, collection of multiple samples at one location will not provide a better estimate of the flux from that location.

4.3 Conclusions

The equations developed in section 4.2 can be used to determine what the major sources of uncertainty are for the calculation of the flux of OCS and selected halocarbons. Table 4-1 is a list of these gases showing some average values for K_ℓ, H, C_g, and C_ℓ along with the estimated uncertainty for these quantities. The values of K_ℓ ($K_\ell = k_\ell$) were taken from Chapter 2. $\tilde{\sigma}_{K_\ell}$ was estimated based on the uncertainties in the values measured by Peng et al. (1979), and errors resulting in the calculation of k_ℓ from the corresponding k_ℓ value for $^{14}CO_2$ or radon. Gases with molar volumes considerably different from CO_2 would

TABLE 4-1

Average Values of Parameters for Two-Film Model and Their Associated Uncertainties

GAS	K_L	$\tilde{\sigma}_K$	H	$\tilde{\sigma}_H$	C_f (pptv)	$\tilde{\sigma}_C$	C_g (pptv)	$\tilde{\sigma}_{C_g}$	$\beta = \frac{HC_f}{C_g}$	$\beta^2 = \frac{1}{S^2}$	$G^2 = \frac{(S+1)^2}{S^2}$	$S = (\beta - 1)$
MeI	11	0.50	0.24	0.10	108	0.40	2	0.25	13	0.007	1.2	12
					49				6	0.04	1.4	5
OCS	12	0.50	2.0	0.15	1000	0.35	470	0.20	4.3	0.09	1.6	3.3
					500				2.1	0.8	4	1.1
CH_3CCl_3	7	0.50	1.7	0.30	108	0.15	154	0.03	1.2	25	36	- 0.2
$CHCl_3$	9	0.50	0.13	0.40	449	0.35	24	0.11	2.4	0.5	3	1.4
PCE	7	0.50	0.6	0.40	113	0.50	40	0.10	1.7	2	6	- 0.7
F-12	8	0.50	10	0.50	42	0.30	335	0.01	1.3	11	19	0.3
CCl_4	8	0.50	1.0	0.40	72	0.20	153	0.01	0.5	4	9	- 0.3
F-11	8	0.50	5.2	0.25	27	0.15	198	0.01	0.7	12	20	- 0.3

be expected to have larger values of $\tilde{\sigma}_{K_\ell}$. H was taken from the "best" available values in Table 3-3. $\tilde{\sigma}_H$ was estimated on the variation between literature values and how well H was known as a function of temperature and salinity. A larger $\tilde{\sigma}_H$ would result in extrapolations from distilled water to seawater when seawater values were not available.

The values of C_ℓ and C_g were taken from the measurements described in Chapter 10. Values from a particular productivity area were averaged to get $\bar{C}_\ell$, and σ_{C_ℓ} was set equal to the standard deviation of the pooled measurements. C_g was taken to be the average of all available air sample data, and σ_{C_g} was the standard deviation. More will be said about the data in Chapter 10, but these values provide a reasonable average for use in the uncertainty analysis procedure.

The data from Table 4-1 were substituted into equation (4.2-4), and the values of ε_T, ε_K, ε_{C_g} , ε_H, and ε_{C_ℓ} were calculated. The results are presented in Table 4-2. This table reports the relative errors as percentages, and shows the contributions to the total error from errors in K, H, C_ℓ , and C_g.

Table 4-2 shows that the total uncertainty, ε_T, is very high for those gases that have saturation values close to zero. These gases are primarily of anthropogenic origin, and have as the major source of uncertainty ε_H. For these gases the collection of multiple samples at one location would not provide a better estimate of the flux.

TABLE 4-2

Major Sources of Error for Average Concentrations

Compound		$\varepsilon_{T_{(\%)}}$	$\varepsilon_{K_{\ell}}^{2}{}_{(\%)}$	$\varepsilon_{C_g}^{2}{}_{(\%)}$	$\varepsilon_{H}^{2}{}_{(\%)}$	$\varepsilon_{C_{\ell}}^{2}{}_{(\%)}$
OCS	(M)	66	25	0.4	0.2	19
	(L)	84	25	3	1	42
CH_3I	(M)	67	25	0.04	0.01	19
	(L)	68	25	0.3	0.04	22
CH_3CCl_3		183	25	2	225	80
$CHCl_3$		82	25	0.6	8	35
PCE		145	25	2	32	150
F-12		220	25	0.1	280	170
CCl_4		115	25	0.04	64	40
F-11		120	25	0.1	75	45

Also, the Henry's constant for these gases is not well known, so $\tilde{\sigma}_H^2$ is also large. For gases produced in the ocean and for which the ocean is a source, the uncertainty is primarily in ε_{K_ℓ} and ε_{C_ℓ}. Improvement in the uncertainty of these gases could be made by collecting more samples, which, according to equation (4.2-11), would result in a reduction of ε_{C_ℓ}. This process would eventually be limited by ε_{K_ℓ}.

PART II

ANALYTICAL METHODOLOGY FOR TRACE GAS MEASUREMENTS IN SEAWATER AND AIR

CHAPTER 5

INSTRUMENTATION FOR MEASUREMENT OF OCS AND HALOCARBONS

5.1 Introduction

The trace gases studied in this project include carbonyl sulfide (OCS), methyl iodide (CH_3I), chloroform ($CHCl_3$), methyl chloroform (CH_3CCl_3), and other halogenated organics. In the atmosphere these gases are present at the parts per trillion by volume (pptv) level which requires sensitive instrumentation and specialized techniques to measure. For this task gas chromatography with an appropriate detector, a mass spectrometer (MS) for OCS and an electron capture detector (ECD) for the halogenated compounds, was chosen. To provide additional sensitivity a freezeout loop immersed in liquid oxygen was used to concentrate the sample from the air or headspace.

The OCS methodology will be described in detail since much of the procedure and evaluation has not appeared in the literature. Included is a discussion of the advantages of the MS detection method, the operating parameters, measurement precision, minimum detectable quantity, peak identification, potential sources of errors, and standardization procedures.

The temperature programmed GC-ECD methodology for the measurement of the halogenated compounds has been described in detail in the literature (Rasmussen et al., 1977; Rasmussen and Khalil, 1980). Only a brief review of this methodology is included.

5.2 OCS Measurement Techniques

OCS was first measured in the atmosphere by Hanst et al. (1975) using an infrared spectrometer. Since then several other researchers (Sandalls and Penkett, 1977; Farwell et al., 1979; Maroulis et al., 1977; Aneja et al., 1979) have published the results of other measurements using gas chromatographic (GC) methods. The most commonly used analytical system is a sample preconcentration loop, a packed column, and a flame photometric detector (FPD). The FPD has a detection limit in the low ppbv region, and with cryogenic preconcentration, ambient levels of 500 pptv can be measured. Maroulis (1977) used a GC/FPD to measure routine samples but used a Finnigan 4010 GC/MS to monitor mass 60 and 62 to verify the OCS peak. Capillary columns have been used by Farwell (1979), but they had problems with peak tailing, losses from adsorption, and resolving the H_2S-OCS peak.

There are several difficulties associated with the measurement of OCS at low atmospheric levels. When using the FPD detector for the measurement of OCS, errors can often result due to poor resolution of the H_2S and OCS peaks. Even when using a capillary column, Farwell was not able to achieve baseline separation of these two peaks when high concentrations of H_2S are present. Also, care must be taken to be sure that the FPD response is linear over the region of interest (Stevens et al., 1969).

More serious problems in the analysis of OCS come from adsorption of OCS onto glass and metal surfaces at active sites. This can arise in the column and sample containers or wherever the sample is in contact with heated glass or stainless steel (Farwell and Gluck, 1980). These adsorption losses can be eliminated either by deactivation of the surfaces involved, or by conditioning with repeated sample injections until a stable signal is reached.

To avoid some of the difficulties associated with poor OCS peak resolution, a quantitative method for OCS was developed using a Finnigan 4021 GC/MS with an automated data acquisition system and a sample freezeout concentration step to improve the sensitivity (Rasmussen et al., 1982a).

The cryogenic preconcentration procedure has been described by Rasmussen et al. (1977). A schematic of the basic valving system is shown in Figure 5.1. The pressure of the gas sample is used to fill a 100 mL syringe through a flow restrictor when toggle valve 1 is open. When the syringe has been filled, valve 1 is closed, the sample valve is turned to "load," and valves 2 and 4 are opened. Gravity forces the air at 100 mL/min through the freezeout loop, a 1/4" x 6" stainless steel tube filled with glass beads. During the filling procedure the loop is kept in liquid oxygen at -183°C. When all of the sample has flowed through the loop, the sample valve is turned to "inject" and the loop is placed in 85°C water and the sample is injected onto the column of the gas chromatograph (GC).

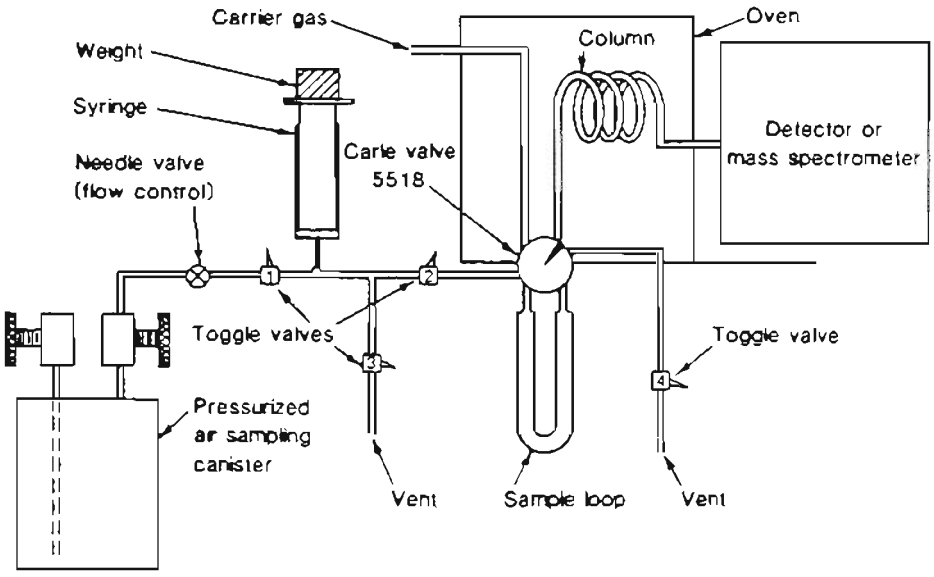

Figure 5.1. Schematic of OCS analytical system.

Several preliminary samples are run through the freezeout loop and the column to condition any active sites. Usually this takes about 30 minutes each day. After this short conditioning, the sample peak height stabilizes. Periodically the system is checked by running a "zero" air sample containing only N_2 and O_2 to verify that no residual OCS is observed. Between runs the system is flushed with 100 mL of zero air.

The OCS sample is separated from the air peak using a 10' x 1/4" stainless steel column packed with 10% SP2100 on 100/120 Supelcoport. SP2100 is a methyl silicone column material that is widely used for general purpose gas analysis. The column is run isothermally at 2°C with a helium carrier gas flow rate of 40 mL/min. Figure 5.2 shows some chromatograms of ambient air samples demonstrating the separation of the OCS from the air peak. The electron multiplier is turned off while the air peak comes through and is turned on just before the OCS peak appears.

The quadrupole mass spectrometer is used as a detector for both quantitation and identification of the peak. The MS is operated in the electron impact mode, using multiple ion detection (MID) with a 0.25 amu window centered at mass 60 for OCS. A copy of the MID descriptor is shown in Figure 5.3. The Finnigan 4021 system is equipped with a pulsed positive ion negative ion chemical ionization (PPINICI) unit which has a modified electron multiplier. The unit is operated in the positive ion mode so it is passive except for the ion conversion dynode which is set at -3000 V; the electron multiplier is operated at -1650 V.

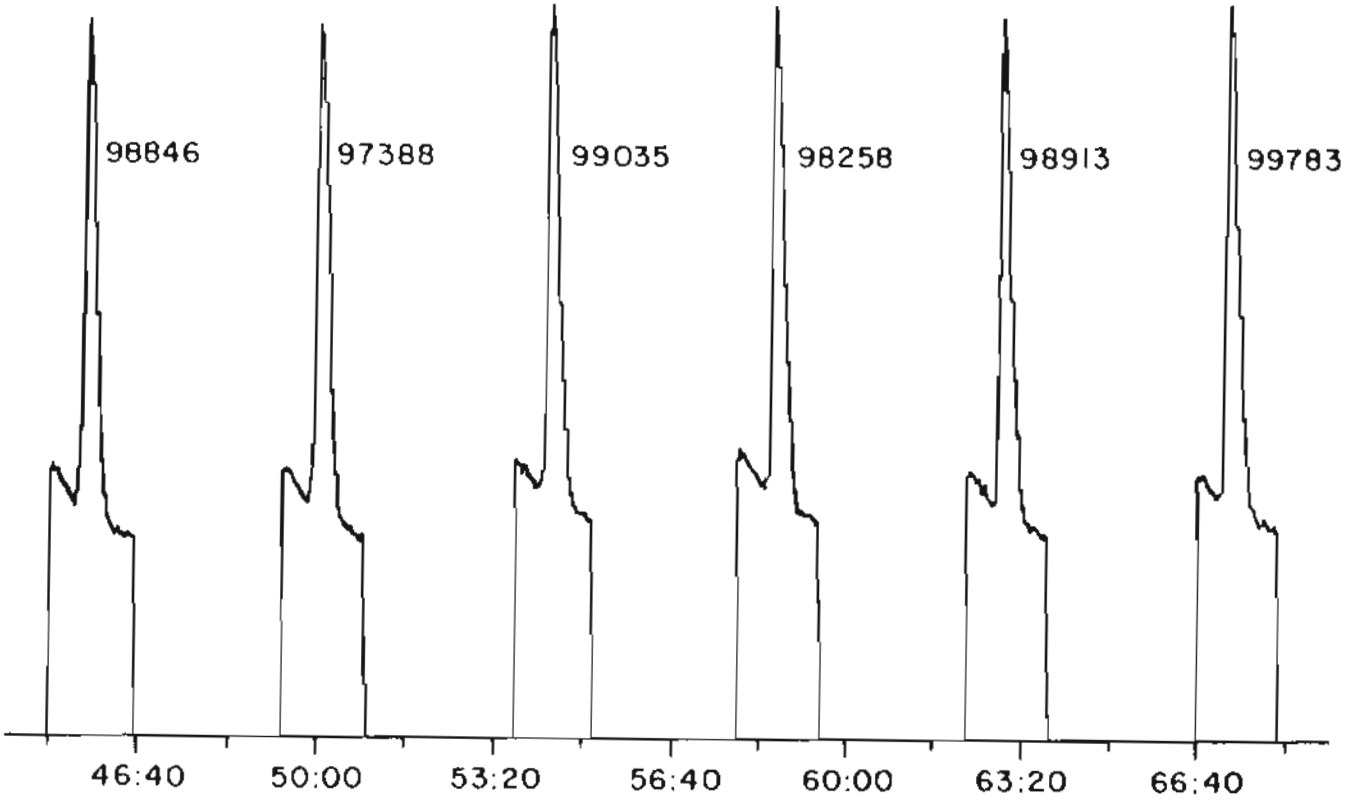

Figure 5.2. Reproducibility of OCS measurements on standard 0-100 over a 20-minute period.

```
ACQUIRE                          RUN 0.COS2                    ALREADY EXISTS
11/06/81 16:25:04                FREE SECTORS:  7775
SAMPLE
CONDS :
FORMULA:                         INSTRUMENT:  4021             WEIGHT:     0.000
SUBMITTED BY:                    ANALYST:                      ACCT. NO :
MODE:  CENTROID POSITIVE ION

MID SCAN                         DESC.  AB                     MASS INTERVALS.  1
SCAN TIME.   0.843 SECS          SAMP. INT.:  0.200 MS         MASTER RATE  32767

 INT #    LO MASS    HI MASS      TIME  MPW MFW  MA  TH  BL  ION
   1       59.875     60.125      0.839   5  80   0   1   1  POS



MID            DESC:  AB
INST:  4021    CAL1:  FC431227813

MASS DEFECT AT 100 AMU     30 MMU
MASTER RATE              32767
TOTAL ACQU TIME          0.839 SECS
TOTAL SCAN TIME          0.843 SECS
CENT SAMP INT            0.200 MS
MASS RANGE           1 TO 1024 AMU
 1       59.875     60.125       1.000     0.000     1   80   0   1   0  POS
INT       BEGIN        END        TIME     (SECS)   MPW  MFW  MA  TH  BL  ION
 #         MASS       MASS     REQUEST     ACTUAL

 1       59.875     60.125       0.900     0.839  5592   80   0   1   1  POS
```

Figure 5.3. GC/MS acquisition parameters and MID descriptor for OCS measurements.

The reproducibility of the analyses was checked by repeated analysis of standards (see Chapter 8). A series of 6 runs on a standard cryogenic air sample collected at Cape Meares, Oregon, is shown in Figure 5.2. The concentration in this tank is 503 pptv, which corresponds to a peak height of almost 100,000 counts with a relative error of 0.8% over a 20-minute period. Occasionally spurious noise is observed, or a slight drift in peak height will take place over the period of operation. However, most of the time stability is observed.

Standard Preparation. The daily working standard, tank 0-100, is a background air sample collected in a specially prepared 35 L stainless steel tank. The sample is collected by cryogenically condensing the air to get a tank pressure of about 400 psig (this procedure is described in more detail in Chapter 6). This standard was originally calibrated against a commercial 5.47 ppm CCS standard (Scott Research Laboratory, Inc.) by a static dilution technique. The 0-100 tank was also intercalibrated against another static dilution standard prepared in S. Penkett's laboratory at A.E.R.E, Harwell, U.K., using a VG Micromass mass spectrometer. Comparing the data from these calibrations, a best value was assigned to the tanks of 503 ± 10 pptv. This standard was used throughout the program to calibrate each sample, providing a uniform calibration base.

Calibration Curve. A calibration curve was prepared covering the concentration range from 89 ppt to 1050 ppt, which is the range of most samples encountered (Figures 5.4 and 5.5). Figure 5.4 shows the actual integration counts plotted against the concentration, and Figure

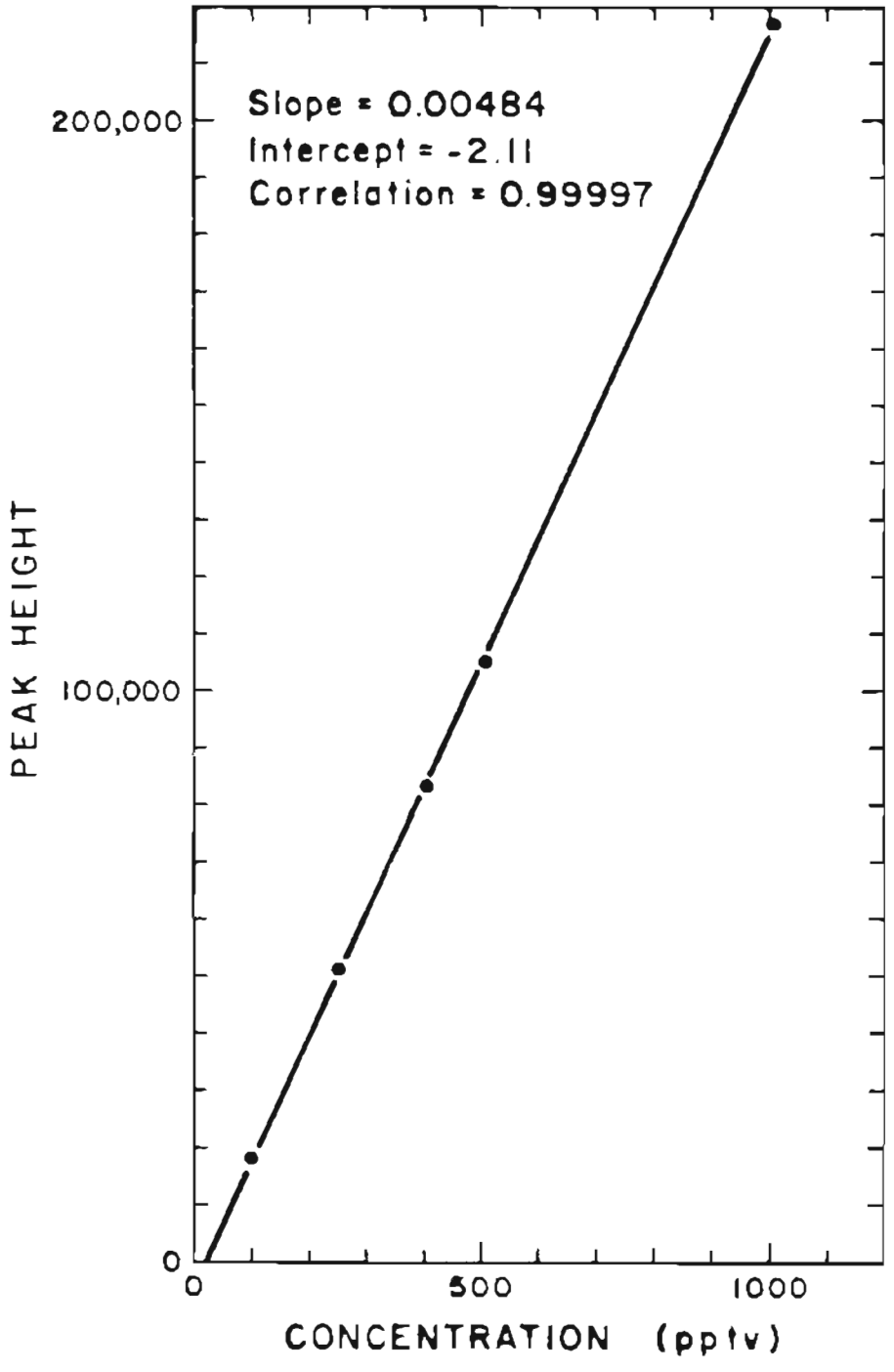

Figure 5.4. Calibration curve for OCS showing measured peak height vs. concentration in pptv.

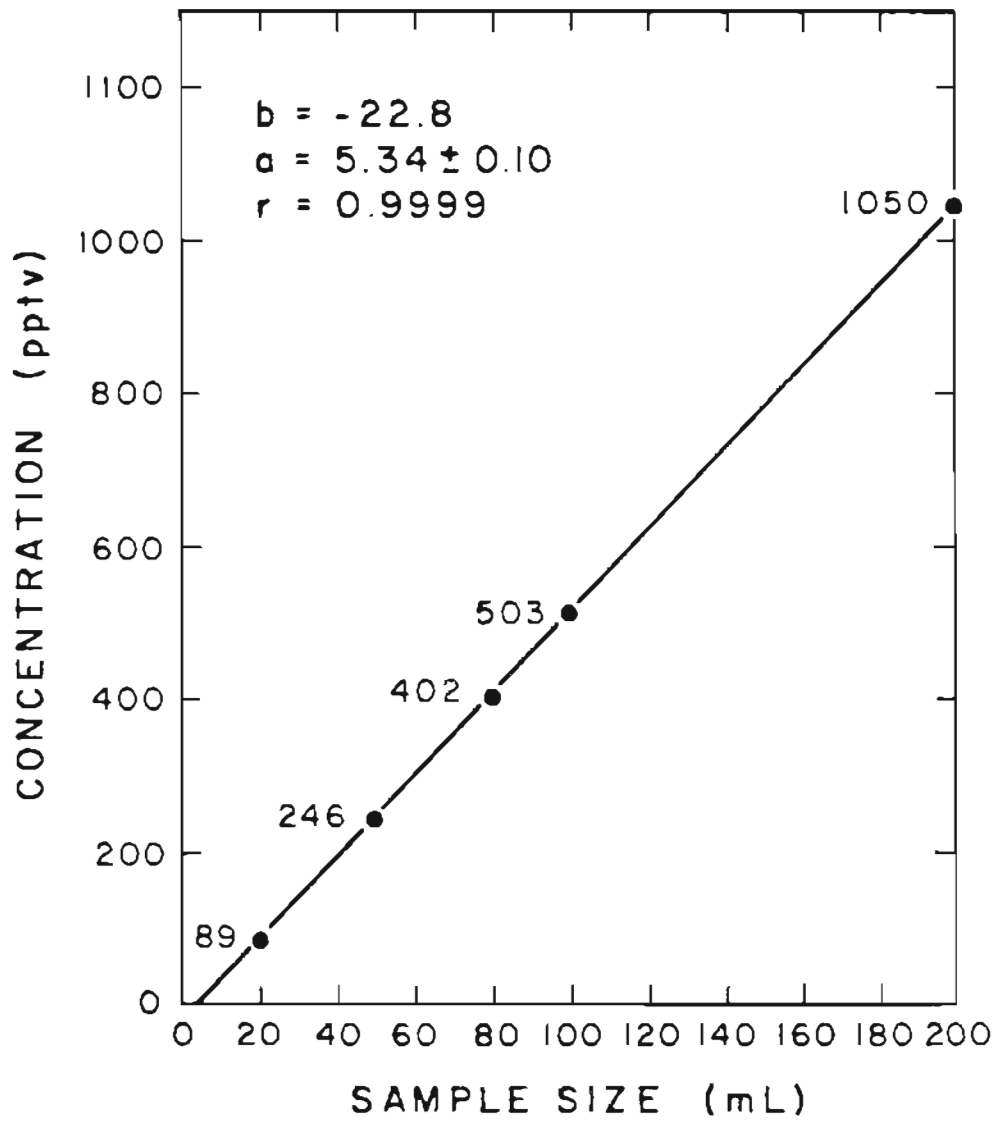

Figure 5.5. Calibration curve showing the measured concentration of OCS vs. the sample size in mL.

5.5 shows the calculated concentration plotted against the actual number of mL injected. The curve is linear and has a high correlation coefficient. The actual reconstructed ion chromatogram (RIC) for each of the concentrations used to prepare the calibration curve is shown in Figure 5.6, with each point on the curve being the average of three measurements.

Identification of OCS Peak. The chromatographic peak that was used to measure OCS in the air and seawater samples was identified by its retention characteristics and its mass spectra. OCS has a boiling point of -50°C, so on an SP2100 column operating at 2°C the peak comes out right after the air peak. Interfering compounds would have to have a similar boiling point and a peak at m/e 60. Examining a list of potential atmospheric compounds shows that no low boiling compounds have any mass spectra peaks within 2 mass units of 60. As an additional precaution, m/e 60 and 62 were monitored on a concentrated sample to see if the correct sulfur isotope ratio was observed. Figure 5.7 shows the RIC for mass 62 and mass 60 plus the total RIC for 60 plus 62. The $^{32}S/^{34}S$ ratio for the sample was 21.8, which corresponds to the normal sulfur isotope ratio (Brownlow, 1979). From this information it was concluded that the peak measured corresponded to OCS.

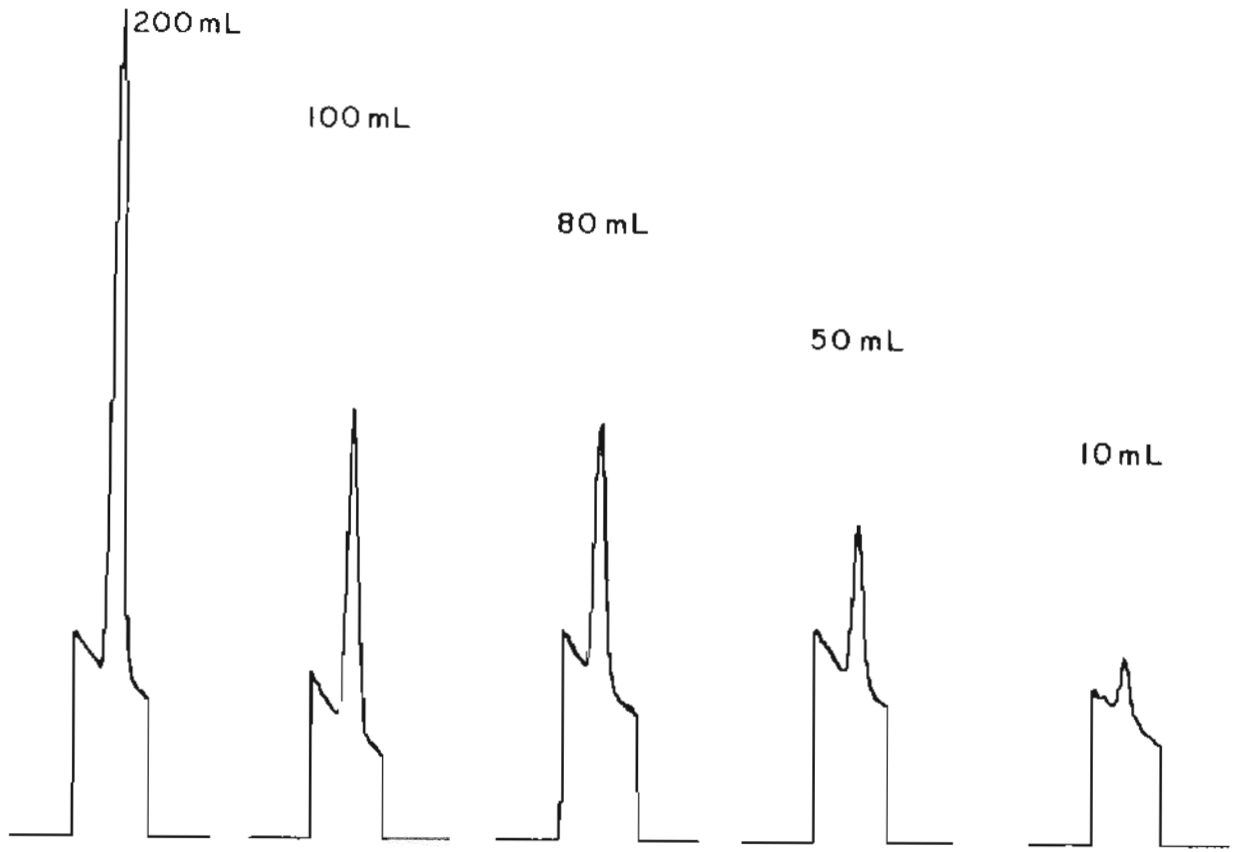

Figure 5.6. Actual GC/MS readout for sample sizes used to construct calibration curve.

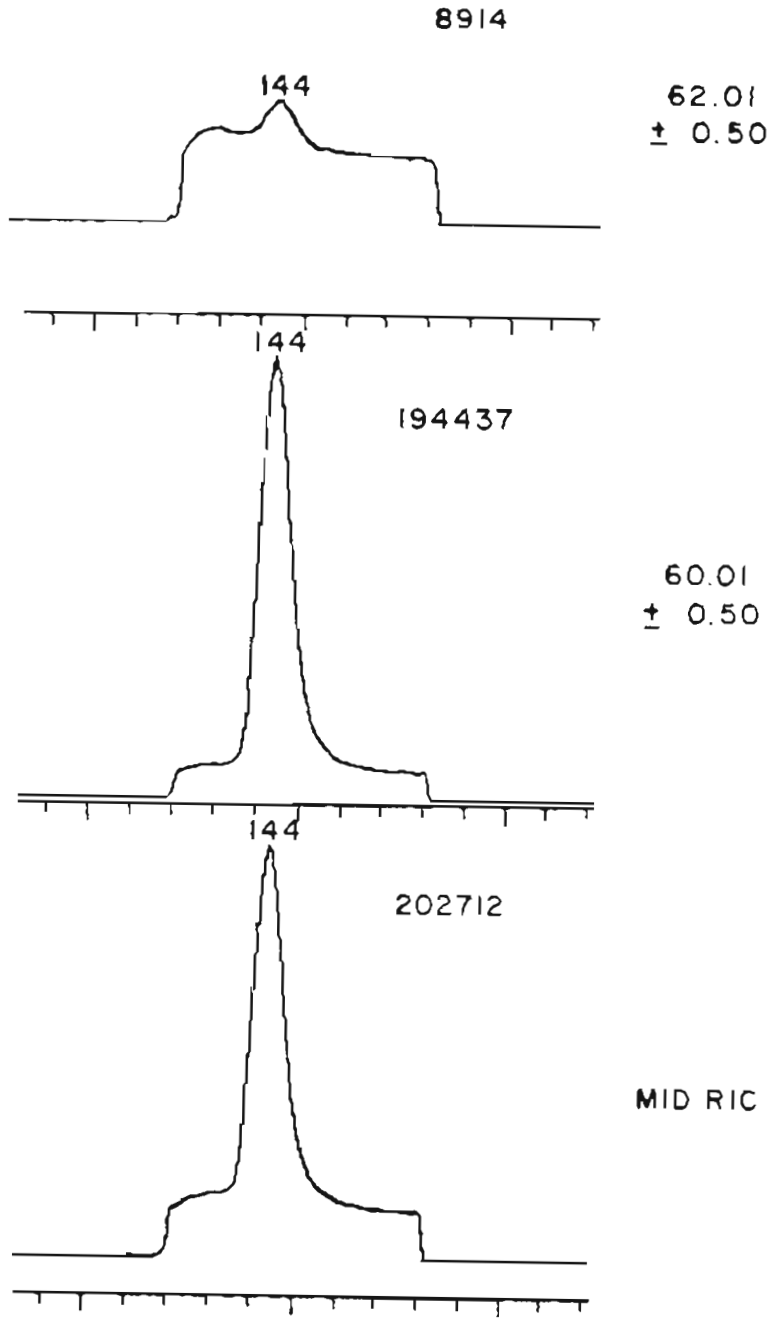

Figure 5.7. Sulfur isotope peaks used to verify identity of OCS peak. Top figure shows ^{34}S isotope, and middle figure shows the ^{32}S isotope. The bottom figure shows the combined RIC signal.

Detection Limit. For the measurement program described the detection limit (minimal detectable quantity) can best be calculated as a confidence limit for the difference between the mean of the sample counts ($\bar{x}_s$) and the mean of the background noise counts ($\bar{s}_b$).

$$\Delta\bar{x} = \bar{x}_s - \bar{x}_b \tag{5.2-1}$$

By using a simple propagation of error equation for subtraction, the standard deviation in $\Delta\bar{x}$ is given by:

$$s_{\Delta\bar{x}} = (s_{x_s}{}^2 + s_{x_b})^{\frac{1}{2}} \tag{5.2-2}$$

This can be written in terms of the individual standard deviations by substituting in the expression for the standard error:

$$s_{\Delta\bar{x}} = \left(\frac{s_{x_s}}{n_s} + \frac{s_{x_b}}{n_b} \right)^{\frac{1}{2}} \tag{5.2-3}$$

where n_s is the number of measurements of the sample and n_b is the number of measurements of the background. The measurement of a signal near the detection limit will be subject to the same noise sources as the background, so $s_{x_s}{}^2$ is approximately equal to $s_{x_b}{}^2$.

$$s_{\Delta\bar{x}} = s_{x_b} \left(\frac{1}{n_s} + \frac{1}{n_b} \right)^{\frac{1}{2}} \tag{5.2-4}$$

The confidence limit for $\bar{x}_s$ being significantly different from $\bar{x}_b$ can be calculated from:

$$C.L. = \pm t(\alpha, f)\, s_{\Delta\bar{x}} \tag{5.2-5}$$

where t is the t statistic for the α significance level and f is the degrees of freedom. By defining the detection limit (D.L.) to correspond to the upper confidence limit, the minimum detectable quantity is given by:

$$D.L. = t(\alpha, f)\, s_{\Delta\bar{x}} \tag{5.2-6}$$

Substituting (5.2-4) into (5.2-6) and by making ten blank measurements to determine s_{x_b} (f = 9), the detection limit for a 97.5% confidence limit can be written as:

$$D.L. = 2.3\, s_{x_b} \sqrt{\frac{1}{n_s} + \frac{1}{n_b}} \tag{5.2-7}$$

where n_s is the number of sample measurements and n_b is the number of blank measurements the sample is compared to. For a single measurement of a sample and blank this becomes:

$$D.L. = 2.3 \sqrt{2}\, S_{x_b} = 3.5\, s_{x_b} \tag{5.2-8}$$

where the units of s_{x_b} are in equivalent concentration as determined by the calibration curve slope (Figure 5.4).

A set of blank signal measurements is listed in Table 5-1. The average noise can be set approximately equal to s_{x_b}. The noise in concentration units is equal to 10 ppt, so the detection limit is equal to 35 pptv, or, in absolute sensitivity, 5 pg.

5.3 Halocarbon Measurement Procedure

Measurement of the halogenated compounds was done by a temperature-programmed gas chromatographic method that operates routinely in the lab (Rasmussen et al., 1977; Rasmussen and Khalil, 1981b). The air samples were concentrated using the same freezeout procedure described in Section 5.2 for OCS. Most measurements were made using 100 mL of sample, but occasionally, for low concentrations, 200 mL was used.

The compounds were separated using a Perkin Elmer Model 3920B gas chromatograph equipped with an electron capture detector using a ^{63}Ni source. The peak heights were measured using a Hewlett-Packard 3388A electronic integrator. The chromatographic column is a 1/4" O.D. by 10' long stainless steel tube packed with 10% SP2100 on 100/120 mesh Supelcoport. The oven temperature is set to 10°C to concentrate the constituents on the front of the column, and is programmed at 16°C/min to 80°C. The carrier gas is a mixture of 95% argon and 5% methane with a flow rate of 63 mL/min. The detector temperature is 350°C.

A chromatograph of an ambient air sample and a seawater sample is shown in Figure 5.8. The identities of the peaks were established

TABLE 5-1

Blank Signal Measurements

Determination No.	Noise Heights (counts)
1	2199
2	2095
3	1467
4	1886
5	2305
6	2514
7	1676
8	2095
9	2619
10	2619

Average noise = 2148 counts

Average noise = 10 ppt

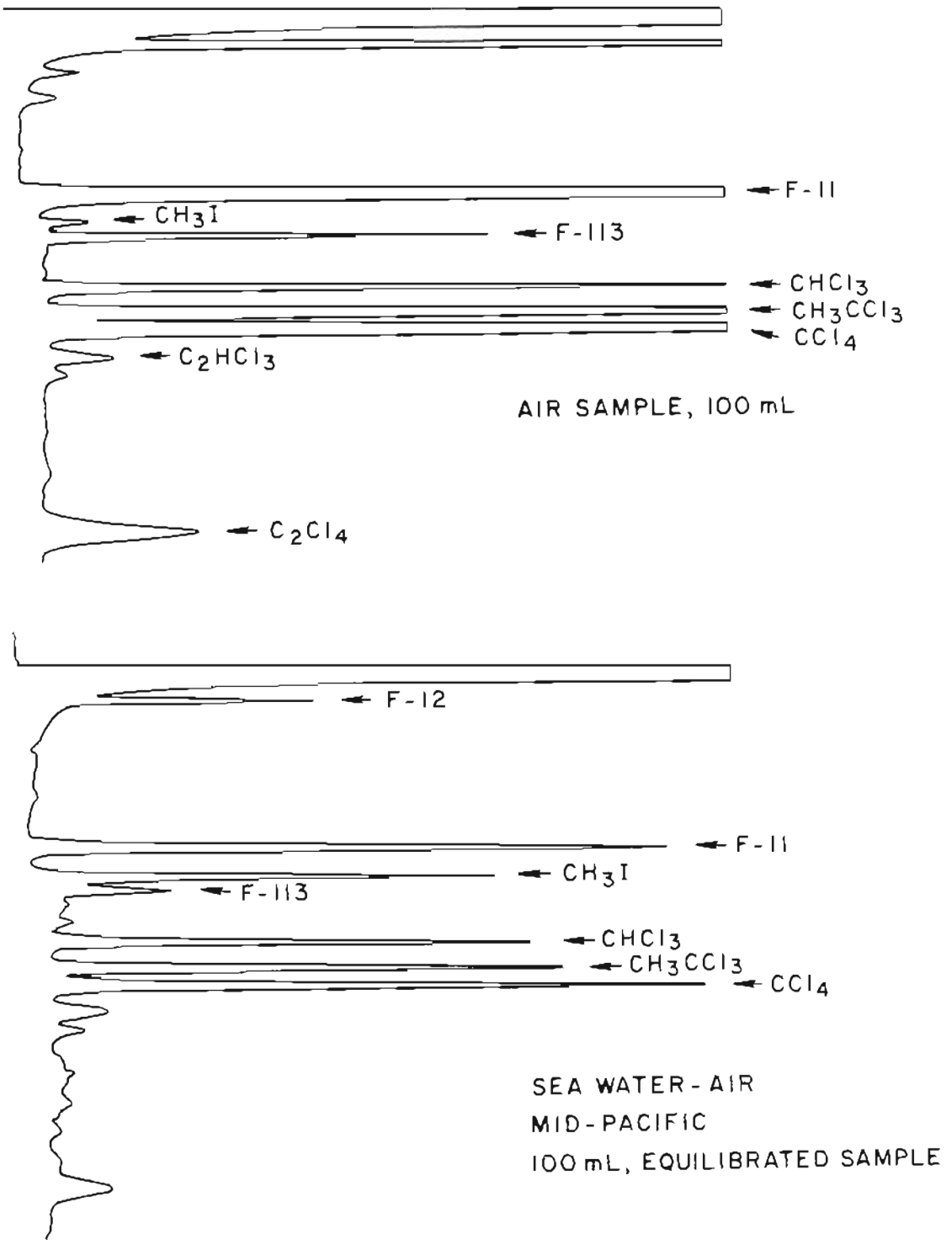

Figure 5.8. Chromatogram of temperature-programmed run of an air and seawater sample.

by running samples at A.E.R.E., Harwell, on a VG Micromass 16F mass spectrometer coupled to a Hewlett-Packard HP5710 gas chromatograph, and by comparison with data obtained on the routine instrument (Rasmussen and Khalil, 1981b) for F-11 and methyl chloroform (CH_3CCl_3). The detection limits for 100 mL of the halogenated compounds are shown in Table 5.2 (Rasmussen et al., 1977).

TABLE 5-2

Detection Limits for Temperature-Programmed Measurements

Halocarbon	D.L. (ppt)	$s/\bar{x}$ (%)
F-12 (CCl_2F_2)	9	1.5
F-11 (CCl_3F)	2	1.4
F-113 ($C_2Cl_3F_3$)	4	1.8
$CHCl_3$	6	5
CH_3CCl_3	4	4.3
CCl_4	2	2.8
CH_3I	0.05	10
C_2HCl_3	2	5
C_2Cl_4	1	8.3

CHAPTER 6

AIR SAMPLING METHODOLOGY

6.1 Introduction

To calculate the flux of a gas from the ocean, the atmospheric concentration of the gas near the ocean's surface must be measured. There are two ways to do this. Either the measurement equipment can be taken to the location and the air analyzed directly, or sample containers can be filled with air and sent back to the laboratory for analysis. The advantages of making field measurements are that many analyses can be made, and there is no need to worry about sample stability in the containers. The advantages of sending samples to the laboratory are that better quality assurance can be maintained, it is easier to analyze samples from many different locations, the precision of the measurements is usually better, and it is less expensive and simpler to maintain the equipment.

All of the atmospheric measurements for this dissertation were obtained by collecting air samples and analyzing them in the laboratory by one of the procedures described in the previous chapter. There were five types of sample bottles and two types of collection procedures used. Samples were collected in 800 mL and 6 L SS bottles and 1.5 L aluminum bottles using a pump, in a 1.6 L SS bottle and a 35 L SS tank using cryogenic pumping.

6.2 Collection Procedures for Atmospheric Air Samples

The 800 mL air sampling bottle is shown in Figure 6.1. The bottle is constructed from 304 stainless steel and is internally electropolished using the SUMMA® process to passivate the inside of the bottle. Each bottle has a filling "T" with two Nupro 4H4 metal bellows valves. The bellows valves substantially reduce contamination. Before use, the bottles are baked out overnight in an oven at 100°C while being flushed with contaminant-free zero air. The bottles are then pressurized to 30 psig with the zero air and checked for leaks and contamination before being sent into the field. The bottles are filled with atmospheric air using a metal bellows pump (MB15, Metal Bellows Corp.) which has been tested for contamination. The bellows pump is attached to a purging "T" which has a pressure gauge and a toggle valve (Figure 6.1). The purge "T" is used to flush the bellows valve. To collect an air sample, the pump is turned on and valve A is flushed; then both valve A and valve B are opened to flush the bottle. The bottle is flushed for 10 minutes, valve B is closed, and the pressure built up to 30 psig. Valve A is closed, and caps are placed on the valves to prevent leaks in transport.

The 6 L cans are shown in Figure 6.2 and are constructed from 6 L stainless steel beakers type 304 with a stainless steel top welded on them (Harsch, 1980). On each side of the beaker a Nupro 4H4 metal bellows valve is welded so the side with the fill tube is set in

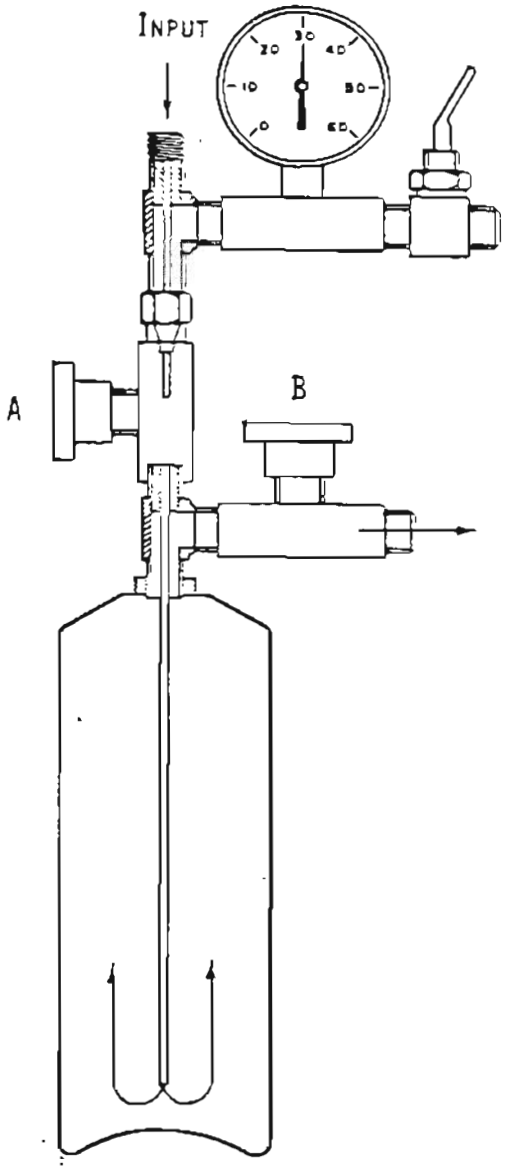

Figure 6.1. 800 mL stainless steel sample bottle.

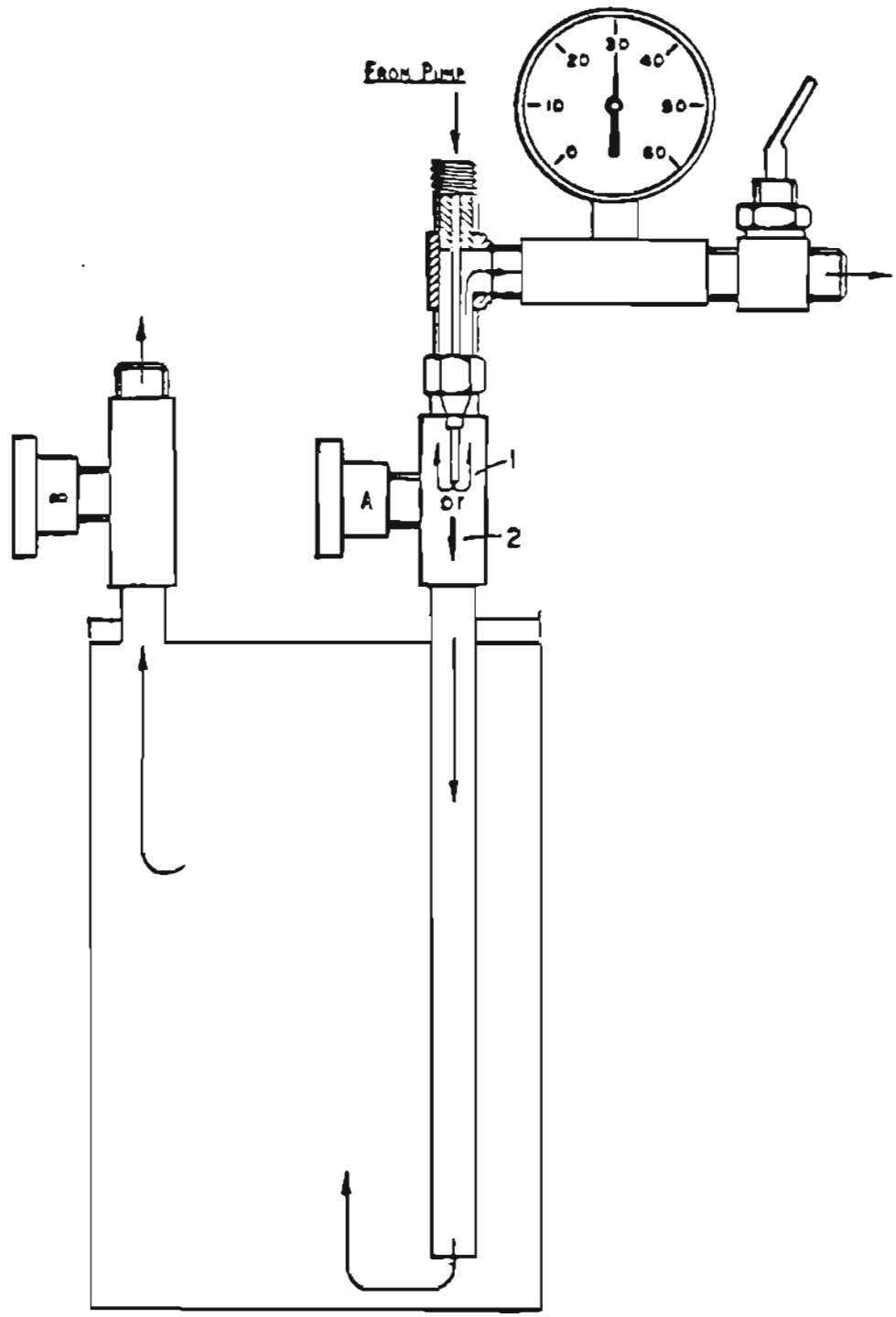

Figure 6.2. Diagram of 6-liter stainless steel sample container and filling "T."

farther than the other side. These containers are conditioned and filled the same way as the 800 mL bottles.

The 1.5 L aluminum bottles are purchased from Luyfer and fitted with a filling "T" and Nupro metal bellows valves. The aluminum bottles are steam-cleaned before use by adding a small amount of water to the bottle and heating to 110°C overnight. The bottles are then flushed with zero air and pressurized to 30 psig before being sent to the field. The bottles are filled the same way as the 800 mL bottles.

The 1.6 L cryo bottles (see Figure 6.3) are type 316 stainless steel which has been electropolished by the SUMMA® process. The bottles have a stainless steel filling "T" with Nupro stainless steel 4H4 bellows valves. Before use the bottles are baked at 110°C and flushed with zero air overnight. Some of the bottles are evacuated before being sent to the field. The air samples are collected by cryogenically condensing air in the bottles. This is done by placing the bottle in a Dewar filled halfway with liquid nitrogen. (A snorkle is placed on valve B to keep liquid nitrogen fumes from being sucked into the bottle and diluting the sample.) When the flask has cooled, valve B is opened and the cold surface of the bottle condenses the air in the bottle which creates a vacuum. Valve B is closed after 10-15 minutes to keep the bottle from becoming over-pressurized. The bottle is removed from the liquid nitrogen and warmed to room temperature. The final pressure in the bottles is usually about 400 psig. The advantages of the cryogenic samples are the elimination of pump contamination and the large amount of air that can be collected in a small

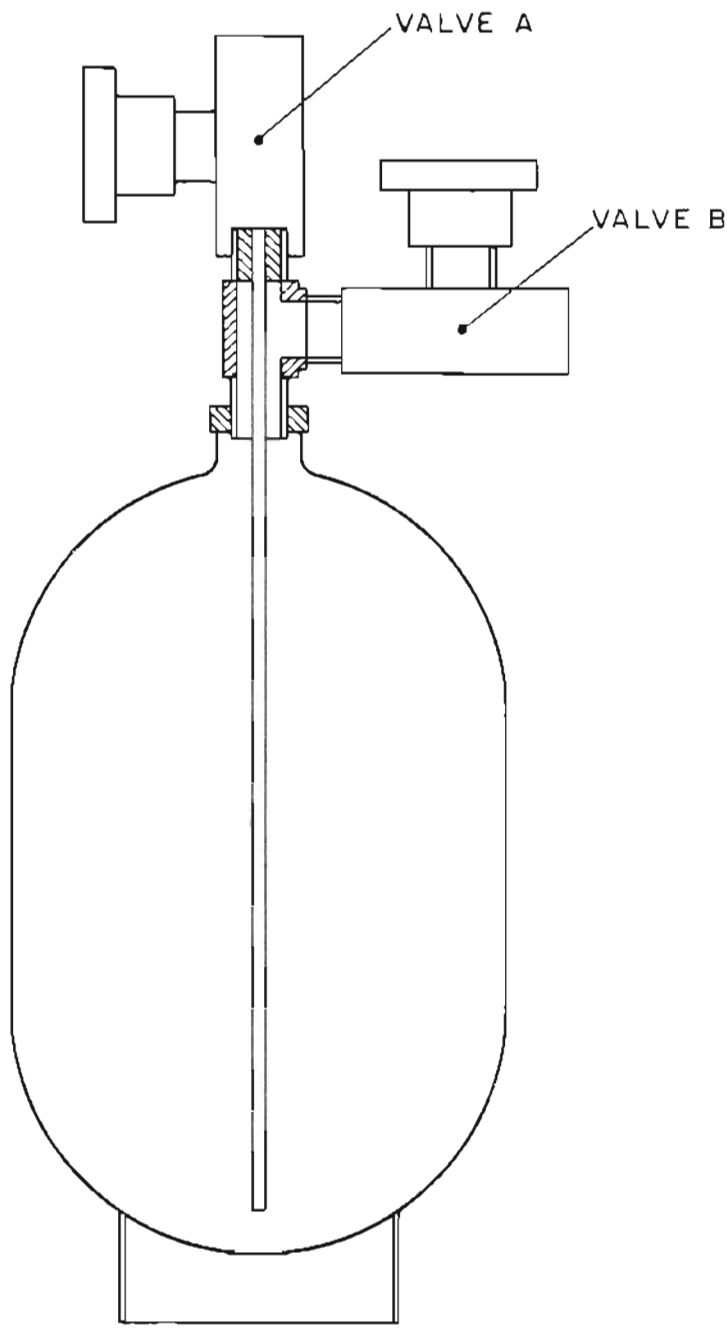

Figure 6.3. Diagram of 1.6 liter stainless steel cryogenic can.

bottle because of the high pressure. The high pressure and the large sample volume to surface area ratio of the cryo sample give better long term stability.

Figure 6.4 shows the 35 L cryogenic sampling tank. These tanks are surplus oxygen tanks constructed from a type B16 stainless steel. The tanks have a stainless steel fill "T" and Nupro 4H4 metal bellows valves. The tanks are conditioned by adding about 100 mL of distilled water to the tank, shutting valves A and B, and heating to 110°C in an oven to pressure-cook the insides of the tank. Near the end of the process (usually about 8 hours) valve B is opened and the tank flushed and filled with zero air. Samples are collected by first flushing the tank with air using a metal bellows pump, and then floating the tank on liquid nitrogen in a large stainless steel Dewar. The pump is disconnected and valve B is opened. Typically the air is sampled long enough to achieve a tank pressure of 400 psig at room temperature. After the tank is returned to the lab, it is inverted and excess water blown out through valve B. Typically the dew point on this tank is about -26°C.

The 35 L cryogenic tank produces the most stable air samples, and because of their large volumes they are ideal for use as working standards. Once calibrated against a primary standard the tank can be used as a secondary standard for at least a 6-month period of time before recalibration. These tanks ahve been used for interlaboratory calibrations (Rasmussen and Khalil, 1981).

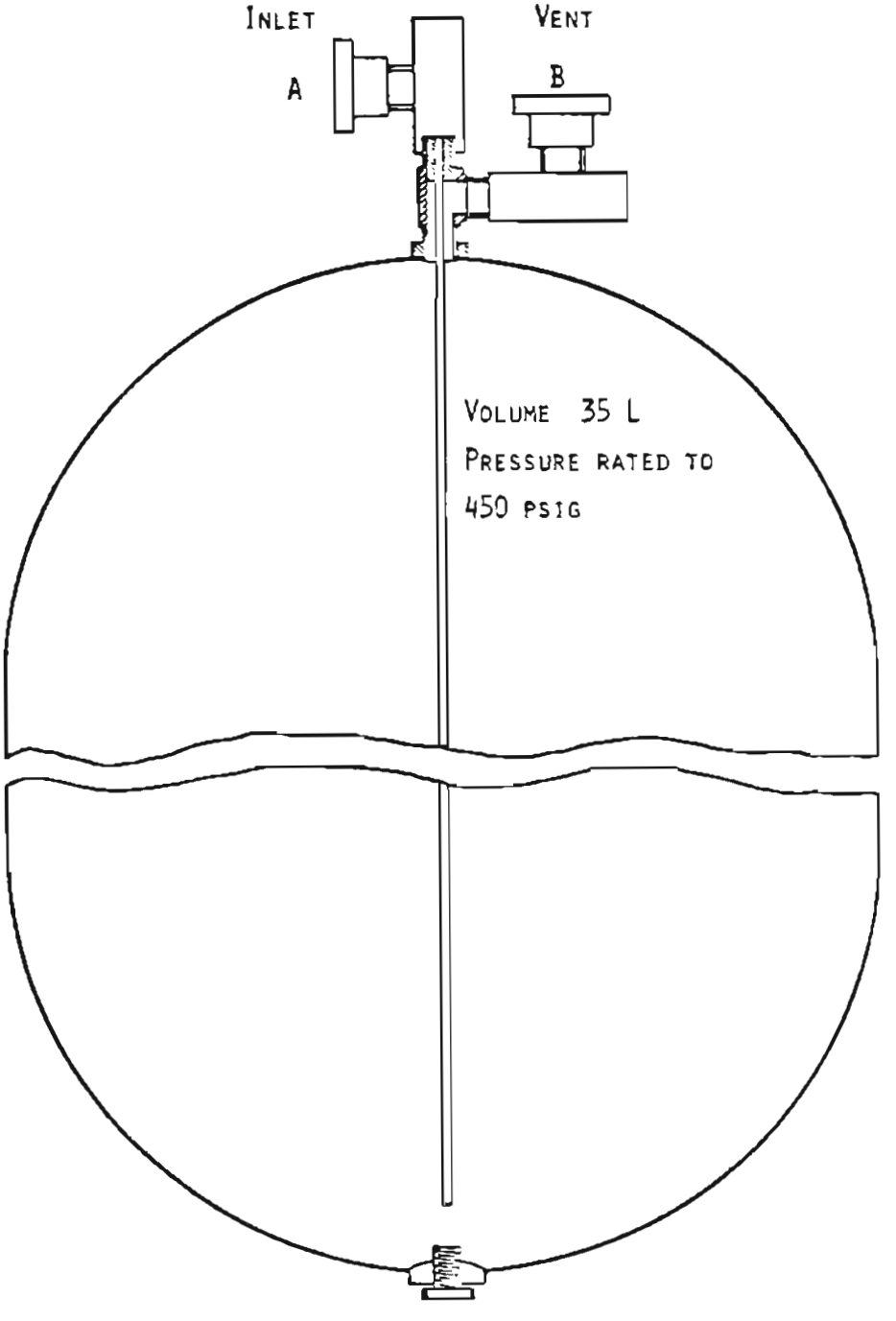

Figure 6.4. Diagram of 35-liter stainless steel cryogenic tank.

Each sample container has its advantages and disadvantages, depending on the particular sampling situation. Table 6-1 gives a comparison of the various containers. Usually a combination of samples is collected for a study, to check for contamination or drift.

TABLE 6-1

Comparison of Air Sampling Containers

Container	Advantages	Disadvantages
800 mL bottle collected w/pump	small inexpensive to mail does not require liquid nitrogen (a problem at remote locations)	not much sample for analysis not stable for certain compounds requires metal bellows pump and electricity pressure limit 200 psig
6 L bottle collected w/pump	does not require liquid nitrogen more stable than 800 mL bottle for some gases more sample than 800 mL bottle	larger than the 800 mL bottle; more difficult to ship requires metal bellows pump and electricity cannot pressurize above 30 psig
1.6 L cryogenic bottle	does not need electricity for pump large amount of sample and small storage space small and not very expensive to mail excellent stability for most gases	requires liquid nitrogen not as convenient to mail as 800 mL bottle does not have the long term stability of the 35 L tank for some compounds pressure limit 500 psig
35 L cryogenic tank (ALE tank)	most stable; suitable for long term storage large sample size dry air sample	expensive to construct costly to ship requires liquid nitrogen, pump, and large Dewar more space to store than 1.6 L cryo pressure limit 450 psig

CHAPTER 7

METHODS OF COLLECTING AND ANALYZING SEAWATER SAMPLES FOR TRACE GASES

7.1 Introduction

The sampling methodology called for seawater samples to be collected and returned to the laboratory for analysis on several different instruments. A procedure was needed for collecting, transporting, and extracting the gases from water without contamination or losses, so it was decided to build a container that could be easily used in the field for sample collection and later in the laboratory for analysis.

The two principal techniques that have been used for the measurement of trace gases in water samples are gas stripping (Grob, 1973; Grob and Zücher, 1976; Swinnerton and Linnenbom, 1976), and headspace analysis (McAuliffe, 1979; Schmidt, 1979; Hachenberg and Schmidt, 1977). A modified version of the McAuliffe headspace technique was chosen because of the simplicity of the technique and the ability to obtain selectivity based on the partition coefficients of the gases.

A special vacuum extraction flask was designed so the water samples could be collected directly in this container in the field, transported back to the lab, and the headspace gas analyzed without having to transfer the water. There are many advantages to this system. Since the flasks are designed to hold pressure to 30 psig and vacuum to 100 mtorr, there is no chance of contamination once the water is sealed in

the flask. The flasks are sent to the field with a 100 mtorr vacuum so water can easily be aspirated into the flask without the need for a pump (an additional source of contamination or degassing). Each sample can be analyzed several times on different instruments to measure the concentrations of several gases.

The next few sections describe the construction and operation of the vacuum extraction flask and show how to calculate the seawater gas concentration from the headspace concentration. Also a propagation of error procedure is used to identify the major sources of uncertain concentration from the headspace concentration. Also a propagation of error procedure is used to identify the major sources of uncertainty in calculating the seawater concentration from the headspace concentration.

7.2 Collection of Water Samples Using the Vacuum Extraction Flask

The design of the vacuum extraction bottle is shown in Figure 7.1. The bottle is made from a 1000 mL Erlenmeyer flask with a Kovar to glass seal attached to the top. A stainless steel 1/4" female pipe coupling is welded to the Kovar to form a gas-tight seal. A Nupro B-4H4 brass bellows valve is connected to the coupling with a 1/4" pipe to 1/4" pipe adaptor. The top of the bellows valve has a Swagelok® 1/4" pipe to 1/4" tubing male connector for leak-free connection to accessories (i.e., funnel, filter, etc.). The pipe connections are sealed with Teflon® tape so the sample is exposed to glass and a small amount of stainless steel, brass, and Teflon®. The system

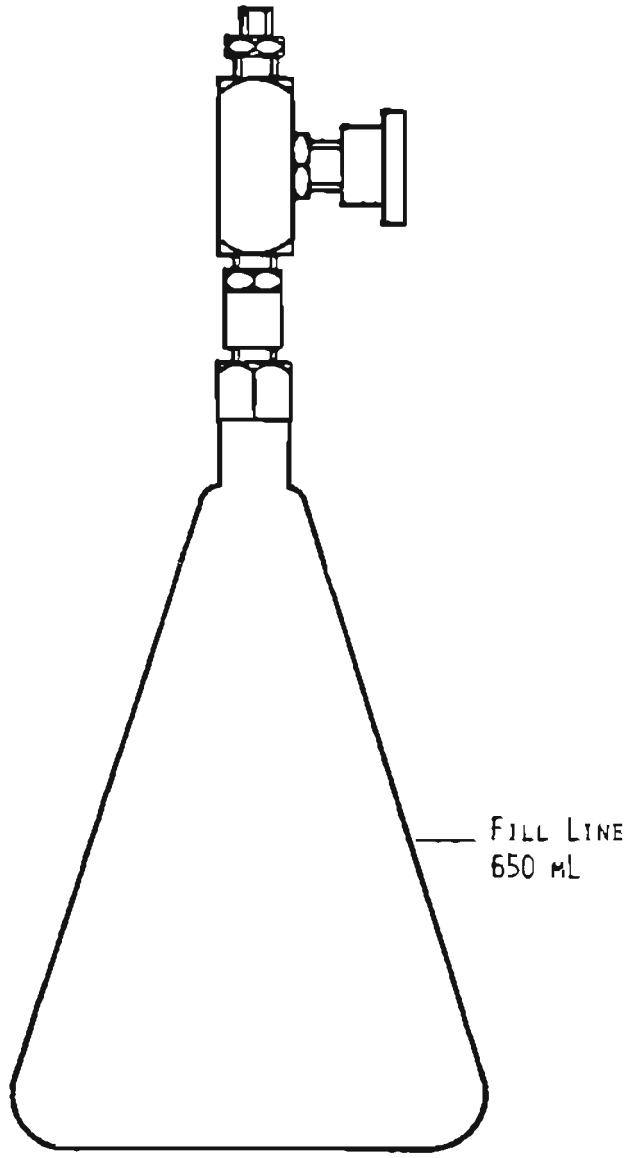

Figure 7.1. Vacuum extraction flask for seawater analysis.

is designed to hold a 0.1 torr vacuum and pressure up to 15 psig without leaks. The final volume of the system is about 1000 mL.

The bottle is cleaned for use in gas analysis by placing the bottle in a heated chamber at 100°C and simultaneously pumping on it with a vacuum pump for one hour. The bellows valve is then closed to keep the bottle under a vacuum of 0.1 torr until use.

The design allows a funnel or filter to be attached in a leak-free manner to the bottle when it is desired to filter the sample. (A Millipore® high pressure stainless steel filter holder works well in this application.)

The sample can be collected either by submerging the bottle and opening the valve or by adding the water sample to a stainless steel funnel and opening the valve to draw the sample in under vacuum. To get the equivalent of a McAuliffe extraction, 700 mL of water are drawn into the bottle and the valve closed before any air can enter. The container is then pressurized to 15 psi with zero air. This gives equal volumes of air and water at 25°C and 1 atmosphere pressure. The positive pressure helps prevent contamination of the headspace and provides pressure to transfer the sample to the gas chromatograph.

After the water sample has been collected, the bottle is placed in a freezer and kept frozen until it is analyzed. The frozen bottles are shipped with dry ice. Freezing the samples reduces both biological and chemical activity in the bottles.

For analysis the bottles are taken from the freezer and put in a water bath where they are agitated for 30 minutes so the system can

reach equilibrium and a temperature of 25°C before measurements are made. The container is connected directly to the chromatograph through the Swagelok® fitting. The headspace air can be analyzed for the compounds of interest by doing either single or multiple extractions of the bottle. The multiple extractions are conveniently done by keeping the bottle stationary after measurement to prevent mixing, then flushing the headspace 5 times with zero air, re-pressurizing to 15 psi, and shaking for another 30 minutes. This process of flushing and re-pressurizing is continued until the desired number of extractions have been made.

7.3 Calculation of Seawater Concentration from Headspace Concentration

The concentration of a gas in seawater collected in the vacuum extraction flask can be calculated from the equations developed for the McAuliffe technique (McAuliffe, 1970). The equations were based on a 1:1 air volume to water volume ratio ($\alpha = 1$), and have been rederived in a general form with no restrictions on α. This allows more versatility in the filling of the flasks, and α can be optimized to provide the best balance between sample volume and sensitivity.

The equations for the gas concentration in seawater are based on the mass balance in the vacuum extraction flask and on the Henry's constant for the gas.

$$V_o^* = V_{gi}^* + V_{\ell i}^* \qquad \text{Mass balance} \qquad (7.3\text{-}1)$$

$$H = \left(\frac{V^*_{gi}}{V_g}\right)\left(\frac{V_L}{V^*_{\ell i}}\right) = \frac{Cg_i}{C\ell_i} \qquad \text{Henry's law} \qquad (7.3\text{-}2)$$

where V^*_o is the total mL of component gas of interest in the system, V^*_{gi} is the mL of component gas in the gas phase with volume V_L, $V^*_{\ell i}$ is the volume of component gas in the liquid phase of V_g, and H is the Henry's law constant. We can rewrite equation (7.3-2) as:

$$\alpha H = \frac{V^*_{gi}}{V^*_{\ell i}} \qquad \text{where } \alpha = \frac{V_g}{V_L} \qquad (7.3\text{-}2a)$$

We can now proceed and derive the equations needed to evaluate a series of extractions using the procedure of McAuliffe (1970), except the equations are generalized to extraction volume ratios other than 1:1 using the factor α.

Equation (7.3-2b) can be written as

$$V^*_{gi} = \alpha H\ V^*_{\ell i} \qquad (7.3\text{-}3)$$

and equation (7.3-1) can be substituted into (7.3-3) to yield

$$V^*_{gi} = \alpha H\ (V^*_o - V^*_{gi})$$

which will simplify to

$$V^*_{gi} = \frac{\alpha H\ V^*_o}{(1 + \alpha H)} \qquad (7.3\text{-}4)$$

The equation for V^*_{gi+1} can be obtained from (7.3-4) by subtracting V^*_{gi} from the total initial mass of the system V^*_i:

$$V^*_{gi+1} = \frac{\alpha H}{(1 + \alpha H)} (V^*_o - V^*_{gi}) \qquad (7.3\text{-}5)$$

Substituting (7.4-3) into (7.3-5) and simplifying:

$$V^*_{gi+1} = \frac{\alpha H \, V^*_o}{(1 + \alpha H)^2} \qquad (7.3\text{-}6)$$

This equation can be generalized to n extractions:

$$V^*_n = \frac{\alpha H \, V^*_o}{(1 + \alpha H)^n} \qquad (7.3\text{-}7)$$

Since concentrations are experimentally measured, equations (7.3-4), (7.3-6), and (7.3-7) can also be written in the concentration form using $\alpha = V_g/V_L$, where C^*_o is the initial water concentration of the gas (by volume) and C^*_{gi} is the headspace concentration (by volume) for the ith extraction.

$$C^*_{gi} = \frac{H \, C^*_o}{(1 + \alpha H)} \qquad (7.3\text{-}4a)$$

$$C^*_{gi+1} = \frac{H \, C^*_o}{(1 + \alpha H)^2} \qquad (7.3\text{-}6a)$$

$$C^*_{gn} = \frac{H \, C^*_o}{(1 + \alpha H)^n} \qquad (7.3\text{-}7a)$$

The value for H can be determined by dividing equation (7.3-4) by (7.3-6):

$$H = \frac{1}{\alpha}\left(\frac{C^*_{gi}}{C^*_{gi+1}} - 1\right) \qquad (7.3\text{-}8)$$

so the value of H can be calculated from two successive gas concentrations.

Equation (7.3-7a) can be linearized by taking the log of both sides:

$$\log C^*_{gn} = \log HC^*_o - n \log (1 + \alpha H) \qquad (7.3\text{-}9)$$

By plotting the concentration from successive extractions (C^*_{gi}, i = 1 ton) on semi-log paper, the initial water concentration (C^*_o) and the Henry's law constant (H) can be found from the following:

$$\text{Intercept} = HC^*_o \qquad (7.3\text{-}10)$$

$$\text{Slope} = -(\alpha H + 1) \qquad (7.3\text{-}11)$$

If $\alpha = 1$, the above equations reduce to the form used by McAuliffe (1971). Even though the 1:1 extraction was shown to lead to easily calculated results, it is not always possible or advantageous to use the 1:1 extraction. The more general equations are not any more complicated to apply and can lead to improved results in the case of the vacuum extraction flask.

The gas concentration in the water, C_o^*, can also be calculated from a single measurement of the headspace gas concentration by using equation (7.3-4a). This equation is rearranged to the form:

$$C_o^* = \frac{C_{gi}^* (1 + \alpha H)}{H} \qquad (7.3\text{-}12)$$

To use this equation, the Henry's constant has to be known at the extraction temperature, and for seawater the Henry's constant in seawater must be used since it is about 20% higher than the distilled water value. It is not necessary to accurately know the salinity of the sample since the Henry's constant does not vary more than a few percent over the salinity range commonly found in the ocean.

7.4 Error Analysis of Headspace Technique

The propagation of error procedure described in Chapter 4 was applied to equation (7.3-12) and equation (7.3-4) to calculate the uncertainty in the seawater gas concentration from the measured headspace concentration. This will provide guidelines for estimating the uncertainties for each gas measured using the headspace analysis technique. There were two measurement procedures described: one using just the initial headspace concentration and the Henry's constant, H, measured by an independent technique; the second using successive extractions and extrapolating the results to get the seawater concentration. The uncertainty analysis is slightly different, depending on the method used, so both procedures will be discussed.

If the seawater concentration is measured by successive extractions and then graphically, the gas concentration in the seawater, C^*_o, is given by equation (7.3-4).

$$C^*_o = \frac{C^{*\,2}_{gi}\,\alpha}{(C^*_{gi} - C^*_{gi+1})} \tag{7.4-1}$$

C^*_o in this case is a function of the independent variables C^*_{gi}, C^*_{gi+1}, and α. The uncertainty in C^*_o, $\sigma_{C^*_o}$, can be found using equation (4.1-1) and substituting the partial derivatives of the independent variables.

$$\frac{\partial C^*_o}{\partial \alpha} = \frac{C^{*\,2}_{gi}}{(C^*_{gi} - C^*_{gi+1})} \tag{7.4-2a}$$

$$\frac{\partial C^*_o}{\partial C^*_{gi}} = -\frac{\alpha C^*_{gi}\, C^*_{gi+1}}{(C^*_{gi} - C^*_{gi+1})^2} \tag{7.4-2b}$$

$$\frac{\partial C^*_o}{\partial C^*_{gi+1}} = \frac{\alpha C^{*\,2}_{gi}}{(C^*_{gi} - C^*_{gi+1})^2} \tag{7.4-2c}$$

Making the above substitutions and calculating the uncertainty as the relative error, $\tilde{\sigma}_{C^*_o}$, is equal to:

$$\tilde{\sigma}_{C^*_o} = \left[\frac{C^{*\,2}_{gi+1}}{(C^*_{gi} - C^*_{gi+1})^2} \left(\tilde{\sigma}^{\,2}_{C^*_{gi}} + \tilde{\sigma}^{\,2}_{C^*_{gi+1}}\right) + \tilde{\sigma}\,\alpha^2 \right]^{\frac{1}{2}} \tag{7.4-3}$$

From this expression is can be seen that $\tilde{\sigma}_{C^*_o}$ depends on C^*_{gi} and C^*_{gi+1}, which are determined by the Henry's constant of the gas, and α as shown by equation (7.3-8).

Even though the Henry's constant is not used in this procedure, it can be substituted into equation (7.4-3) in order to see how the first term will behave for different gases and different ratios of α. Equation (7.3-8) can be solved for C^*_{gi+1}:

$$C^*_{gi+1} = \frac{C^*_{gi}}{(\alpha H + 1)} \qquad (7.4\text{-}4)$$

This can be substituted into the first expression in equation (7.4-3):

$$\frac{C_{gi+1}}{(C^*_{gi} - C^*_{gi+1})}$$

to give $1/\alpha$ H. The expression for the relative error can be rewritten:

$$\tilde{\sigma}_{C^*_o} = \left[\left(\frac{1}{\alpha H}\right)^2 \left(\tilde{\sigma}_{C^*_{gi}}{}^2 + \tilde{\sigma}_{C^*_{gi+1}}\right)^2 + \tilde{\sigma}_{\alpha}{}^2\right]^{1/2} \qquad (7.4\text{-}5)$$

For more soluble gases, as H becomes small, $1/\alpha$ H will become large, so $\tilde{\sigma}_{C^*_o}$ will be larger for the more soluble gases. Also, the larger the air to water volume ratio, α, the smaller the value of $\tilde{\sigma}_{C^*_o}$ will become. A secondary effect is that for large values of H, C^*_{gi+1} will be much smaller than C^*_{gi+1}, so the measurement standard deviation $\tilde{\sigma}_{C^*_{gi+1}}$ will be larger than $\tilde{\sigma}_{C^*_{gi}}$. For the more soluble gases $\tilde{\sigma}_{C^*_{gi}}$ will be about equal to $\tilde{\sigma}_{C^*_{gi+1}}$.

If the Henry's constant, H, is determined by some independent method such as described in Chapter 9, the seawater concentration can be determined using equation (7.3-12), with C^*_{g1} being the headspace concentration of the first extraction.

$$C_o^* = \frac{C_{g1}^* (1 + \alpha H)}{H} \qquad (7.3\text{-}12)$$

In this case C_o^* is a function of the independent variables C_{g1}^*, H, and α. Again using equation (4.1-1), the relative error in the seawater concentration $\tilde{\sigma}_{C_o^*}$ can be determined:

$$\tilde{\sigma}_{C_o^*} = \left[\tilde{\sigma}_{C_{g1}^*}^2 + \frac{1}{(1 + \alpha H)^2} \tilde{\sigma}_H^2 + \left(\frac{H\alpha}{(1 + \alpha H)} \right)^2 \tilde{\sigma}_\alpha^2 \right]^{\frac{1}{2}} \qquad (7.4\text{-}6)$$

$$A = \frac{1}{(1 + H)^2} \qquad B = \frac{H\alpha}{1 + \alpha H}$$

The dependence of the uncertainty is more complicated than in equation (7.4-5). For the gases studied these values have been calculated for different values of α and are shown in Table 7-1.

The values in Table 7-1 show that for all gases, $\tilde{\sigma}_{C_{g1}}$ will provide a major contribution to the total uncertainty. For the more soluble gases, less material will be in the headspace and C_{g1} will be small, causing $\tilde{\sigma}_{C_{g1}^*}$ to become large. This can often limit the usefulness of the technique unless the seawater concentrations are high.

In the case of CH_3I and $CHCl_3$, which are highly soluble, the values of C_{g1}^* were large since the ocean is a source, so the uncertainty, $\tilde{\sigma}_{C_{g1}^*}$, is not large. Another aspect shown by Table 7-1 is that as α goes from 0.25 to 4, the value of A (Table 7-1) becomes smaller while B (Table 7-1) becomes larger. Thus, there is a tradeoff in the uncertainties due to H and α. By judiciously selecting α

TABLE 7-1

Values of Equation (7.4-6)

GAS	$\alpha = 0.25$		$\alpha = 0.5$		$\alpha = 1.0$		$\alpha = 2.0$		$\alpha = 4.0$	
	A	B	A	B	A	B	A	B	A	B
OCS	0.44	0.11	0.25	0.25	0.11	0.44	0.04	0.64	0.01	0.79
CH_3I	0.89	0.003	0.78	0.01	0.65	0.04	0.46	0.10	0.26	0.24
$CHCl_3$	0.94	0.001	0.88	0.004	0.78	0.01	0.62	0.04	0.43	0.12
CCl_4	0.64	0.04	0.44	0.11	0.25	0.25	0.11	0.44	0.04	0.64
CH_3CCl_3	0.49	0.09	0.29	0.21	0.14	0.40	0.05	0.59	0.02	0.76
F-11	0.25	0.25	0.11	0.44	0.04	0.64	0.01	0.79	0.003	0.88
F-12	0.08	0.51	0.03	0.69	0.008	0.83	0.002	0.91	0.0006	0.95

$$A = \frac{1}{(1 + \alpha H)^2} \qquad B = \left(\frac{H\alpha}{1 + \alpha H} \right)^2$$

large uncertainties due to α or H can be minimized. Table 7-1 also shows that for highly soluble gases such as CH_3Cl, B will be very small, so large uncertainties in the air-water ratio, α, can be tolerated without a significant contribution to the total uncertainty.

In Table 7-2 an α value of 1.0 was selected and some typical values of $\tilde{\sigma}_{C_{gl}}$, $\tilde{\sigma}_H$, and $\tilde{\sigma}_\alpha$ for various gases were used to calculate $\tilde{\sigma}_{C^*_D}$ from equation (7.4-6). The value of $\tilde{\sigma}_{C^*_{gl}}$ is the uncertainty in the gas measurement, which is less than 10% for all gases listed. The values for $\tilde{\sigma}_H$ were taken from Chapter 4. Values for $\tilde{\sigma}_\alpha$ can be estimated to be about 0.25, which represents a typical "filling" error in the vacuum extraction flasks. One important course of uncertainty not included in the equation is from instabilities of the gases in the sample bottles resulting from production or loss mechanisms. These will be dealt with in Chapter 8.

Table 7-2 shows that the total uncertainty for the extraction flask is about 20% for most gases. The uncertainty is higher for the more soluble gases as would be expected since the distribution would favor more of the gas being in the water than in the headspace. For gases such as the fluorocarbons the fill ratio α is an important parameter since the uncertainty in α is multiplied by a larger B^2 than the other gases.

TABLE 7-2

Uncertainties in 1:1 Vacuum Extraction Flask Measurement of Gases in Seawater (Equation (7.4-6))

GAS	A^2	B^2	$\tilde{\sigma}_{C_{gl}}$	$\tilde{\sigma}_H$	$\tilde{\sigma}_\alpha$	$\epsilon^2_{C_{gl}}$	ϵ^2_H	ϵ^2	ϵ^2_T
OCS	0.11	0.44	0.10	0.15	0.10	0.01	0.003	0.004	0.15
CH_3I	0.65	0.04	0.10	0.15	0.10	0.01	0.015	0.0004	0.16
$CHCl_3$	0.78	0.01	0.05	0.40	0.10	0.0025	0.12	0.0001	0.35
CCl_4	0.25	0.25	0.10	0.40	0.10	0.01	0.04	0.003	0.23
CH_3CCl_3	0.14	0.40	0.05	0.30	0.10	0.01	0.013	0.004	0.16
F-11	0.04	0.64	0.05	0.25	0.10	0.0025	0.0025	0.006	0.10
F-12	0.008	0.83	0.05	0.50	0.10	0.0025	0.002	0.008	0.11

CHAPTER 8

STABILITY OF OCS IN SAMPLE CONTAINERS

8.1 Introduction

Since all of the data obtained on the distribution of OCS in the atmosphere and the ocean are based on samples that have been collected and shipped to the laboratory for analysis, it is important to determine how stable the samples are in the collection containers.

There have been several studies indicating that the OCS may react with stainless steel or glass (Farwell and Gluck, 1980) and with water (Thompson et al., 1935; Graedel et al., 1981). For this reason experiments were conducted using all of the containers that the OCS would come in contact with. Both air samples and seawater samples were tested for stability to ensure sample integrity.

8.2 Stability of OCS in 35 Liter Cryogenic Tanks

Of primary importance in studying the stability of OCS is to see how it behaves in the high pressure 35 L tanks containing cryogenically collected air which are used for long-term storage and as secondary standards for the calibration of the other samples.

A tank designated 0-100 was selected as the standard and was calibrated according to the procedure described in Chapter 5. To follow the stability of tank 0-100 and other tanks, a pool of four tanks was established. The same three tanks were analyzed against tank 0-100 at

about monthly intervals. The data and the standard deviation of the measurements are shown in Table 8-1. If there was a problem with tank stability, the values of the tanks would drift apart in the 8 months of the study, since it is unlikely that all four tanks would drift in the same manner. The actual percentage drift of the tanks from their initial value is shown in Figure 8.1. From the graph it can be seen that at no time did the tanks ever drift more than 5% from their initial concentrations, and at the end of the study they are tightly (within 1%) grouped around the initial concentration. The ±5% drifts which did occur appear to be random, thus containing no evidence that OCS is either systematically destroyed or created in the large high pressure 35 L tanks. Another indication of the stability of OCS in the 35 L tanks is that there is no systematic trend in a series of 22 tanks which were collected over a one-year period of time (see Appendix A).

From these two sets of data it is apparent that the 35 L tanks provide a stable sample that does not drift, at least over an 8-month period of time. For this reason they are ideal for long-term storage and for use as calibration standards.

8.3 Stability of OCS in Metal Sample Cans

The sample bottles and collection procedures were described in Chapter 6. Each of the sample bottles was tested for stability with zero air, a dry air standard, and real atmospheric samples collected using normal sampling procedures.

TABLE 8-1

35L Cryogenic Tanks - Stability Study

Date Analyzed	0-135		0-134		0-125	
	Conc. (pptv)	S (pptv)	Conc. (pptv)	S (pptv)	Conc. (pptv)	S (pptv)
04/01/81	444	± 7	391	± 4	324	± 14
05/12/81	462	± 13	398	± 12	322	± 5
07/18/81	437	± 3	387	± 6	322	± 4
09/08/81	449	± 5	378	± 9	323	± 2
10/13/81	466	± 19	--		--	
10/17/81	440	± 23	379	± 19	318	± 5
10/29/81	448	± 8	385	± 3	312	± 2
12/07/81	447	± 6	392	± 8	323	± 7

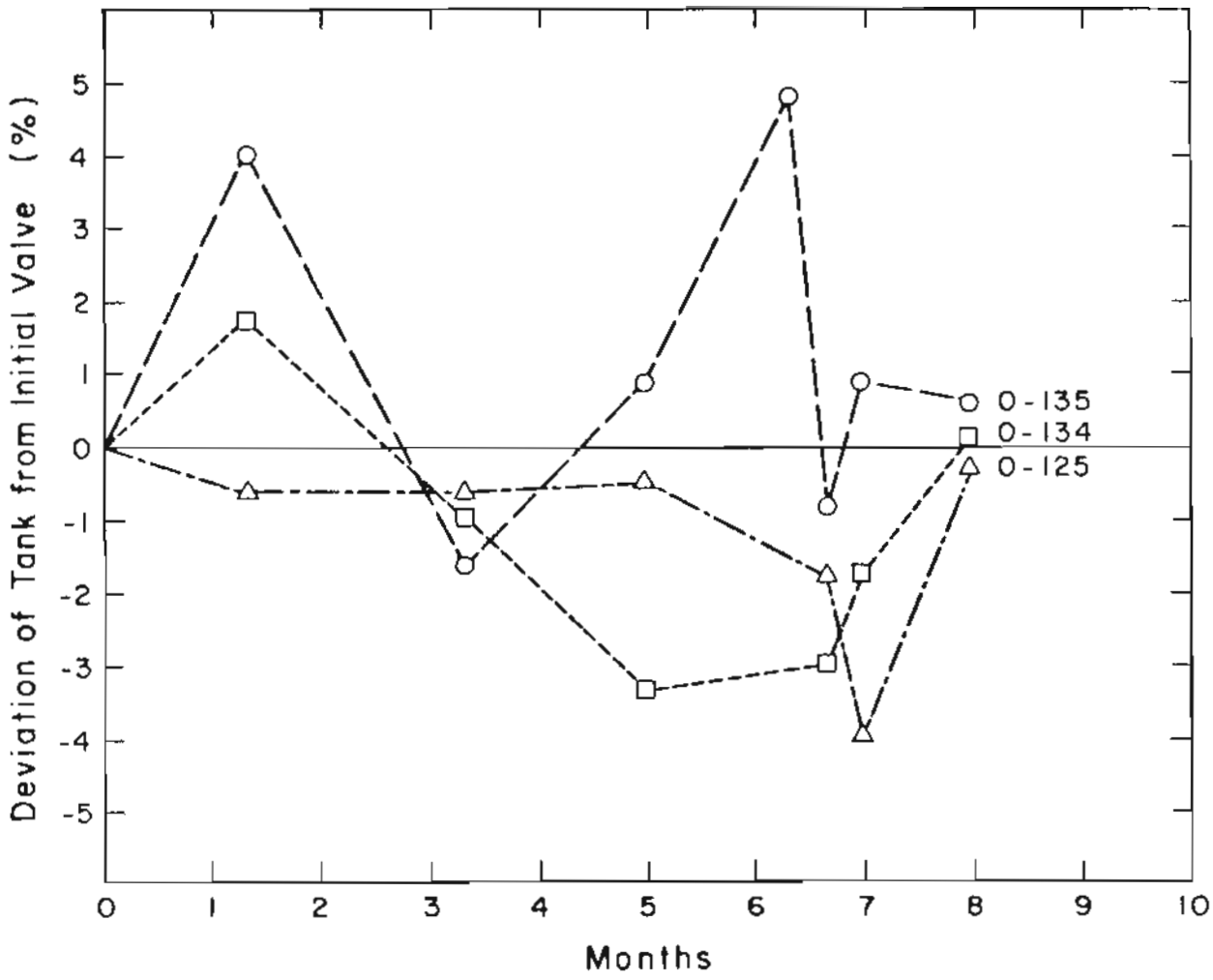

Figure 8.1. Long-term stability of OCS in 35 liter cryogenic tanks. Tanks are measured against the standard, 0-100.

The 1.6 L stainless steel bottles used for cryogenic sample collection were cleaned and baked out, then filled with zero air. The results after 21 days are shown in Table 8-2. In two of the three bottles there appeared to be significant change in OCS concentration, and in one bottle the growth was substantial. Additional bottles were filled with air from a 35 L tank which had already been analyzed. This air is exceptionally dry since all the water is removed from the tank after collection. The results of this study are shown in Table 8-3. The OCS level in some of the cans remained the same while in some of the others it increased or decreased. There did not appear to be any clear trend in the study or in the zero air studies. The stability of OCS did not appear to be suitable in dry, low pressure samples.

Next the 1.6 L bottles were filled with air samples using the cryogenic procedure described in Chapter 6. The samples were analyzed immediately after collection and then at later dates. The results are listed in Table 8-4. The first samples at Cape Meares, Oregon, increased by as much as 45% over a period of one month. However, this was observed for only two cans collected on the same day using a pump to flush the bottles. The other sets of samples showed only an average increase of 10% over one month. It is possible that contamination from the pump could have resulted in the two high values observed. The samples collected at the Oregon Graduate Center, Oregon (OGC), appear to be stable for a period of 18 days, after which they showed an average increase of 12% over a period of 1-2 months. The results indicate that most of the 1.6 L cryogenically collected samples are

TABLE 8-2

Zero Air Stability Studies

6 L Stainless Steel Cans (21 days)		
	S42	< 28 ppt
	S202	< 28
	S225	< 28
Glass Seawater Sampling Flasks (35 days)		
	G-33	< 28 ppt
	G-23	< 28
	G-5	< 28
1.5 L Stainless Steel Bottle (21 days)		
	C060	< 30 ppt
	C237	<316
	C190	< 28

TABLE 8-3

Stability of 1.6 L Bottle Filled with

Dry Air Standard

Bottle No.	Initial Conc. (pptv)	Conc. 17 days (pptv)
C236	385	382
C111	385	197
C022	385	197
C239	385	425
C269	385	412
C214	385	401

TABLE 8-4

Stability of 1.6 L Cryogenic Samples

Cape Meares, Oregon, collected 11/05/81:

Sample	0 Days	37 Days	53 Days	94 Days
C144	388 pptv	566 pptv	590 pptv	657 pptv
C176	358	510	561	592

Oregon Graduate Center, Oregon, collected 12/10/81:

Sample	0 Days	1 Day	18 Days	58 Days
C190	395 pptv	402 pptv	399 pptv	422 pptv
C060	411	418	410	449
C237	400	401	405	492

Oregon Graduate Center, Oregon, collected 12/31/81:

Sample	3 Days	37 Days
C269	338 pptv	392 pptv
C022	334	356
C111	345	376

Cape Meares, Oregon, collected 12/30/81:

Sample	1 Day	38 Days
C253	366 pptv	370 pptv
C173	362	444

stable, but some can grow in concentration. For this reason each sample should be analyzed twice, once just after collection and a second time about one month later. Actual cryogenic samples collected on the Pacific and Atlantic cruises (Appendix A) were analyzed several times after collection, and the OCS concentrations were found to have increased slightly but not enough to contribute to the total uncertainty in the calculated ocean flux (see Chapter 4).

The 6 L stainless steel cans were baked and filled with zero air. The results are shown in Table 8-2. Over the 21 days of the study there was no generation of OCS by the cans. Additional cans were filled with dry air from a 35 L tank and analyzed 19 days later. The data in Table 8-5 show that 3 of the cans were very stable, and the 4th can decreased 7% in concentration. These cans appear to be stable when filled with dry air. Cans from the NOAA Pacific Cruise (Appendix A) were studied two and three months after they were first analyzed. All of the samples showed an increase in concentration, up to 30%; again this increase does not significantly affect the calculated OCS flux.

8.4 Stability of Seawater Samples in Glass Bottles

The glass sampling bottles, described in Chapter 7, for the sampling and analysis of seawater were tested for their stability. First the bottles were checked by baking and evacuating them, and then filling them with zero air. The results in Table 8-2 show no production of OCS by the bottles.

TABLE 8-5

Stability of 6 L Stainless Steel Cans Filled with Dry Air Standard

Can No.	Initial Conc. (pptv)	Conc. 19 days (pptv)
S26	385	372
S180	385	387
S209	385	357
S14	385	389

To simulate the actual conditions of sample collection and storage, bottles were filled with seawater, partially degassed by vacuum, and then repeatedly equilibrated with air of a known concentration from a standard tank. The bottles were then frozen and analyzed 21 days later. The results shown in Table 8-6 suggest that under these collection procedures the gas concentration in the seawater decreased only 9% on the average with a relative standard deviation of 17%. At the bottom of Figure 8.6 the average and standard deviation for the analysis of the bottles just before the final pressurization are given. These data show that even without storage there is an uncertainty of about 12% (one standard deviation) due to the equilibration process. These data demonstrate that the freezing process effectively preserves the OCS in the seawater samples until the time of analysis to within about 10 to 20% of the initial value.

Additional preservative methods were tested to see if a procedure could be found other than freezing the samples. (Acidification to a pH < 2 was tried, and the concentration of OCS increased greatly in 3 days. The reason for the increase is not known.) The results in Table 8-7 show that the addition of mercuric chloride ($HgCl_2$) resulted in a decrease in OCS concentration over a 7-day period. This was probably due to loss by the reaction of OCS with seawater. With no preservative in the bottles the concentration was found to decrease rapidly, probably by reaction with seawater, as for the $HgCl_2$ addition.

TABLE 8-6

Stability of Seawater in Glass Bottles

Bottles filled with seawater saturated with O-186. Headspace filled with O-186 and tested for equilibration.

Bottle No.	Initial Concentration 12/12/81	Final Concentration 01/03/81
9	400	313
11	400	310
31	400	371
21	400	437
39	400	317
7	400	442

$\bar{x}$ = 365 ppt S = 61.9 ppt

$\frac{S}{\bar{x}}$ = 17%

Before final pressurization:

$\bar{x}$ = 306 S - 37.6

$\frac{S}{\bar{x}}$ = 12.2% ← Bottle filling variability

TABLE 8-7

OCS Seawater Stability

Measured Initial Concentration: 1,180 pptv *

Calculated Initial Flask Concentration: 1,180 pptv

Acidification (< pH2) 3 days

9,170 pptv		
9,610		
10,000	$\bar{C}_\ell$ = 9,950 pptv	

$HgCl_2$ 7 days

140 pptv		
130		
145	$\bar{C}_\ell$ = 138 pptv	S = 8 pptv

No Preservative 3 days

698 pptv		
935		
900	$\bar{C}_\ell$ = 840 pptv	S = 130 pptv

No Preservative 7 days

280 pptv		
230		
140	$\bar{C}_\ell$ = 220 pptv	S = 71 pptv

* Concentration measured using vacuum extraction flask and calculated using equation (7.3-12).

The results of these studies indicate that freezing the samples is the best method of preservation for the OCS, and probably works well for other gases produced in the ocean. Using this procedure, the measured concentrations will be within 20% of the actual seawater concentration for OCS.

CHAPTER 9

MEASUREMENT OF THE HENRY'S CONSTANT FOR OCS IN SEAWATER

9.1 Introduction

The Henry's constants for substances which are gases at room temperature have historically been determined as the solubility of the pure gas at a pressure of about one atmosphere. The solubility is usually reported as the Bunsen solubility coefficient (β) or the Ostwald adsorption coefficient (α), which were discussed in Chapter 3. The solubility can be measured by either physical or chemical methods. Excellent reviews of solubility measurements have been written by Markham and Kobe (1941) and Battino and Clever (1966).

The early solubility measurements were made using physical methods to measure the volume of gas absorbed by a liquid. For this method gas-free water must be prepared. The widely adopted procedure for this has been to boil the water and then cool it under a vacuum. Usually trace amounts of the gas or other gases do not lead to serious errors since high concentrations are used. A known volume of the gas-free water is then brought into contact with a measured volume of the pure gas at about 1 atmosphere pressure in a constant temperature bath. The gas and water are mixed until they reach equilibrium, and the final volume of gas is measured. The difference in the gas volume is equal to the amount dissolved in the liquid. The volume is adjusted to STP and reported as the Bunsen solubility coefficient.

More recently Douglas (1964) and Weiss (1971) used a microgasometric procedure to measure the solubility of gases in distilled water and seawater. The procedure is basically the same as the physical method described above, but was specially modified to use a smaller volume of water and give high precision results in less time. In their procedure pure gas which had been saturated with water is separated from degassed water by mercury. To start the experiment, the apparatus is tipped and the gas and water mix, leaving the same total volume in the system. A micrometer is used to adjust the mercury level to determine the amount of gas absorbed by the water, and when the experiment is done, the micrometer is used to determine the total water volume. The gas volume is reduced to STP and reported as the Bunsen solubility coefficient.

One source of error in the physical absorption procedure is the expansion of the liquid due to the dissolving of the gas. This can be corrected by using the molar volume of the gas. Weiss (1971) found that this effect amounted to only a 0.1-0.2% change in the solubility data. Since the solubility is dependent on temperature, a water bath is used to control the temperature, and solubility measurements are made over a range of temperatures (0-40°C). Solubility is also a function of ionic strength, so in seawater it is often measured at various salinities. The seawater was prepared by dilution with distilled water or by evaporation to give salinities between 20 o/oo and 40 o/oo,

Since the physical methods measure volume differences, the resulting solubilities can be determined very precisely (four significant figures). The difficulty with the procedure is that the measurements are made at about 760 torr partial pressure of the gas, and in the actual environment the concentration is often at the parts per billion level. The ability of Henry's law to hold over these ranges for various gases is not well documented (Meadows and Spedding, 1974).

An alternative to the physical methods, which require the use of pure gas, are the chemical methods, which actually measure the concentration distribution between the air and water. The solubility of CO was measured by Schmidt (1979) using the HgO method where CO reacts with HgO to produce mercury vapor, which was measured by atomic absorption. The solubility measurements were made by placing a distilled water or seawater sample in a temperature-regulated, water-jacketed cylinder. A standard gas of known concentration was bubbled through the solution until equilibrium was reached (30 minutes at a flow of 1 L/min). A water sample was removed and measured by headspace analysis, and the solubility calculated from the standard gas concentration and the headspace gas concentration. The precision of the measurements (about 7%) was not as good as the microgasometric method, but the results for CO were found to agree to within 10% with the physical methods. Schmidt (1979) concluded that the data for CO followed Henry's law down to the ppb range, but cautioned that the more soluble gases such as N_2O may not.

9.2 Experimental

To model the flux of OCS between the ocean and the atmosphere, the Henry's constant for OCS in seawater at various temperatures must be known. Table 3-4 shows that OCS solubility data exist for distilled water, but have to be estimated for seawater. As part of this project an apparatus similar to Schmidt's (1979) was constructed and used to measure the Henry's constant for OCS in seawater at various temperatures using air concentrations in the parts per billion range. The solubility data of different temperatures will then be fitted using equation (3.2-19). A diagram of the apparatus is shown in Figures 9.1 and 9.2. One portion is a water-jacketed equilibrium sparging column where the air standard and water sample are brought to equilibrium. The other part is a vacuum extraction flask for the analysis of the gas in water, as described in Section 9.7.

The jacketed sparging column is built around a 1 L graduated cylinder accurate to ±2 mL. The water jacket is connected to an NBS Model G67 and RF10 refrigerated shaker bath which controls the temperature to ±0.05°C. The bottom of the cylinder has a fritted gas diffuser to achieve maximum air-water contact and mixing in the cylinder. The thermometer at the top of the cylinder monitors the temperature during the equilibration process.

Measurement of the liquid concentration in the purging column in equilibrium with the gas concentration is done using the vacuum

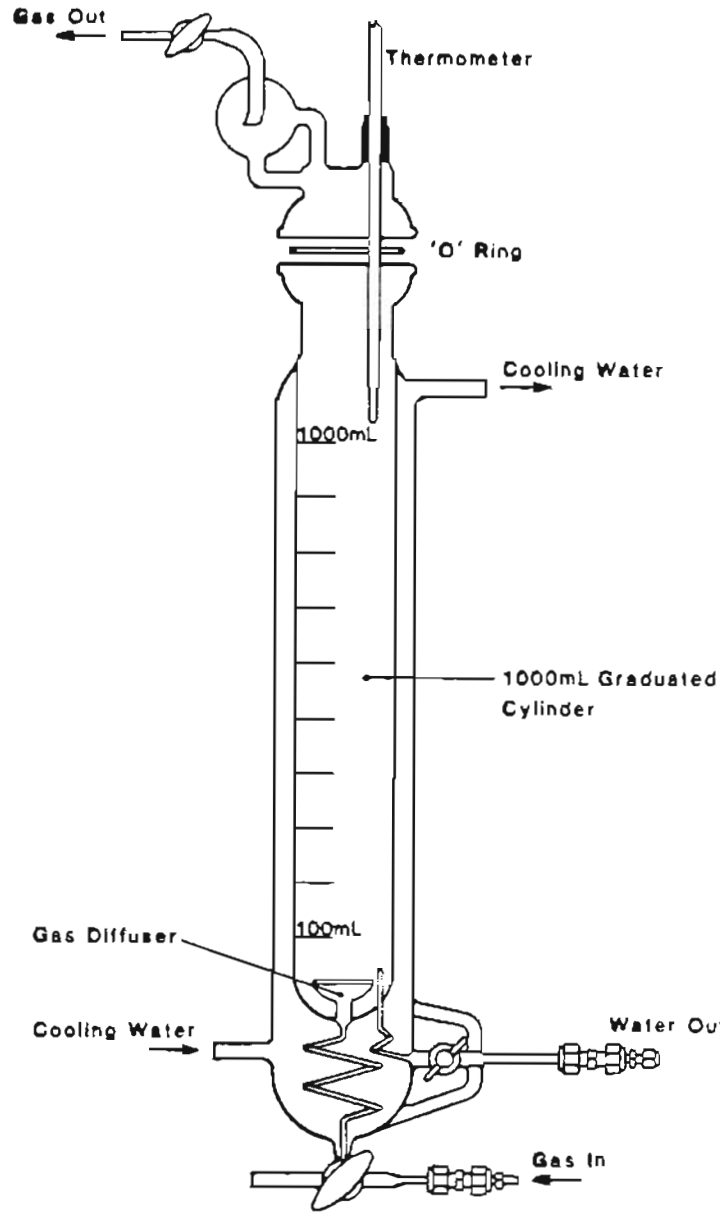

Figure 9.1. Equilibration column for measuring Henry's constant and the preparation of solutions of known gas concentration.

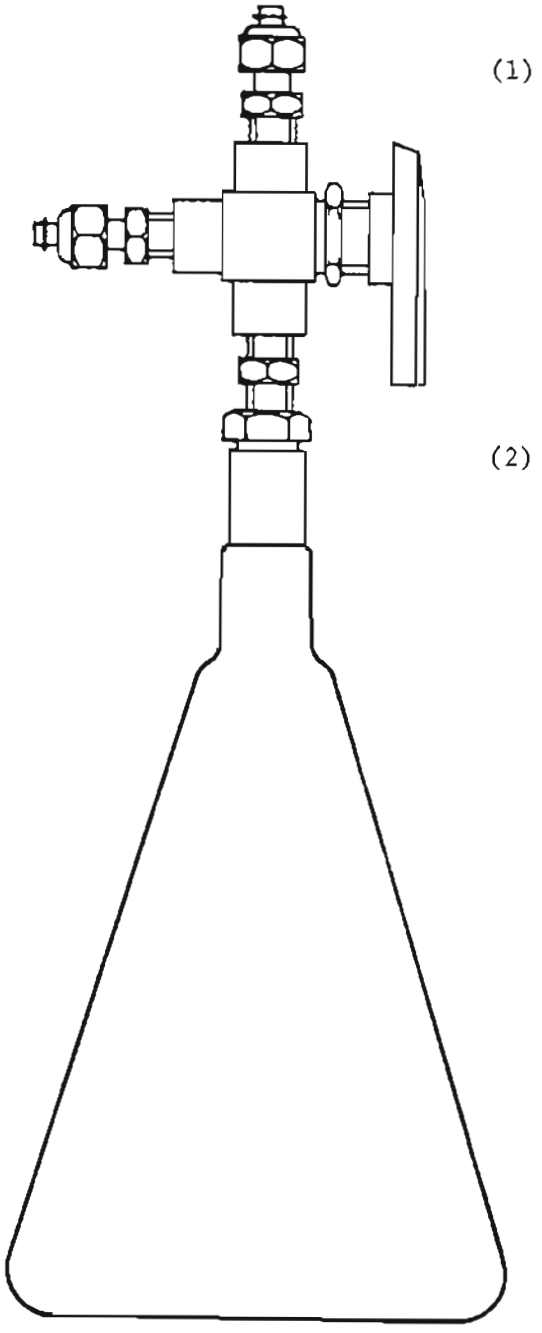

Figure 9.2. Vacuum extraction flask with 3-way ball valve for the measurement of the Henry's constant.

extraction flask. When the ball valve on the vacuum flask (Figure 9.2) is in the 1st position, the valve and connecting line can be purged. In the 2nd position the solution can run into the flask.

A standard OCS gas sample in the ppbv range was prepared by cryogenically collecting a known volume of commercially prepared OCS standard and an appropriate dilution volume of zero air in a 35 L SUMMA® polished stainless steel container at a pressure of 150 psi. This is equivalent to about 350 L at 1 atm pressure. The gas dilution was calibrated against stable laboratory OCS standards. The standardized OCS sample is then used with the equilibrium sparging column to establish an equilibrium concentration in the solution.

To measure the Henry's constant, the equilibrium sparging vessel is first filled to about 50 mL above the zero mark with the water to be studied. The standard gas is bubbled through the solution at a rate of 1 L per minute for 30 minutes. At the end of this time period the gas was tested and found to be in equilibrium with the water at the desired temperature. The gas flow is shut off and the water is lowered to the zero mark by flushing through the connecting line and the 3-way valve on the vacuum extraction flask. The valve is turned to position 2, and the volume of equilibrated water (about 700 mL) needed to get a 1:1 extraction is sucked into the vacuum flask. The flask is accurately pressurized to about 15 psi with a Valadyne pressure gauge accurate to 1 torr.

The vacuum flask is used to measure the liquid concentration (C_ℓ) using equation (7.3-12), which gives C_ℓ (C_o^*) in terms of the headspace gas concentration (C_{g1}^*), with $\alpha = 1$.

$$C_\ell = \frac{C_{g1}^* (H+1)}{H} \tag{9.2-1}$$

The liquid concentration in the sparging column is related to the gas concentration (C_g) by Henry's law.

$$C_\ell = \frac{C_g}{H} \tag{9.2-2}$$

These equations can be set equal to each other and solved for H:

$$H = \frac{C_g - C_{g1}^*}{C_{g1}^*} \tag{9.2-3}$$

This gives H in terms of the headspace gas concentration (C_{g1}^*) and the standard tank concentration (C_g). Notice that the absolute calibration of the standard does not enter the calculation using this method.

Seawater for the solubility measurements was collected from the Oregon coast. The salinity of the water was found to be approximately 35 o/oo. This water was filtered through a coarse cellulose filter to remove any large material and placed in the sparging column without any additional treatment. Experiments on the extraction flasks show that

over the time periods used to make the measurements, biological activity is not important at a 2 ppb level.

Using equation (9.2-3) the Henry's constant for OCS in seawater has determined at four different temperatures. Duplicate data points were collected for each temperature. The results are shown in Table 9-1. These data were used to obtain a least squares fit of the Henry's constant against temperature using the first three terms of equation (3.2-19).

$$\ln H = A_1 + A_2 \left(\frac{100}{T}\right) + A_3 \ln \left(\frac{T}{100}\right) \qquad (9.2\text{-}4)$$

The results of the fitting program are listed in Table 9-2 and plotted in Figure 9.3. The figure also shows the 4 original data points to provide a comparison of the fits and the values for A_1, A_2, and A_3. The figure shows a comparison of the seawater values and the distilled water values obtained by Winkler (see Seidell, 1940). This graph shows that the seawater values of H are about 20% higher than the distilled water values, which is the difference generally found for most gases (see Table 3-3).

TABLE 9-1

Henry's Constant for OCS

Experimental

T°C	T°K	$\bar{H}$ *
10	283	1.5
15	288	1.9
20	293	2.2
25	298	2.7

*Average of 2 measurements.

TABLE 9-2

Henry's Constant for OCS in Seawater

Interpolated Values (±10%) *

T(°C)	T(°K)	H
0	273	1.0
1	274	1.0
2	275	1.1
3	276	1.1
4	277	1.2
5	278	1.2
6	279	1.3
7	280	1.3
8	281	1.4
9	282	1.5
10	283	1.5
11	284	1.6
12	285	1.7
13	286	1.7
14	287	1.8
25	288	1.9
16	289	2.0
17	290	2.0
18	291	2.1
19	292	2.2
20	293	2.3
21	294	2.4
22	295	2.4
23	296	2.5
24	297	2.6
25	298	2.7
26	299	2.8
27	300	2.9
28	301	3.0
29	302	3.1
30	303	3.2

* Data of Table 9-1 fitted using equation (9.2-4).

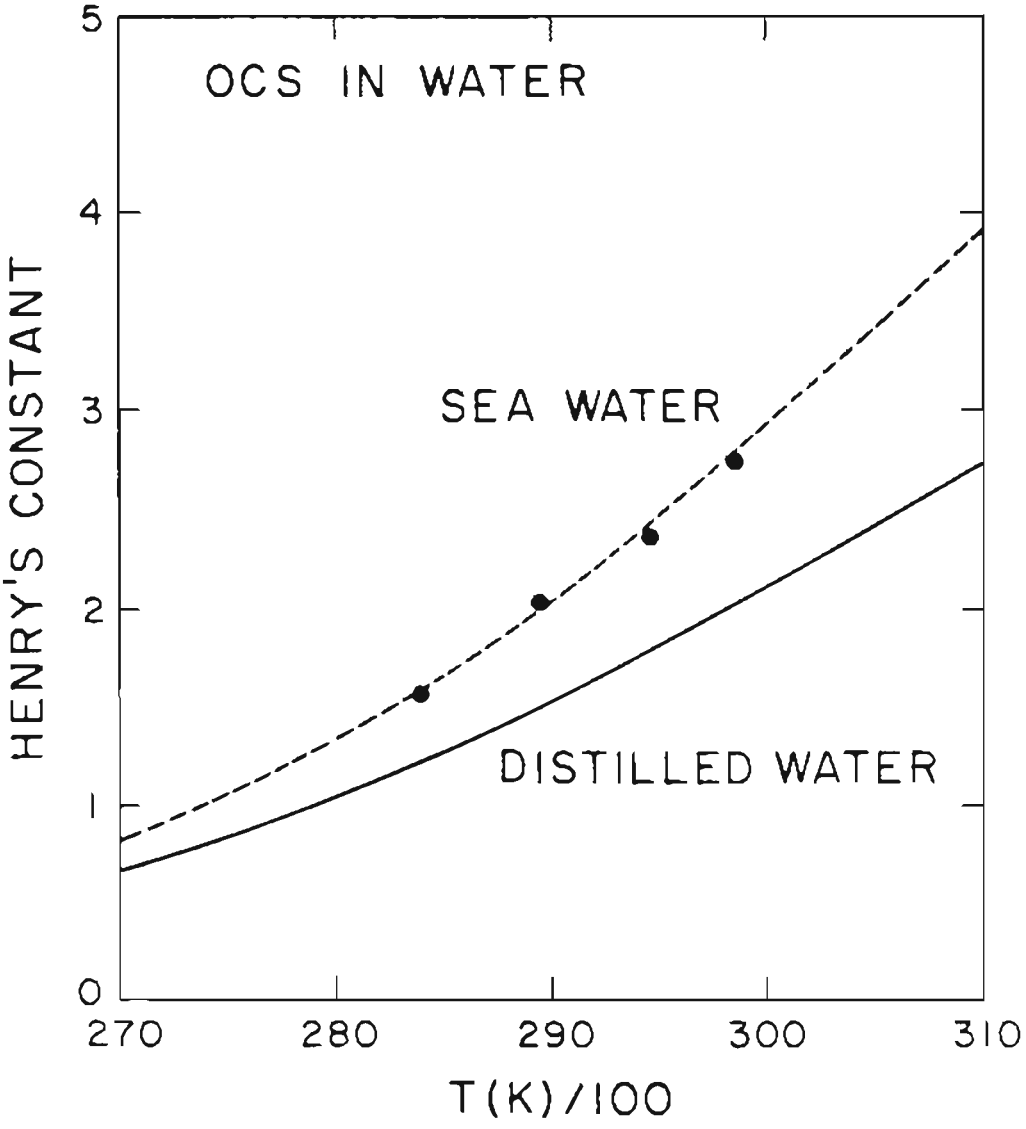

Figure 9.3. Variation of Henry's constant with temperature for seawater and distilled water. The distilled water values were from Seidell. The points indicate the experimentally measured values.

CHAPTER 10

MEASUREMENT OF THE OCEAN FLUX OF OCS, CH_3I, $CHCl_3$, CCl_4, CH_3CCl_3, F-11, F-12, PCE

10.1 Trace Gas Flux Calculations

The determination of the flux of a trace gas to or from the ocean is important in understanding how oceans can affect atmospheric composition and the environment. Recently it has been realized that man's activities can produce substantial quantities of gases that can modify the earth's climate or other features such as the stratospheric ozone layer. These effects have been reviewed in several publications (Kellogg, 1980; Kellogg and Schware, 1981; Hansen et al., 1981; NAS, 1979). To calculate how trace gases can change in concentration, models have been developed utilizing data on the sources and sinks of these gases. Because of its size the ocean has often been considered to be an important sink for gases such as CO_2, OCS, and the chlorofluoromethanes (Bolin, 1960; Revelle and Suess, 1957; Rowland, 1979; Junge, 1976; Gammon et al., 1982). To actually determine whether the ocean is a source or a sink and its magnitude, a model along with actual data collected at various locations in the ocean must be used.

Using the two-film model described in Chapter 2 with the sampling and analysis procedures of Chapters 5-8, the ocean flux of the trace gases OCS, CH_3I, $CHCl_3$, CCl_4, CH_3CCl_3, F-11, F-12, TCE, and PCE was calculated. The locations where the air and seawater samples were

collected will be described along with the physico-chemical parameters used in the model. The importance of the ocean flux is then discussed in terms of other sources or sinks for these gases.

The oceanic flux, F, of the trace gases was calculated using the two-film air-sea exchange model described in Section 2.2:

$$F = K_\ell\left(\frac{C_g}{H} - C_\ell\right) \qquad (2.2\text{-}9)$$

The Henry's constant, H, was taken from Tables 3-3 and 9-2. The overall transfer coefficient, K_ℓ, was calculated from equation (2.2-8b):

$$\frac{1}{K_\ell} = \frac{1}{k_\ell} + \frac{1}{Hk_g} \qquad (2.2\text{-}8b)$$

k_ℓ was taken to be the average of the experimentally determined liquid transfer coefficients measured by Peng et al. (1979), which is 12 cm/hr for Rn. This value was adjusted for other gases as described in Chapter 3, and the values of k_ℓ for the gases are shown in Table 3-4. The value of k_g was taken as 1000 cm/hr. Putting these data and the value of H at 20°C into equation (2.2-8b), a value of K_ℓ was calculated. The results are shown in Table 10-1.

The atmospheric concentration, C_g, of the gases studied can be obtained from their latitudinal profiles, and do not have to be collected at exactly the same time or location as the water samples, since experience has shown that atmospheric concentrations of long-lived

TABLE 10-1

Transfer Coefficients

Gas	K_ℓ (cm/hr)
OCS	12
CH_3I	11
$CHCl_3$	9
CCl_4	8
CH_3CCl_3	7
F-11	8
F-12	8
PCE	7

Values of K_ℓ are based on Table 3-4 calculated using the Radon values of Peng et al. (1979) and corrected using equation (2.2-8b).

gases are uniform in each hemisphere due to rapid mixing, and any seasonal fluctuations are too small to be of significance (Torres et al., 1980; Pierotti et al., 1980; Rasmussen et al., 1982c). The values of C_g were determined by averaging all of the available air sample data for each of the gases. The concentrations are reported as parts-per-trillion by volume adjusted to 25°C.

The value of the seawater concentration, C_ℓ, at each sampling location was used in equation (2.2-8), since the ocean concentration is not uniform and H will vary with temperature. C_ℓ is reported as parts-per-trillion by volume, with the gas volume adjusted to 25°C for direct comparison with the air samples. The seawater samples were collected in a vacuum extraction flask and analyzed for the gas content using the methodology described in Chapters 5 and 7. The single extraction procedure was used in all cases and the seawater concentration calculated using equation (7.3-12):

$$C_\ell = \frac{C_{g1}(\alpha H+1)}{H} \qquad (7.3\text{-}12)$$

All extractions were set up with a gas to liquid ratio, α, of 1.

A flux was calculated for each seawater sample using the value of C_ℓ, the average value of C_g for that latitude, and the value of H corresponding to the temperature of the seawater at the time of collection (Appendix A). The samples were grouped according to biological productivity area, since biological activity is often responsible for

the flux (this was not necessary for purely anthropogenic gases) (Rasmussen et al., 1982d; Lovelock et al., 1972; NAS, 1975). The sampling locations are shown in Figures 10.1 and 10.2.

10.2 Carbonyl Sulfide

Carbonyl sulfide (OCS) has recently been recognized as an important trace atmospheric gas because it is the most stable sulfur gas in the troposphere and has a long lifetime. For this reason it is now thought that OCS may be responsible for maintaining the stratospheric sulfate layer (Crutzen, 1976), and changes in its concentration could cause a change in the radiation balance and global climate.

The stratospheric sulfate layer was first discovered by Junge et al. (1961) and has been of interest because of its potential effect on the earth's climate. The layer is at an altitude of 15 to 30 km and is composed of water-sulfuric acid droplets. It was first thought that the sulfate aerosol was formed from conversion of sulfur dioxide (SO_2) adsorbed by water droplets and oxidized (Scott et al., 1969; Friend, 1973; Castleman et al., 1975). Since it is unlikely that the SO_2 can cross the cold trap at the tropopause and enter the stratosphere, it was postulated that major volcanic eruptions directly injected SO_2 into the stratosphere and might be responsible for the layer (Lazrus et al., 1979; Castleman, 1973; Cronin, 1971).

OCS was first measured in the troposphere by Hanst et al. (1975) using infrared spectrometry, and later by other groups using gas chromatography (Sandalls and Penkett, 1977; Maroulis et al., 1977;

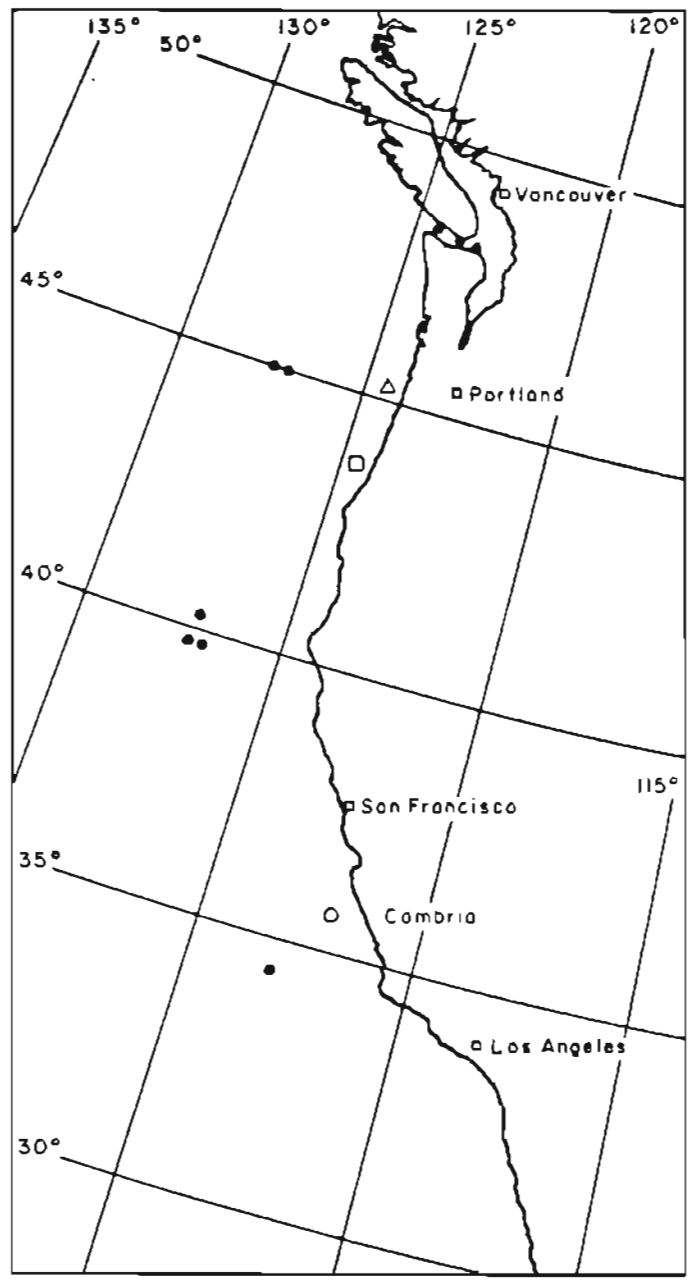

Figure 10.1. Sites where samples were collected by fishing boat (open circles) and by Scripps Institution coastal cruise (solid circles).

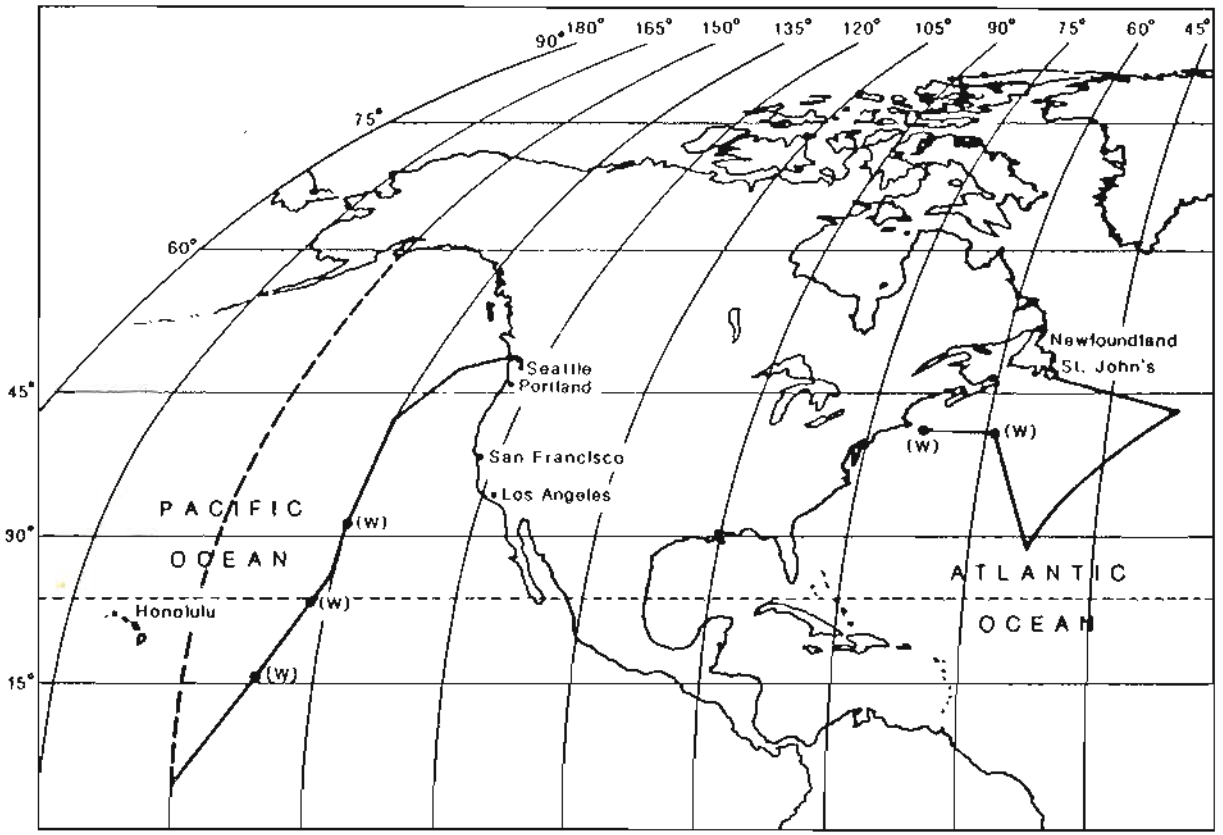

Figure 10.2. Site locations for seawater samples collected on Atlantic and Pacific oceanographic cruises.

Rasmussen et al., 1982c; Torres et al., 1980). The average values of the measurements along with the locations are shown in Table 10-2. Using the data of Hanst et al. (1975), Crutzen (1976) was able to calculate that the stratospheric sulfate layer could be maintained by the photodissociation of OCS and have transient variations due to volcanic sulfur emissions. Turco et al. (1980) showed that the stratospheric sulfate layer was more sensitive to OCS than SO_2 or CS_2. All of this information, with the recent findings of Rasmussen et al. (1982a) which show that the dominant gases following the reuption of Mt. St. Helens, Washington, were OCS and CS_2, suggests that OCS may be the gas which controls the sulfate layer. For this reason it is important to understand what the sources and sinks are in order to evaluate what potential climatic implications this species may have. If OCS were found to be increasing due to increased anthropogenic emissions, i.e., combustion, wood burning (Crutzen et al., 1979), auto exhaust, then there is a potential for global cooling due to an increase in the amount of aerosol in the stratosphere.

Using the atmospheric values shown in Table 10-3 and the estimated sources listed in Table 10-4, global budgets were proposed for OCS indicating a lifetime of about one year (Turco et al., 1980; Kurlo, 1978). These estimates of the lifetime were based on the reaction of CS_2 with hydroxyl radical (OH) as the major source and the subsequent reaction of OCS with OH as the major sink:

TABLE 10-2

Atmospheric OCS Concentration

Average Concentration (pptv)	Location	Reference
200	East Coast	Hanst et al. (1975)
510	Harwell, England	Sandalls & Penkett (1977)
466	S.W. & Eastern U.S.	Maroulis et al. (1977)
512	GAMETAG Flights	Torres et al. (1980)

TABLE 10-3

Atmospheric OCS Measurements

Average Conc. (pptv)	Location	Reference
200	East Coast, USA	Hanst et al. (1975)
510	Harwell, England	Sandalls and Penkett (1977)
466	Southwest and Eastern USA	Maroulis et al. (1977)
512	GAMETAG Data	Torres et al. (1980)

TABLE 10-4

Non-Oceanic Sources of OCS

Source	Average Flux (Tg/yr)	
$CS_2 + OH \rightarrow OCS + SH$	1 - 2	(a)
Soils	0.02 - 0.2	(b)
Biomass burning	0.2 - 0.45	(c)
Anthropogenic	0 - 1	(d)
Total Average	2.5 Tg/yr	

(a) Kurylo (1978); Leu and Smith (1981); Ravishankara et al. (1980); Sze and Ko (1979), (1980), (1981); Molina et al. (1981); Jones et al. (1979); Wine and Ravishankara (1982).

(b) Aneja (1979); Adams (1981).

(c) Crutzen et al. (1979).

(d) Anthropogenic contribution must be small since there is no significant Northern-Southern Hemisphere difference in concentration (Khalil and Rasmussen, 1980; Khalil, 1979).

$$CS_2 + OH \rightarrow OCS + SH$$

$$OCS + OH \rightarrow CO_2 + SH$$

Recently there has been some controversy over the reaction rate of CS_2 with OH because the reaction is apparently catalyzed by O_2. It is now thought that CS_2 may be responsible for about 1-2 Tg/yr OCS (Jones et al., 1982; Wine and Ravishankara, 1982), but the OCS reaction with OH is too slow to be a sink for OCS in the troposphere (Atkinson et al., 1978; Cox and Sheppard, 1980; Ravishankara et al., 1980; Leu and Smith, 1981).

This means that the OCS budgets previously proposed with a lifetime of one year are no longer valid. In the ensuing search for an OCS sink, the ocean has been proposed because of the alkaline hydrolysis reaction of OCS with seawater (Rowland, 1979; Turco et al., 1980). This reaction has been studied by Thompson et al. (1935) and Phillip and Dautzenberg (1965) and found to give a rate of 4.8×10^{10} exp (-6643/T) liters $mole^{-1}$ s^{-1}. This would be responsible for a lifetime of 2.8 days in the ocean. However, it can be shown that the rate limiting step for the ocean sink is not the hydrolysis reaction but rather the transfer rate of OCS to the ocean, which would give OCS a lifetime of 11 years.

Because many sulfur compounds including OCS have biogenic sources (Adams et al., 1981; Aneja et al., 1979; Adams et al., 1979) and the ocean has been found to be a source for sulfur compounds such as dimethylsulfide (DMS) and carbon disulfide (CS_2)(Lovelock et al.,

1972; Lovelock, 1974), it was decided to investigate whether the ocean was also a source for OCS.

The value of C_g for OCS was determined using data from air samples collected in stainless steel bottles according to the procedures described in Chapter 6. The results are shown in Figure 10.3 (detailed data tables are in Appendix A). The data points are shown for the different types of containers used to collect the samples. This arrangement was selected for OCS because the stability studies indicated that different types of sample bottles have different stability (Chapter 8).

To measure if there was any significant difference between air samples collected in different containers, a "t" test was run on the average concentrations for each set of bottles. This can be done because the atmospheric concentration of OCS is uniform and does not vary much with latitude (Torres et al., 1980). The average concentrations are shown in Table 10-5. Table 10-6 shows that there is no significant difference ($\alpha = 0.1$) in air samples collected in the 1.6 liter cryogenic bottles and low pressure bottles, but there is a significant difference ($\alpha = 0.1$) between these bottles and the 35 liter cryogenic tanks. This was expected because the stability studies showed that the 35 liter cryogenic tanks gave the best long-term stability, while the other bottles often showed a slight increase ($\sim$20%).

Based on the results of the "t" test the data for the 1.6 liter cryogenic bottles and the low pressure bottles were combined to give one average value which represents an upper limit to the OCS

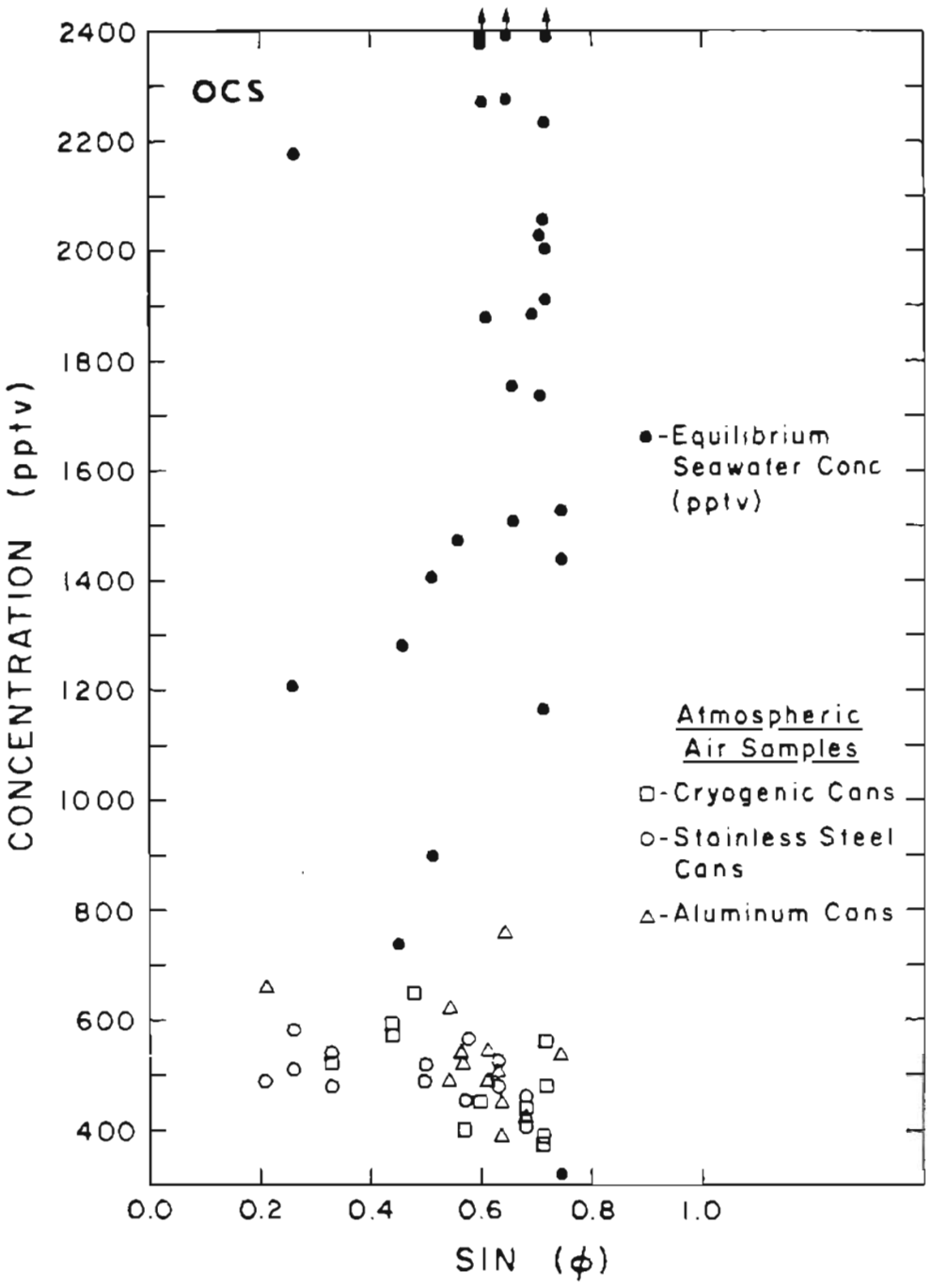

Figure 10.3. Atmospheric and equilibrium seawater concentrations of OCS.

TABLE 10-5

Average OCS Concentrations in Air Samples

1.6 Liter Stainless Steel Cryogenic Cans

$\bar{C}_g$ = 498 pptv s = 91 pptv n = 11

Low Pressure Cans

$\bar{C}_g$ = 517 pptv s = 77 pptv n = 26

35 Liter Stainless Steel Cryogenic Tanks

$\bar{C}_g$ = 417 pptv s = 48 pptv n = 20

Average of 1.6 liter Cans and Low Pressure Cans

$\bar{C}_g$ = 505 pptv s = 75 pptv n = 37

TABLE 10-6

Test for Significant Difference in Concentrations

in OCS Sample Bottles

	Significant Difference ? (α = 0.1)		
	1.6 Liter Cryo	Low Pressure Cans	35 Liter Cryo
1.6 Liter Cryo	--	No	Yes
Low Pressure Cans	No	--	Yes
35 Liter Cryo	Yes	Yes	--

atmospheric concentration. The OCS flux will be calculated using both the average of the 35 liter cryogenic tank data and the average of the other sample bottles. These values for C_g are shown in Table 10-5.

The seawater concentrations, C_ℓ, of OCS are listed in Appendix A. The samples are arranged according to productivity area, and the flux for each sample was calculated using the two average values of C_g, 417 pptv and 505 pptv. The fluxes for all samples in a productivity area were averaged and are shown in Table 10-7, along with the standard deviation of the flux.

A "t" test was used to determine if there is any significant difference ($\alpha = 0.1$) between the flux for the different productivity areas. The results at the bottom of Table 10-7 show that the two moderate groups, one collected from a fishing boat and the other from an oceanographic research vessel, are not significantly different. The low productivity area samples did show a significant difference. The data for the two moderate areas were combined and a new average calculated (Table 10-7).

The flux calculated using the 35 liter cryogenic tanks was compared to the flux calculated using the other pooled sample bottles, and it was found that there was no significant difference ($\alpha = 0.1$). Therefore, for the final flux determination the 35 liter cryogenic tank data were used to give the most conservative estimate of the flux. The total oceanic flux was calculated by multiplying the flux per cm^2

TABLE 10-7

OCS Ocean Flux Calculated by Productivity Area

Moderate Productivity (1) Fishing Boat Samples n = 10

35 Liter Cryo $F = (3.6 \mp 1.3) \times 10^{-11}$ $g/cm^2 \cdot hr$

Low Pressure $F = (3.5 \mp 1.3) \times 10^{-11}$

Moderate Productivity (2) Coastal n = 11

35 Liter Cryo $F = (2.9 \mp 1.7) \times 10^{-11}$

Low Pressure $F = (2.7 \mp 1.7) \times 10^{-11}$

Low Productivity n = 6

35 Liter Cryo $F = (1.3 \mp 0.6) \times 10^{-11}$

Low Pressure $F = (1.2 \mp 0.6) \times 10^{-11}$

Moderate (Combined) n = 21

35 Liter Cryo $F = (3.3 \mp 1.5) \times 10^{-11}$

Low Pressure $F = (3.1 \mp 1.5) \times 10^{-11}$

Test for Significant Difference Between Productivity Areas ($\alpha = 0.1$)

	M(1)	M(2)	L
M(1)	-	No	Yes
M(2)	No	-	Yes
L	Yes	Yes	-

by the total oceanic area of that productivity region, as shown in Table 2-2. The areas of the moderate and high regions were added together to calculate the combined region. The total oceanic flux for each region is:

$$\bar{F}_M = 0.6 \text{ Tg/yr}$$

$$\bar{F}_L = 0.2 \text{ Tg/yr}$$

The total oceanic flux is equal to the sum of these fluxes: 0.8 Tg/yr. A 90% confidence limit based on the standard deviation of the measurements in the particular region is equal to 0.1 Tg/yr, but the uncertainty from the propagation of error in the two-film model is 0.5 Tg/yr (Chapter 4). These results indicate that the ocean is a source of OCS with a total flux of about 0.8 ± 0.5 Tg/yr. When compared to other sources of OCS listed in Table 10-4, the ocean could be responsible for about 25% of the yearly flux.

10.3 Methyl Iodide

Methyl iodide (CH_3I) was first measured in the atmosphere and in seawater by Lovelock et al. (1973) when they reported a mean atmospheric concentration of 1.2 pptv and a mean ocean concentration of 135 pptv. Even though CH_3I is present at extremely low concentrations, it is believed to play an important role in atmospheric organic iodine chemistry (Cicerone, 1981; see also Chameides and Davis, 1980).

The ocean was found to a source of CH_3I by Lovelock et al. (1973) when they found high concentrations of CH_3I in seawater.

Lovelock (1975) also found CH_3I to be a product of marine algae and kelp, and that seawater concentrations in kelp beds had an average concentration of 120,000 pptv. Liss and Slater (1974) calculated an ocean flux of CH_3I of 0.27 Tg/yr, using the data of Lovelock et al. (1973), which suggested an additional source of gaseous iodine needed to make up the 1-2 Tg/yr flux that was calculated by Zafiriou (1974) to balance the gaseous iodine budget.

Extensive atmospheric methyl iodide measurements were made by Rasmussen et al. (1982d). 375 samples were collected at locations from the Arctic to the South Pole and averaged according to latitude. The results are shown in Figure 10.4 where the atmospheric concentration of CH_3I is shown to vary with latitude, with the highest concentration in the tropics. Exceptionally high values, 7-22 pptv, were found in air samples from regions of high biomass productivity where production of CH_3I would be expected to be the largest.

The equilibrium seawater concentrations are plotted in Figure 10.5, showing a flux of CH_3I from the ocean. The flux (per unit area) for the different productivity regions was calculated and is shown in Table 10-8. There is a significant difference ($\alpha = 0.1$) in the CH_3I flux for the three regions:

High Productivity
Flux = 0.06 Tg/yr
Moderate Productivity
Flux = 0.14 Tg/yr
Low Productivity
Flux = 0.05 Tg/yr

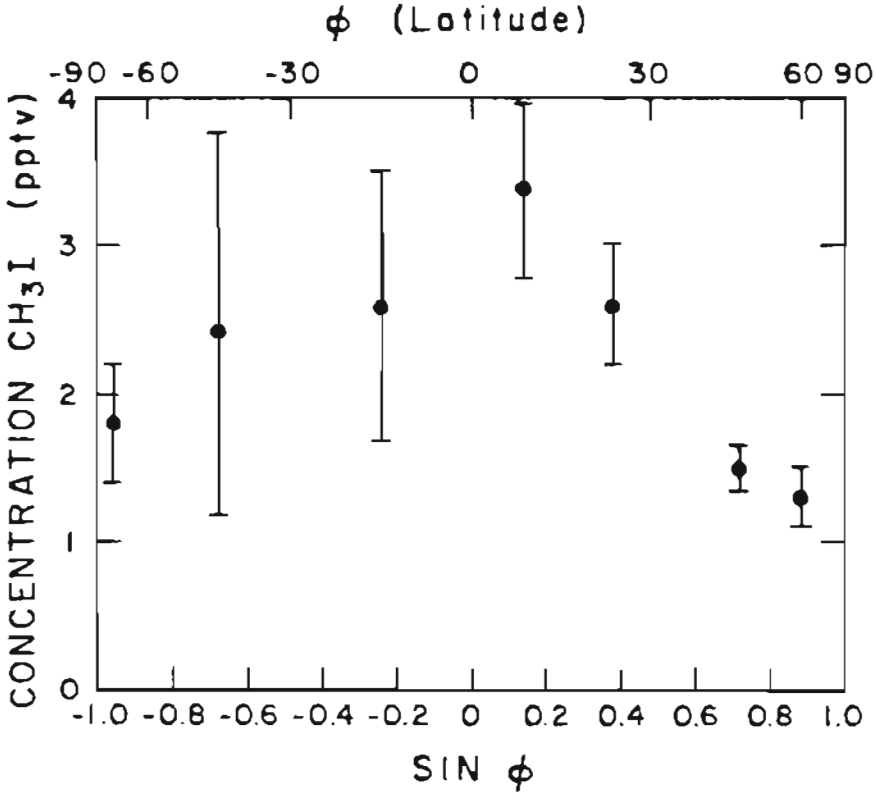

Figure 10.4. Variation in CH_3I concentration with latitude.

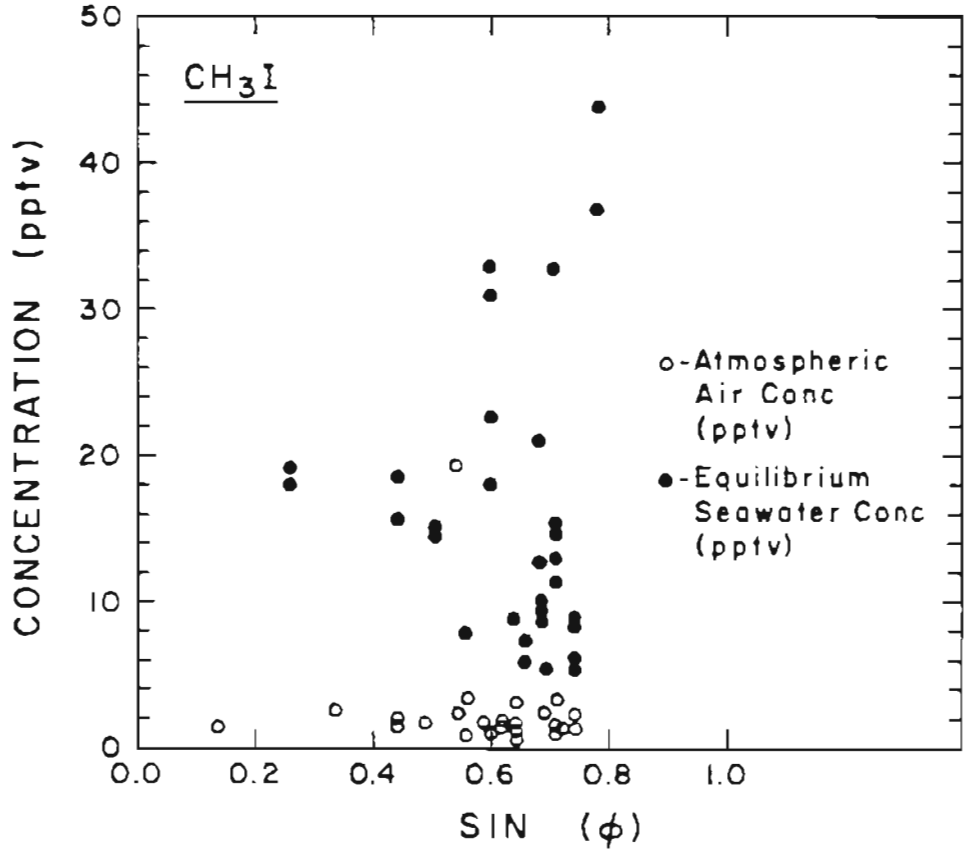

Figure 10.5. Atmospheric and equilibrium seawater concentrations of methyl iodide.

TABLE 10-8

CH_3I Flux from the Ocean Calculated

by Productivity Area

High n = 3

$F = (18.1 \mp 2.8) \times 10^{-12}$ g/cm^2 hr

Moderate n = 8

$F = (8.8 \mp 3.8) \times 10^{-12}$

Low

$F = (4.0 \mp 1.6) \times 10^{-12}$

The data for the high productivity region probably represent a lower limit since samples collected by Lovelock (1975) gave CH_3I concentrations of 3400 pptv. Using Lovelock's value, a much higher total flux can be estimated for the high productivity region:

High Productivity
Flux = 0.20 Tg/yr

Adding this in gives a total global oceanic flux of about 0.5 Tg/yr with the largest portion of the flux coming from the high productivity areas. This is an example of how a small region of the ocean can be responsible for a large portion of the flux.

10.4 Chloroform

It was first thought that the ocean might be a source of chloroform by Su and Goldberg (1976) when they observed large concentrations of $CHCl_3$ in open ocean samples. However, they did not have enough samples to discount the possibility of contamination. High concentrations (40 pptv) of $CHCl_3$ observed over the ocean and lower concentrations (25 pptv) over land along with data which show a vertical decrease in $CHCl_3$ concentration in the troposphere support the idea of an oceanic source of $CHCl_3$ (Singh, 1977; Pierotti et al., 1980b; Rasmussen and Khalil, 1981c). Although the ocean is thought to be a source of $CHCl_3$, there is little firm evidence for this conclusion. On the Atlantic and Pacific Cruises seawater measurements of $CHCl_3$ have been made providing evidence of an oceanic source of $CHCl_3$.

The average atmospheric chloroform concentration over the ocean was 24 ± 2.7 pptv with n = 9. The atmospheric concentrations and the equilibrium seawater concentrations are shown in Figure 10.6. Individual data points are in Appendix A. The equilibrium seawater concentration was calculated using H = 0.19, since the temperature dependence of the Henry's constant was not known. Using these data a flux of 0.65 Tg/yr was calculated. These samples were collected in a low productivity area, on the open ocean far away from any shoreline contamination. Compounds such as F-11, F-12, CH_3CCl_3, and PCE, which are known to be man-made, were simultaneously measured with results indicating that there was no contamination in the seawater samples (see section on methylchloroform, F-11, F-12, and PCE).

An oceanic flux of 0.65 Tg/yr fits in with the total global $CHCl_3$ budget proposed by Yung et al. (1975). Yung estimated a dispersed global source of 0.99 Tg/yr. From production figures of 1976 the upper limit of the annual anthropogenic release of $CHCl_3$ is 0.3 Tg/yr. Additional chloroform is thought to be produced by paper bleaching and water chlorination with an upper limit of 0.3 Tg/yr. Remembering that these represent upper limits that were arrived at in an attempt to balance the budget, an oceanic source of 0.65 Tg/yr fits into the budget within the uncertainty limits.

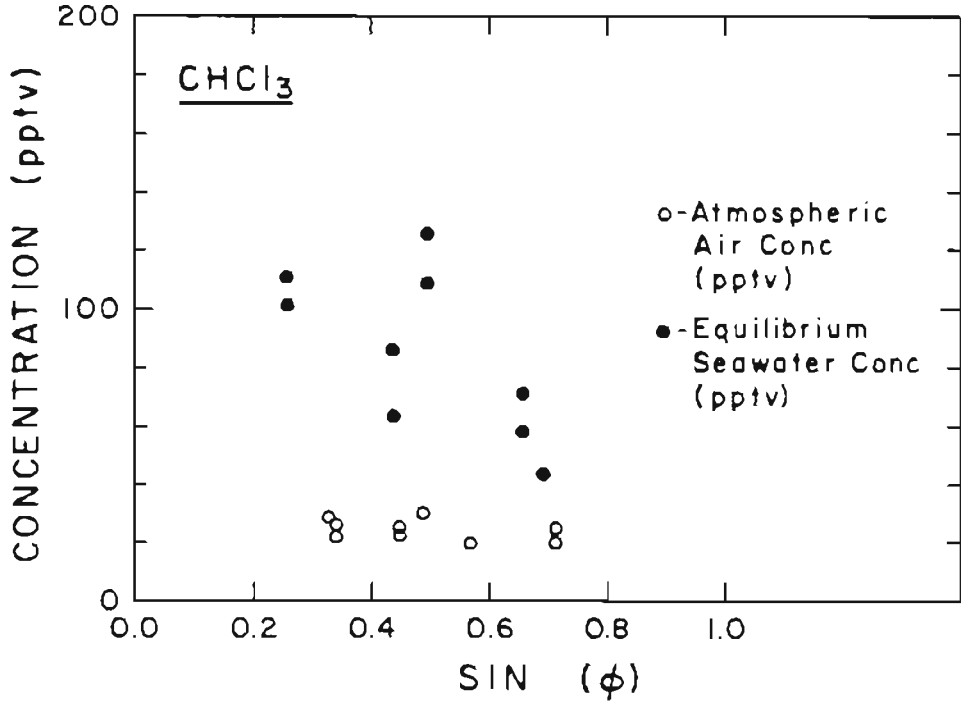

Figure 10.6. Atmospheric and equilibrium seawater concentrations of chloroform.

10.5 Other Halocarbon Gases

Carbon Tetrachloride

The production and source data are more complete for carbon tetrachloride (CCl_4), and there do not appear to be any natural sources (NAS, 1975; Lovelock et al., 1973; Singh et al., 1981). The annual production of CCl_4 in 1973 was estimated to be 1×10^{11} grams, of which it is estimated that 9×10^{10} enter the atmosphere (Galbally, 1976). Air and seawater measurements of CCl_4 have been made by Lovelock (1973) who found CCl_4 to be essentially in equilibrium. The air and seawater data collected on the three cruises are plotted in Figure 10.7, which shows the ocean to be a 0.2 Tg/yr sink for CCl_4. This was larger than Lovelock found and may be the result of storage problems for CCl_4. However, since the Henry's constant temperature dependence is not well known for CCl_4 in seawater, the uncertainty in the calculation is so large it is difficult to estimate what the magnitude of the ocean sink is, or even to rule out the ocean's being in equilibrium.

Methylchloroform, F-11, F-12, PCE

These compounds are of anthropogenic origin and are not expected to have an oceanic flux (Rasmussen and Khalil, 1981a, 1982e). Since these compounds have been released for several years, it is expected that the surface waters of the ocean will be close to equilibrium with the atmospheric concentration (Junge, 1976). As shown in Chapter 4, when a gas is close to equilibrium, the uncertainties in the flux

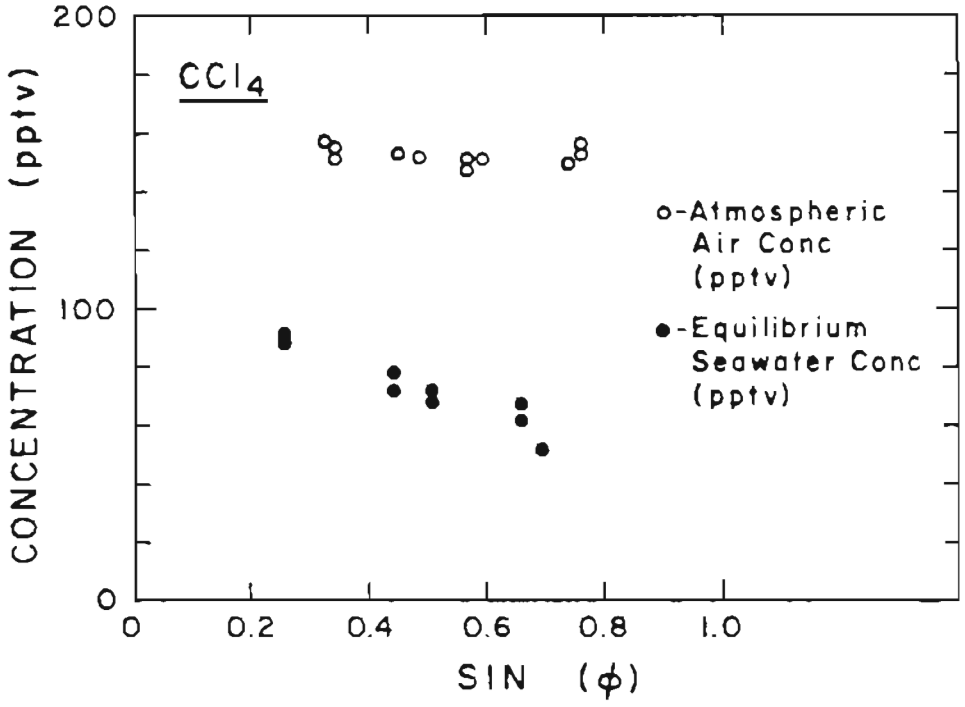

Figure 10.7. Atmospheric and equilibrium seawater concentrations of carbon tetrachloride.

calculation become very large. The atmospheric concentrations and equilibrium seawater concentrations for these gases are shown in Figures 10.8 to 10.11. Methylchloroform (CH_3CCl_3) clearly shows that the air and seawater samples are in equilibrium. For the case of F-11 ($CFCl_3$) the seawater is undersaturated with respect to the air samples. This is probably due to the uncertainty in the Henry's constant, which varies widely in the literature. There was a lot of variability in the F-12 data with some points showing saturation and some undersaturation. The wide distribution in points is partly due to the large Henry's constant, used to calculate the equilibrium seawater concentration and potential F-12 contamination from the ship. The data for perchloroethylene ($Cl_2C=CCl_2$) show equilibrium between air and seawater for most points. The one set of high points may be due to coastal contamination in the seawater or contamination from the boat. The calculated fluxes for these gases are shown below where a positive flux indicates transfer into the ocean.

CH_3CCl_3	$\bar{F}$ = 0.008 Tg/yr
F-11	$\bar{F}$ = 0.04 Tg/yr
F-12	$\bar{F}$ = -0.01 Tg/yr
PCE	$\bar{F}$ = 0.10 Tg/yr

Due to the uncertainties in the flux calculations, these are not a significant indication that the ocean is a source or a sink for these compounds. To get a better estimate of the flux, the Henry's constant needs to be accurately measured in seawater.

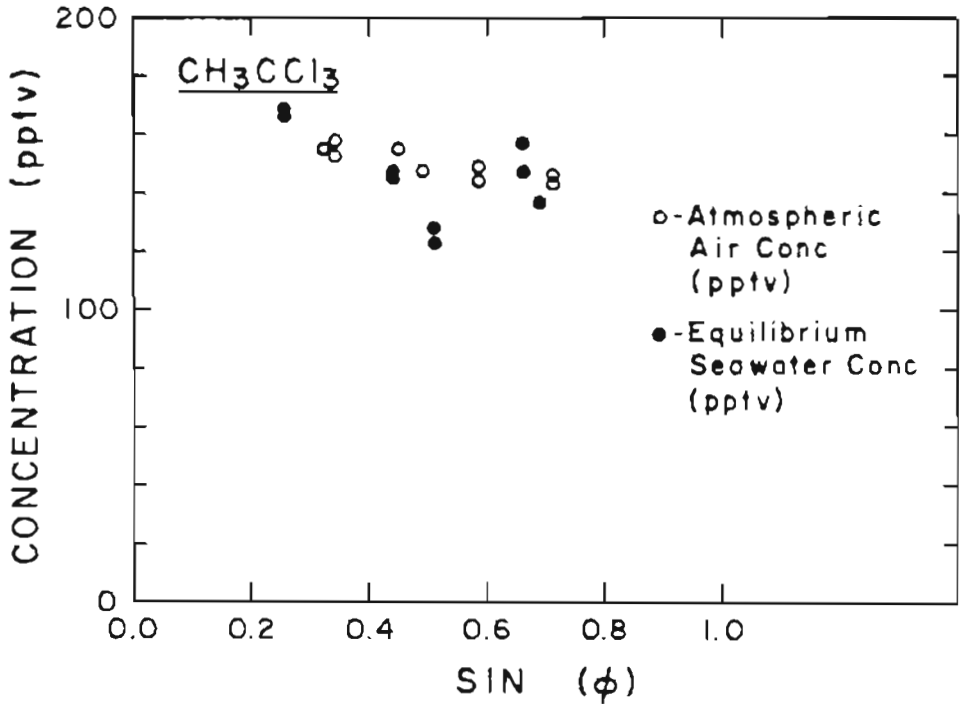

Figure 10.8. Atmospheric and equilibrium seawater concentrations of methyl chloroform.

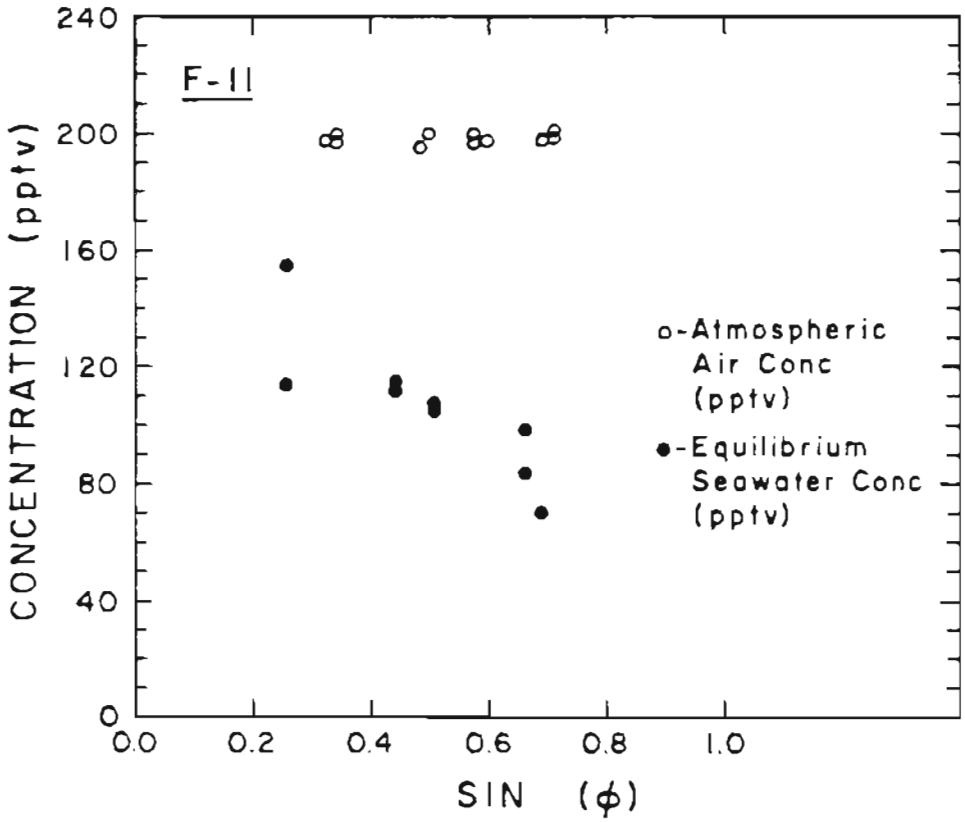

Figure 10.9. Atmospheric and equilibrium seawater concentrations of F-11.

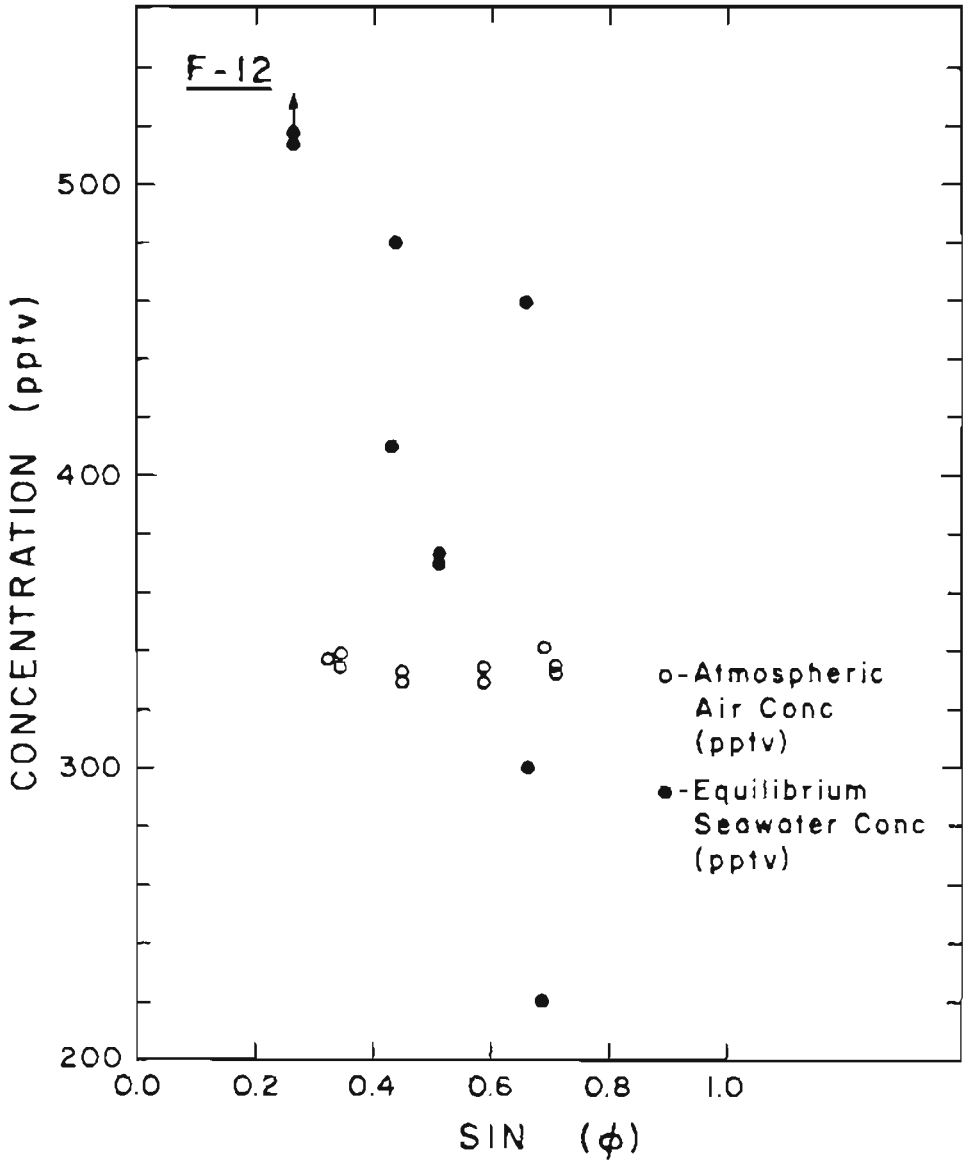

Figure 10.10. Atmospheric and equilibrium seawater concentrations of F-12.

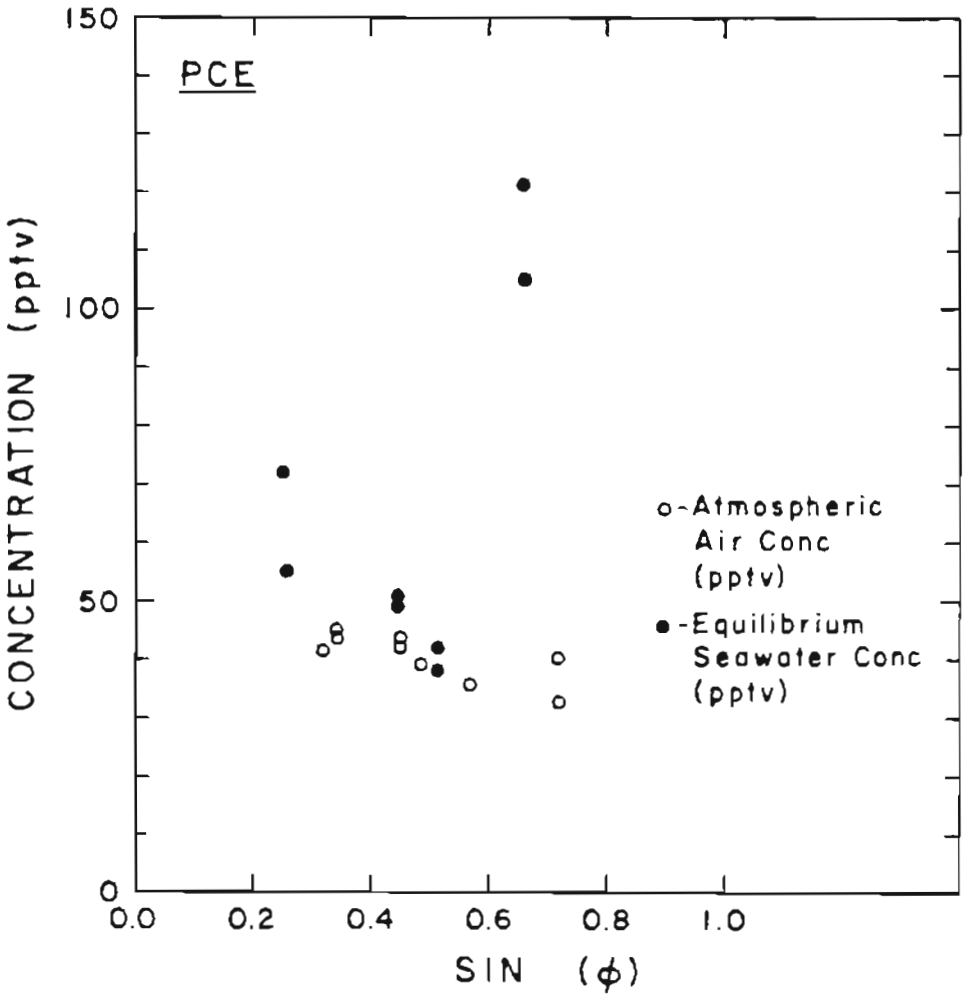

Figure 10.11. Atmospheric and equilibrium seawater concentrations of perchloroethylene.

10.6 Conclusions

The data collected on the seawater concentrations of OCS and halocarbons have provided new evidence that the ocean may be an important source for OCS and $CHCl_3$. In addition, the oceanic source strength of CH_3I has been verified. Since the flux of these three gases appears to be dependent on the primary productivity of the ocean, it would seem that the ocean source would be biological. The calculated fluxes of these gases along with the uncertainty calculated using the values in Table 4-2 are summarized in Table 10-9 along with the totals for atmospheric sources.

Data for the anthropogenic halocarbons are summarized in Table 10-9, which shows them to be essentially in equilibrium in the surface waters of the ocean (within experimental uncertainty). To give some idea of the magnitude of the uncertainty, the estimated yearly emissions are included for comparison. From this it can be seen that a small difference in the ocean and atmospheric concentration can result in a calculated yearly flux equivalent to the anthropogenic release. Better estimates of the flux await better measurements of the Henry's constant, which is a major source of uncertainty. However, just because the surface waters are close to equilibrium does not mean that the ocean does not act an as important sink, since there are cold surface currents that rapidly move to the deep ocean, bringing much of this material into unsaturated areas (Gammon et al., 1972). Research into this area awaits more data on depth profiles of gases such as F-11, F-12, and CH_3CCl_3.

TABLE 10-9

Ocean Flux of OCS and Halocarbons with

the Estimated Uncertainty

Gas	P		Flux * (Tg/yr)	Uncertainty Table 4-2	Total Non-Oceanic Sources (Tg/yr)
OCS	M	-	0.6	∓ 0.4	
	L	-	0.2	∓ 0.2	
	Total	-	0.8	∓ 0.5	1.2 - 3.7
CH_3I	M	-	0.14	∓ 0.09	
	L	-	0.05	∓ 0.03	
	Total	-	0.2	∓ 0.1	-0-
$CHCl_3$	L	-	0.7	∓ 0.6	0.6
CCl_4	L	+	0.2	∓ 0.2	9×10^{10} g
CH_3CCl_3	L	+	8×10^9 g	∓ 15×10^9 g	6×10^9 g
F-11	L	+	3×10^{10} g	∓ 4×10^{10} g	6×10^9 g
F-12	L	-	1×10^{10} g	∓ 2×10^{10} g	6×10^9 g
PCE	L	+	0.1	∓ 0.15	4×10^{11} g

* (-) indicates flux from ocean to air

CHAPTER 11

CONCLUSIONS

This dissertation began as a project to determine if the ocean was a source of carbonyl sulfide (OCS), an atmospheric trace gas that is believed to maintain the stratospheric sulfate layer. OCS has recently generated interest among atmospheric chemists, since its sources and sinks are not well known, and changes in its concentration could have important climatic impacts. While surveying methods to determine gas fluxes from the ocean, it became clear that previous efforts to calculate the ocean fluxes of trace gases were based on old and limited sets of data and model parameters. To get a good estimate of the OCS ocean flux it would be necessary to thoroughly evaluate the available models, update the material on the physio-chemical constants, and develop a method for collecting and measuring seawater gas concentrations in the laboratory.

The results of this research project were not just the calculation of the OCS flux and the flux of some other important atmospheric gases, but served to update and tie together the material on ocean-air exchange. In the pursuit of this goal several important conclusions on flux calculation methods were reached, and some new measurement methodology was developed.

When comparing the widely used two-film model for ocean flux calculations to the more complicated surface renewal models, it was

found that the two models were fundamentally different because they predicted a different dependence of the transfer coefficient, K, on the diffusion coefficient. However, in actual use, with experimentally measured transfer coefficients, the models give similar results with the differences being small compared to the experimental variations observed for K. Using the recently published data base for transfer coefficients measured at 110 stations in the Atlantic and Pacific Oceans, along with an improved correction procedure for the different diffusion roles of gases based on their molar volumes, an updated table of transfer coefficients for the different gases was made.

The values of the Henry's constant, H, were found to be important in determining whether the ocean is a source or a sink for a gas. For OCS no measurements of H have been made in seawater, so an experimental procedure was developed to determine H for OCS as a function of temperature using atmospheric partial pressures of the gas. These were found to agree favorably with the values measured in distilled water using the pure gas. This result also demonstrates for OCS that Henry's law holds from atmospheric pressure down to the parts per billion range, a question that is always of concern in applying laboratory measurements of H to environmental applications.

To better understand some of the limitations of the two-film model, a propagation of error analysis was done to determine what the major sources of uncertainty were in using the model for flux calculations. The results were interesting because they show that the major sources of uncertainty are different for each gas and depend on

the gas saturation level in the seawater. For man-made gases such as the chlorofluoromethanes, which have saturation values close to zero, the major source of uncertainty is in the Henry's constant of the gas, and the closer to zero the saturation becomes, the larger the uncertainty will be. For a gas produced in the ocean, the major sources of uncertainty will be the seawater concentration and the transfer coefficient. In all cases the atmospheric concentration is not a limiting factor.

Most measurements of gas concentrations in seawater have been made on board a ship because attempts to collect seawater gas samples have been plagued with problems of sample losses from the headspace and contamination. For this project, a method was developed for collecting samples to be brought back to the laboratory for analysis. This allows more compounds to be measured per sample, and makes the sample collection procedure more flexible and less expensive. The result was the development of the vacuum extraction flask in which the sample could be collected, stored, and analyzed in a single bottle with a minimum of loss and contamination. Using this procedure many compounds can be analyzed in each sample, increasing the data base for ocean-air exchange calculations of trace gases. In addition, this technique has made it possible to determine that the ocean is a source of chloroform, $CHCl_3$, because simultaneous analysis of the flasks showed elevated $CHCl_3$ and low values for gases indicative of contamination.

The two-film model with the updated values for K_ℓ and H was used with the seawater sampling methodology to calculate the OCS ocean flux and the flux of some halocarbon gases from seawater and air samples collected on oceanographic cruises in the Atlantic and Pacific Oceans. The results were summarized in Table 10-9, showing the ocean to be a source of OCS and $CHCl_3$. The large ocean source of OCS is an important finding since it indicates that anthropogenic sources were not as large as previously thought, reducing the potential for climatic impacts from man's increasing activities.

The initial thrust of the research was to determine the magnitude of the ocean source of OCS. The results of the work have been of more general application to the field of ocean-air exchange because they provide a unified pathway to get from air and seawater concentration measurements to the final flux values for gases. The major sources of uncertainty can be estimated beforehand, and the best sampling and measurement program can be developed. It is anticipated that these techniques will be useful since the importance of ocean-atmosphere exchange in trace gas cycles is just being fully realized.

REFERENCES

Adams, D. F., S. O. Farwell, M. R. Pack, and W. L. Banesberger (1979). "Preliminary Measurements of Biogenic Sulfur-Containing Gas Emissions from Soils." J. Air Pollut. Control Assoc. 29, 380.

Aneja, V. P., J. H. Overton, Jr., L. T. Cupitt, J. L. Durham, and W. E. Wilson (1979). "Direct Measurements of Emission Rates of Some Atmospheric Biogenic Sulfur Compounds." Tellus 31, 174.

Atkinson, L. P. (1973). "Effect of Air Bubble Solution on Air-Sea Gas Exchange." J. Geophys. Res. 78, 962.

Atkinson, R., R. A. Perry, and J. N. Pitts, Jr. (1978). "Rate Constants for the Reaction of OH Radicals with COS, CS_2, and CH_3CCl_3 over Temperature Range 299-430K." Chem. Phys. Lett. 54, 14.

Barnard, W. R., M. O. Andreae, W. E. Watkins, H. Bingemer, H.-W. Georgii. "The Flux of Dimethyl Sulfide from the Oceans to the Atmosphere." J. Geophys. Res. in press (1982).

Bathen, K. H. (1972). "On the Seasonal Changes in the Depth of the Mixed Layer in the North Pacific Ocean." J. Geophys. Res. 77, 7138.

Battino, K., and H. L. Clever (1966). "The Solubility of Gases in Liquids." Chem. Rev. 66, 395.

Bauer, E. (1979). "A Catalog of Perturbing Influences on Stratospheric Ozone, 1955-1975." J. Geophys. Res. 84, 6929.

Benson, B. B., and D. Krause, Jr. (1976). "Empirical Laws for Dilute Aqueous Solutions of Nonpolar Gases." J. Chem. Phys. 64, 689.

Boggs, J. E., and A. E. Buck, Jr. (1958). "The Solubility of Some Chloromethanes in Water." J. Am. Chem. Soc. 62, 1459.

Bolin, E. (1960). "On the Exchange of Carbon Dioxide Between the Atmosphere and the Sea." Tellus 12, 274.

Broecker, H. C., J. Petermann, and W. Siehs (1978). "The Influence of Wind on CO_2 Exchange in Wind-Wave Tunnel, Including the Effects of Monolayers." J. Mar. Res. 36, 595.

Broecker, W. S. (1963). "Radioisotopes and Large Scale Oceanic Mixing." in The Sea, Volume 2, p. 88.

Broecker, W. S. (1966). "Radioisotopes and the Rate of Mixing Across the Main Thermoclines of the Ocean." J. Geophys. Res. 71, 5827.

Broecker, W. S., and Y. H. Li (1970). "Interchange of Water Between the Major Oceans." J. Geophys. Res. 75, 3545.

Broecker, W. S., and T. H. Peng (1974). "Gas Exchange Rates Between Air and Sea." Tellus 26, 21.

Brownlow, A. H. Geochemistry. (Prentice-Hall, Inc., Englewood Cliffs, New Jersey, 1979).

Castleman, A. W., Jr., H. R. Munkelwitz, and B. Manowitz (1973). "Contribution of Volcanic Sulfur Compounds to the Stratospheric Aerosol Layer." Nature 244, 345.

Castleman, A. W., Jr., R. E. Davis, H. R. Munkelwitz, I. N. Tang, and W. P. Wood. Kinetics Data for the Upper and Lower Atmosphere. (J. Wiley, New York, 1975), p. 629.

Cicerone, R. J., R. S. Stolarski, and S. Walters (1975). Stratospheric Ozone Destruction by Man-Made Chlorofluoromethanes." Science 185, 1165.

Cicerone, R. J. (1981). "Halogens in the Atmosphere." Rev. Geophys. and Space Phys. 19, 123.

Cohen, Y., W. Cocchio, and D. Mackay (1978). "Laboratory Study of Liquid-Phase Controlled Volatilization Rates in the Presence of Wind Waves." Environ. Sci. Technol. 12, 553.

Cox, R. A., and D. Sheppard (1980). "Reaction of OH Radicals with Gaseous Compounds." Nature 284, 330.

Craig, H. (1957). "The Natural Distribution of Radiocarbon and the Exchange Time of Carbon Dioxide Between Atmosphere and Sea." Tellus 9, 1.

Craig, H. (1969). "Abyssal Carbon and Radiocarbon in the Pacific." J. Geophys. Res. 74, 5491.

Cronin, J. F. (1971). "Recent Volcanism and the Stratosphere." Science 172, 847.

Crutzen, P. J. (1976). "The Possible Importance of CSO for the Sulfate Layer of the Stratosphere." Geophys. Res. Lett. 3, 73.

Crutzen, P. J., I. S. A. Isaksen, and J. R. McAfee (1978). "The Impact of the Chlorocarbon Industry on the Ozone Layer." J. Geophys. Res. 83, 345.

Crutzen, P. J., L. E. Heidt, J. P. Krasnec, W. H. Pollock, and W. Seiler (1979). "Biomass Burning as a Source of Atmospheric Gases CO, H_2, N_2O, NO, CH_3Cl, and COS." Nature 282, 253.

Danckwerts, P. V. (1951). "Significance of Liquid-Film Coefficients in Gas Absorption." Ind. and Eng. Chem. 43, 1460.

Danckwerts, P. V. (1955). "Gas Absorption Accompanied by Chemical Reaction." J. Amer. Inst. Chem. Eng. 1, 456.

Danckwerts, P. V. Gas-Liquid Reactions. (McGraw-Hill Book Co., New York, 1970).

Daniels, F., and R. A. Alberty. Physical Chemistry. (John Wiley & Sons, Inc., New York, 1975).

Deacon, E. L. (1977). "Gas Transfer to and across an Air-Water Interface." Tellus 29, 363.

Defant, A. Physical Oceanography, Vols. I, II. (Pergamon Press, London, 1961).

Denbigh, K. The Principles of Chemical Equilibrium, 3rd Edition. (Cambridge University Press, Cambridge, 1971).

Dilling, W. L. (1977). "Interphase Transfer Processes. II. Evaporation Rates of Chloro methanes, Ethanes, Ethylenes, Propanes, and Propylenes from Dilute Aqueous Solutions. Comparison with Theoretical Predictions." Environ. Sci. Technol. 11, 405.

Douglas, E. (1964). "Solubilities of Oxygen, Argon, and Nitrogen in Distilled Water." J. Phys. Chem. 68, 169.

Douglas, E. (1967). "Carbon Monoxide Solubilities in Sea Water." J. Phys. Chem. 71, 1931.

Farwell, S. O., and R. A. Rasmussen (1976). "Limitations of the FPD and ECD in Atmospheric Analysis: A Review." J. Chromatogr. Sci. 14, 224.

Farwell, S. O., S. J. Gluck, W. L. Banesberger, T. M. Schutte, and D. F. Adams (1979). "Determination of Sulfur-Containing Gases by a Deactivated Cryogenic Enrichment and Capillary GC System." Anal. Chem. 51, 609.

Farwell, S. O., and S. J. Gluck (1980). "Glass Surface Deactivants for Sulfur-Containing Gases. Anal. Chem. 52, 1968.

Friend, J. P. "The Global Sulfur Cycle" in Chemistry of the Lower Atmosphere, S. I. Rasool, Editor (Plenum, New York, 1973).

Gage, D. R., and S. O. Farwell (1980). "Nonflame Source-Induced Sulfur Fluorescence Detector for Sulfur-Containing Compounds." Anal. Chem. 52, 2422.

Galbally, I. E. (1976). "Man-Made Carbon Tetrachloride in the Atmosphere." Science 193, 573.

Gammon, R. H., J. Cline, and D. Wisegarver (1982). "Chlorofluoromethanes in the Northeast Pacific Ocean: Measured Vertical Distributions and Application as Transient Tracers of Upper Ocean Mixing." J. Geophys. Res. (in press).

Glew, D. N., and E. A. Moelwyn-Hughes (1953). "Chemical Statics of the Methyl Halides in Water." Disc. Faraday Soc. 15, 150.

Hackenberg, H., and A. P. Schmidt. Gas Chromatographic Headspace Analysis (Heyden, London, 1977).

Hansen, J., D. Johnson, A. Lacis, S. Lebedeff, P. Lee, D. Reid, and G. Russel (1981). "Climate Impact of Increasing Atmospheric Carbon Dioxide." Science 213, 957.

Hanst, P. L., L. L. Spiller, D. M. Watts, J. W. Spence, and J. F. Miller (1975). "Infrared Measurements of Fluorocarbons, Carbon Tetrachloride, Carbonyl Sulfide, and Other Atmopsheric Trace Gases." J. Air Pollut. Control Assoc. 25, 1220.

Harsch, D. E. (1980). "Evaluation of a Versatile Gas Sampling Container Design." Atmos. Environ. 14, 1105.

Hasse, L., and P. S. Liss (1980). "Gas Exchange Across the Air-Sea Interface." Tellus 32, 470.

Higbie, R. (1935). "The Rate of Absorption of a Pure Gas into a Still Liquid During Short Periods of Exposure." Trans. Amer. Inst. Chem. Engrs. 31, 365.

Hildebrand, J. E., and R. L. Scott. The Solubility of Nonelectrolytes, 3rd Edition (Dover Publications, Inc., New York, 1964).

Hilerman, B. (1982). "The Greenhouse Effect." Environ. Sci. Technol. 16, 90A.

Hoover, T. E., and D. C. Berkshire (1969). "Effects of Hydration of Carbon Dioxide Exchange Across an Air-Water Interface." J. Geophys. Res. 74, 456.

Houtermans, J., H. E. Suess, and H. Oeschger (1973). "Reservoir Models and Production Rate Variations of Natural Radiocarbon." J. Geophys. Res. 78, 1897.

Jones, B. M. R., J. P. Burrows, R. A. Cox, and S. A. Penkett. "OCS Formation in the Reaction of OH with CS_2." Personal Communication, 1982.

Junge, C. (1972). "The Cycle of Atmopsheric Gases -- Natural and Man-Made." J. Royal Meteorological Soc. 98, 711.

Junge. C. (1976). "The Role of the Oceans as a Sink for Chlorofluoromethanes and Similar Compounds." Z. Naturforsch 31A, 482.

Kanwisher, J. (1963). "On the Exchange of Gases Between the Atmosphere and the Sea." Deep Sea Res. 10, 195.

Keeling, C. D., R. B. Bacastow, A. E. Bainbridge, C. A. Ekdahl, P. R. Guenther, L. S. Waterman, and J. F. S. Chin (1976). "Atmospheric Carbon Dioxide Variations of Mauna Loa Observatory, Hawaii." Tellus 28, 538.

Kellogg, W. (1980). "Modeling Future Climate." Ambio 9, 216.

Kellogg, W. W., and R. Schware. Climate Change and Society. (Westview Press, Boulder, Colorado, 1981).

Khalil, M. A. K. (1979). "Topics in the Behaviour of Atmospheric Trace Gases." Ph.D. Dissertation, Oregon Graduate Center.

Khalil, M. A. K., and R. A. Rasmussen (1981a). "Increase in the Atmospheric Concentrations of Halocarbons and N_2O." Geophysical Monitoring for Climatic Change, No. 9, J. J. DeLuisi, Editor, U. S. Dept. of Commerce, NOAA, p. 134.

Khalil, M. A. K., and R. A. Rasmussen (1981b). "Atmospheric Trace Gases: Possibility of Sources in the Southern Hemisphere." Atmos. Environ. 15, 1331.

Klug, W. (1974). "Eddy Viscosity Profile in Upper Oceanic Layers Derived from Radon Measurements." Tellus 26, 36.

Koblentz-Mishke, O. J., V. V. Volkovinsky, and J. G. Kabanova (1970). "Plankton Primary Production of the World Ocean." Scientific Exploration of the South Pacific -- Proceedings of a Symposium, p. 183.

Kondo, J. (1976). "Parameterization of Turbulent Transport in the Top Meter of the Ocean." J. Phys. Oceanography 6, 712.

Kurylo, M. J. (1978). "Flash Photolysis Resonance Fluorescence Investigation of the Reactions of OH Radicals with OCS and CS_2." Chem. Phys. Lett. 58, 238.

Lamontagne, R. A., J. W. Swinnerton, V. J. Linnenbom, and W. D. Smith (1973). "Methane Concentrations in Various Marine Environments." J. Geophys. Res. 78, 5317.

Lazrus, A. L., R. D. Cadle, B. W. Gandrud, J. P. Greenberg, B. J. Huebert, and W. I. Rose, Jr. (1979). "Sulfur and Halogen Chemistry of the Stratosphere and of Volcanic Eruption Plumes." J. Geophys. Res. 84, 7869.

Leu, M. T., and R. H. Smith (1981). "Kinetics of the Gas-Phase Reaction Between Hydroxyl and Carbonyl Sulfide over the Temperature Range 300-517K." J. Phys. Chem. 85, 2570.

Lewis, G. N., and M. Randall. Thermodynamics, Second Edition (McGraw-Hill, New York, 1961).

Liss, P. S. (1973). "Processes of Gas Exchange Across an Air-Water Interface." Deep Sea Res. 20, 221.

Liss, P. S., and P. G. Slater (1974). "Flux of Gases Across the Air-Sea Interface." Nature 247, 181.

Lovelock, J. E., R. J. Maggs, and R. A. Rasmussen (1972). "Atmospheric Dimethyl Sulphide and the Natural Sulphur Cycle." Nature 237, 452.

Mackay, D. (1979a). "Finding Fugacity Feasible." Environ. Sci. Technol. 13, 1218.

Mackay, D. (1979b). "Transfer Rates of Gaseous Pollutants Between Lakes and the Atmosphere." ACS Meeting, Washington, D.C., September 9-14.

Mackay, D., W. Y. Shiu, and R. P. Sutherland (1979). "Determination of Air-Water Henry's Law Constants for Hydrophobic Pollutants." Environ. Sci. Technol. 13, 333.

Mackay, D., A. T. K. Yuen. "Transfer Rates of Gaseous Pollutants Between the Atmosphere and Natural Waters." In Atmospheric Input of Pollutants to Natural Waters, S. J. Eisenreich, Editor, Ann Arbor Science Publishers, 1980).

Mackay, D., and S. Paterson (1981). "Calculating Fugacity." Environ. Sci. Technol. 15, 1006.

Markham, A. E., and K. A. Kobe (1941a). "The Solubility of Gases in Liquids." Chem. Rev. 28, 519.

Markham, A. E., and K. A. Kobe (1941b). "The Solubility of Carbon Dioxide and Nitrous Oxide in Aqueous Salt Solutions." J. Am. Chem. Soc. 63, 449.

Maroulis, P. J., A. L. Torres, and A. R. Bandy (1977). "Atmospheric Concentrations of Carbonyl Sulfide in the Southwestern and Eastern United States." Geophys. Res. Lett. 4, 510.

McAuliffe, C. (1971). "GC Determination of Solutes by Multiple Phase Equilibria." Chem. Tech. 1, 46.

McConnell, G., D. M. Ferguson, and C. R. Pearson (1975). "Chlorinated Hydrocarbons and the Environment." Endeavor, p. 13.

McGaughey, J. F., and S. K. Gangwal (1980). "Comparison of Three Commercially Available Gas Chromatographic-Flame Photometric Detectors in the Sulfur Mode." Anal. Chem. 52, 2079.

McGovern, E. W. (1943). "Chlorohydrocarbon Solvents." Ind. and Eng. Chem. 35, 1230.

Molina, M. J., and F. S. Rowland (1974). "Stratospheric Sink for Chlorofluoromethanes: Chlorine Atom Catalysed Destruction of Ozone." Nature 249, 810.

Moore, W. J. Physical Chemistry, 3rd Edition (Prentice-Hall, Inc., Englewood Cliffs, N. J., 1972).

Murray, C. N., and J. P. Riley (1971). "The Solubility of Gases in Distilled Water and Sea Water. IV. Carbon Dioxide." Deep Sea Res. 18, 533.

National Academy of Sciences, Washington, D. C. Understanding Climatic Change: A Program for Action. 1975a.

National Academy of Sciences, Washington, D. C. Assessing Potential Ocean Pollutants. 1975b.

National Academy of Sciences, Washington, D. C. The Tropospheric Transport of Pollutants and Other Substances to the Ocean. 1978a.

National Academy of Sciences, Washington, D. C. Chloroform, Carbon Tetrachloride, and Other Halomethanes. 1978b.

National Academy of Sciences, Washington, D. C. Causes and Effects of Stratospheric Ozone Reduction. 1982.

Neely, W. B. Chemicals in the Environment (Marcel Dekker, Inc., New York, 1980).

Neuman, G., and W. J. Pierson, Jr. Principles of Physical Oceanography (Prentice-Hall, Inc., Englewood Cliffs, N. J., 1966), p. 422

Nguyen, B. C., A. Gaudry, B. Bonsang, and G. Lambert (1978). "Reevaluation of the Role of Dimethyl Sulphide in the Sulphur Budget." Nature 275, 637.

Nielsen, E. S. (1951). "Measurement of the Production of Organic Matter in the Sea by Means of Carbon-14." Nature 167, 684.

Nydal, R. (1968). "Further Investigation on the Transfer of Radiocarbon in Nature." J. Geophys. Res. 73, 3617.

Oeschger, H., V. Siegenthaler, V. Schotterer, and A. Gugelmann. "A Box Diffusion Model to Study the Carbon Dioxide Exchange in Nature." Tellus 27, 168.

Pierotti, D., and R. A. Rasmussen (1980). "Nitrous Oxide Measurements in the Eastern Tropical Pacific Ocean." Tellus 32, 56.

Pierotti, D., R. A. Rasmussen, and R. Dalluge (1980). "Measurements of N_2O, CF_2Cl_2, $CFCl_3$, CH_3CCl_3, CCl_4 and CH_3Cl in the Troposphere and Lower Stratosphere over North America." J. Geomag. Geoelectr. 32, 181.

Peng, T.-H., T. Takahashi, and W. S. Broecker (1974). "Surface Radon Measurements in the North Pacific Ocean Station Paper." J. Geophys. Res. 79, 1772.

Peng, T.-H., W. S. Broecker, G. G. Mathieu, Y.-H. Li, and A. A. Bainbridge (1979). "Radon Evasion Rates in the Atlantic and Pacific Oceans as Determined During the Geosecs Program." J. Geophys. Res. 84, 2471.

Rasmussen, R. A., D. E. Harsch, P. H. Sweany, J. P. Krasnec, and D. R. Cronn (1977). "Freezeout Method for EC Gas Chromatographic Analysis of Atmospheric Halocarbons Not Measurable by Direct Injection." J. Air Pollut. Control Assoc. 27, 579.

Rasmussen, R. A., D. Pierotti, T. F. Bidleman, and P. Wilkniss. "Halogenated Hydrocarbons." Tropospheric Transport of Pollutants to the Ocean, J. Prospero, Editor, National Academy of Sciences, 1977.

Rasmussen, R. A., and M. A. K. Khalil. "Atmospheric Halocarbons: Measurements and Analyses of Selected Trace Gases." Proceedings of the NATO Advanced Study Institute on Atmospheric Ozone: Its Variation and Human Influences, A. C. Aikin, Editor, Report No. FAA-EE-50-20, Department of Transportation, Washington, D. C., 1980, p. 209.

Rasmussen, R. A., and M. A. K. Khalil (1981a). "Global Atmospheric Distribution and Trend of Methylchloroform (CH_3CCl_3)." Geophys. Res. Lett. 8, 1005.

Rasmussen, R. A., and M. A. K. Khalil (1981b). "Interlaboratory Comparison of Fluorocarbons 11, 12, Methyl Chloroform, and Nitrous Oxide Measurements." Atmos. Environ. 15, 1559.

Rasmussen, R. A., and M. A. K. Khalil (1981c). "Increase on the Concentration of Atmospheric Methane." Atmos. Environ. 15, 883.

Rasmussen, R. A., M. A. K. Khalil, R. W. Dalluge, S. A. Penkett, and B. Jones (1982a). "Carbonyl Sulfide and Carbon Disulfide from the Eruptions of Mt. St. Helens." Science 215, 665.

Rasmussen, R. A., M. A. K. Khalil, and S. D. Hoyt (1982b). "Oceanic Source of Carbonyl Sulfide (OCS)." Accepted by Atmospheric Environment.

Rasmussen, R. A., S. D. Hoyt, and M. A. K. Khalil (1982c). "Atmospheric Carbonyl Sulfide (OCS): Techniques for Measurement in Air and Water." Accepted for publication in Chemosphere.

Rasmussen, R. A., M. A. K. Khalil, R. Gunawardena, and S. D. Hoyt (1982d). "Atmospheric Methyl Iodide (CH_3I)." J. Geophys. Res. 87, 3086.

Rasmussen, R. A., and M. A. K. Khalil (1982e). "Latitudinal Distribution of Trace Gases In and Above the Boundary Layer." Chemosphere 11, 227.

Ravishankara, A. R., N. M. Kreuther, R. C. Shah, and P. H. Wine (1980). "Rate of Reaction of OH with COS." Geophys. Res. Lett. 7, 861.

Redfield, A. C. (1948). "The Exchange of Oxygen Across the Sea Surface." J. Marine Res. 7, 347.

Reid, R. C., and T. K. Sherwood. The Properties of Gases and Liquids. (McGraw-Hill, New York, 1966).

Revelle, R., and H. E. Suess (1957). "Carbon Dioxide Exchange Between Atmosphere and Ocean and the Question of an Increase of Atmospheric CO_2 During the Past Decades." Tellus 9, 18.

Roether, W., and B. Kramer (1978). "Field Determination of Air-Sea Gas Exchange by Continuous Measurement of Radon-222." Pageoph 116, 476.

Rowland, F. S. (1979). "The Atmospheric and Ocean Sinks of Carbonyl Sulfide." Abstract IV-6, Commission on Atmospheric Chemistry and Global Pollution, Boulder, Colorado.

Sandalls, F. J., and S. A. Penkett (1977). "Measurements of Carbonyl Sulfide and Carbon Disulfide in the Atmosphere." Atmos. Environ. 11, 197.

Schmidt, V. (1979). "The Solubility of Carbon Monoxide and Hydrogen in Water and Seawater at Partial Pressures of About 10^{-5} Atmospheres." Tellus 31, 68.

Scott, W. D., D. Lamb, and D. Duffy (1969). "The Stratospheric Aerosol Layer and Anhydrous Reactions Between Ammonia and Sulfur Dioxide." J. Atmos. Sci. 26, 727.

Seidell, A. Solubilities of Inorganic and Metal Organic Compounds. (Van Nostrand Co., Inc, New York, 1940).

Singh, H. B., L. J. Salas, and H. Shigeishi (1979). "The Distribution of Nitrous Oxide (N_2O) in the Global Atmosphere and the Pacific Ocean." Tellus 31, 313.

Singh, H. B., L. J. Salas, A. J. Smith, and H. Shigeishi (1981). "Measurements of Some Potentially Hazardous Organic Chemicals in Urban Environments." Atmos. Environ. 15, 601.

Stevens, R. K., A. E. O'Keeffe, and G. C. Ortman (1969). "Absolute Calibration of a Flame Photometric Detector to Volatile Sulfur Compounds at Sub-Part-per-Million Levels." Environ. Sci. Technol. 3, 653.

Stevens, R. K., J. D. Mulik, A. E. O'Keeffe, and K. J. Krost (1971). "Gas Chromatography of Reactive Sulfur Gases in Air at the Part-per-Billion Level." Anal. Chem. 43, 827.

Stumm, W., and J. J. Morgan. Aquatic Chemistry. (Wiley-Interscience, New York, 1970).

Su, C., and E. D. Goldberg. "Environmental Concentrations and Fluxes of Some Halocarbons." In Marine Pollutant Transfer (Lexington Books, D. C. Heath and Co., 1976).

Swain, C. G., and E. R. Thornton (1962). "Initial-State and Transition-State Isotope Effects of Methyl Halides in Light and Heavy Water." J. Am. Chem. Soc. 84, 822.

Swinnerton, J. W., and R. A. Lamontagne (1974). "Carbon Monoxide in the South Pacific Ocean." Tellus 26, 136.

Thompson, H. W., Kearton, C. F., and S. A. Lamb (1935). "The Kinetics of the Reaction Between Carbonyl Sulfide and Water." J. Chem. Soc., p. 1033.

Torgerson, T., G. Mathieu, R. H. Hesslein, and W. S. Broecker (1982). "Gas Exchange Dependency on Diffusion Coefficient: Direct ^{222}Rn and ^{3}He Comparisons in a Small Lake." J. Geophys. Res. 87, 546.

Turco, R. P., R. C. Whitten, O. B. Toon, and J. B. Pollock (1980). "OCS, Stratospheric Aerosols and Climate." Nature 283, 283.

Vitenberg, A. G., B. V. Loffe, and V. N. Borisov (1974). "Application of Phase Equilibria to Gas Chromatographic Analysis." Chromatographia 7, 610.

Weiss, R. F. (1970). "The Solubility of Nitrogen, Oxygen, and Argon in Water and Seawater." Deep Sea Res. 17, 721.

Weiss, R. F. (1971). "Solubility of Helium and Neon in Water and Seawater." J. Chem. and Eng. Data 16, 235.

Weiss, R. F., and B. A. Price (1980). "Nitrous Oxide Solubility in Water and Seawater." Mar. Chem. 8, 347.

Weiss, R. F. (1981). "The Temporal and Spatial Distribution of Tropospheric Nitrous Oxide." J. Geophys. Res. 86, 7185.

Whitman, W. G. (1923). "The Two-Film Theory of Gas Absorption." Chem. and Metall. Eng. 29, 146.

Wilke, C. R., and P. Chang (1955). "Correlation of Diffusion Coefficients in Dilute Solutions." AIChE J, page 264.

Wine, P. H., and A. R. Ravishankara. "Kinetics of OH Reactions with Tropospheric Sulfur Compounds." Second Symposium on the Composition of the Nonurban Troposphere, Williamsburg, Virginia, May 1982.

Wu, J. (1969). "Wind Stress and Surface Roughness at Air-Sea Interface." J. Geophys. Res. 74, 444.

Young, J. A., and A. W. Fairhall (1968). "Radiocarbon from Nuclear Weapons Tests." J. Geophys. Res. 73, 1185.

Yung, Y. L., M. B. McElroy, and S. C. Wofsy (1975). "Atmospheric Halocarbons: A Discussion with Emphasis on Chloroform." Geophys. Res. Lett. 2, 397.

Zafiriou, O. C. (1974). "Photochemistry of Halogens in the Marine Atmosphere." J. Geophys. Res. 79, 2730.

APPENDIX A

Atmospheric OCS Measurements

OCS Seawater Concentrations and Flux Calculations

Atmospheric CH_3I Measurements

CH_3I Seawater Concentrations and Flux Calculations

Atmospheric $CHCl_3$ Measurements

$CHCl_3$ Seawater Concentrations and Flux Calculations

Atmospheric F-11 Measurements

F-11 Seawater Concentrations and Flux Calculations

Atmospheric F-12 Measurements

F-12 Seawater Concentrations and Flux Calculations

Atmospheric CH_3CCl_3 Measurements

CH_3CCl_3 Seawater Concentrations and Flux Calculations

Atmospheric CCl_4 Measurements

CCl_4 Seawater Concentrations and Flux Calculations

Atmospheric PCE Measurements

PCE Seawater Concentrations and Flux Calculations

Atmospheric OCS Measurements

C_g (pptv)	Sine ϕ	Date (1981)	Container	Latitude (ϕ)-Longitude	Location
403	0.57	10-11	C	35°N 56°N	North Atlantic Ocean
650	0.48	10-8	C	29°N 54°W	" " "
452	0.60	10-2	C	37°N 46°W	" " "
441	0.68	9-28	C	43°N 41°W	" " "
566	0.72	7-23	C	46°N 130°W	Pacific Ocean
488	0.72	7-23	C	46°N 130°W	" "
575	0.44	7-18	C	26°N 137°W	" "
599	0.44	7-23	C	26°N 137°W	" "
525	0.33	7-16	C	19°N 142°W	" "
388	0.72	11-5	C		Cape Meares, Oregon
388	0.72	11-5	C		" " "
409	0.68	7-22	S	43°N 134°W	Pacific Ocean
455	0.68	7-22	S	43°N 134°W	" "
535 478	0.63	7-21	S	39°N 135°W	" "
458	0.57 564	7-20	S	35°N 135°W	" "
520 489	0.50	7-19	S	30°N 135°W	" "

Atmospheric OCS Measurements (continued)

C_g (pptv)	Sine ϕ	Date (1981)	Container	Latitude (ϕ)-Longitude	Location
537 474	0.33	7-16	S	19°N 135°W	Pacific Ocean
586 502	0.26	7-15	S	15°N 145°W	" "
655 491	0.21	7-14	S	12°N 147"W	" "
540	0.74		A1	48°N 124°W	Pacific Coast Cruise
418	0.69		A1	44°N 123°W	" " "
450 396	0.64		A1	40°N 124°W	" " "
513 751	0.64		A1	40°N 125°W	" " "
494 545	0.62		A1	38°N 125°W	" " "
540 525	0.56		A1	34°N 121°W	" " "
628 496	0.54		A1	33°N 110°W	" " "
454 379	0.72	1-15	A		Cape Meares, Oregon

Atmospheric OCS Measurements (continued)

C_g (pptv)	Sine ϕ	Date (1981)	Container	Latitude (ϕ)-Longitude	Location
440	0.72	2-25	A		Cape Meares, Oregon
388 367		3-11	A		" " "
499		3-18	A		" " "
441		4-17	A		" " "
438		5-13	A		" " "
504		5-27	A		" " "
499		6-17	A		" " "
325		7-15	A		" " "
420		8-19	A		" " "
367		9-2	A		" " "
397		9-16	A		" " "
413		9-30	A		" " "
385 400		10-28	A		" " "
370		11-20	A		" " "
441 420		12-30	A		" " "

OCS Seawater Concentrations and Flux Calculations

C (pptv)	Date (1981)	P	T (°C)	H	C_g/H (pptv)	$-[C_g/H-C]$ (pptv)	Flux $x10^{11}$	Latitude-Longitude	Sine ϕ	Location
840	10-18	M	14	1.8	230	610	2.29	41°N 68°W	0.66	North Atlantic
975	10-18	M	14	1.8	230	745	2.79	41°N 68°W	0.66	" "
946	10-15	M	17	2.0	205	741	2.78	44°N 60°W	0.69	" "
1120	5-29	M	13	1.7	240	880	3.30	46°N 125°W	0.72	Tillamook Boat
1180	5-29	M	13	1.7	240	940	3.53	"	"	" "
1210	5-29	M	13	1.7	240	970	3.64	"	"	" "
1320	5-29	M	13	1.7	240	1080	4.05	"	"	" "
1800	5-29	M	13	1.7	240	1560	5.85	"	"	" "
683	5-29	M	13	1.7	240	443	1.66	"	"	" "
1198	7-9	M	15	1.9	222	976	3.66	37°N 122°W	0.60	Cambria, CA, Boat
1291	7-9	M	15	1.9	222	1069	4.01	"	"	" "
1809	7-9	M	15	1.9	222	1587	5.95	"	"	" "
993	7-9	M	15	1.9	222	771	2.89	"	"	" "
761	5-8	M	14	1.8	230	531	1.99	48°N 123°W	0.74	Pacific Coast Cruise

OCS Seawater Concentrations and Flux Calculations (continued)

C_l (pptv)	Date (1981)	P	T (°C)	H	C_g/H (pptv)	$-[C_g/H-C_l]$ (pptv)	Flux $x10^{11}$	Latitude-Longitude	Sine ϕ	Location
170	5-8	M	14	1.8	230	-60	-0.23	48°N 124°W	0.74	Pacific Coast Cruise
900	5-8	M	14	1.8	230	670	2.51	"	"	" " "
1027	5-6	M	13	1.7	240	787	2.95	45°N 127°W	0.71	" " "
1196	5-6	M	13	1.7	240	956	3.59	"	"	" " "
1900	5-5	M	14	1.8	230	1670	6.26	40°N 125°W	0.64	" " "
1270	5-5	M	14	1.8	230	1040	3.90	"	"	" " "
736	5-5	M	16	2.0	213	523	1.96	34°N 121°W	0.56	" " "
585	7-19	L	21	2.4	177	408	1.53	31°N 135°W	0.52	Pacific Ocean
391	7-19	L	21	2.4	177	214	0.80	"	"	" "
315	7-18	L	22	2.4	171	144	0.54	26°N 137°W	0.44	" "
547	7-18	L	22	2.4	171	376	1.41	"	"	" "
778	7-15	L	26	2.8	149	628	2.36	15°N 140°W	0.26	" "
432	7-15	L	26	2.8	149	283	1.06	"	"	" "

Atmospheric CH_3I Measurements

C_g (pptv)	Sine ϕ	Date (1981)	Container	Latitude (ϕ)-Longitude	Location
3.4 0.9	0.72	7-23	C	46°N 130°W	Pacific Ocean
2.0 1.6	0.44	7-18	C	26°N 137°W	" "
2.6	0.33	7-16	C	19°N 142°W	" "
1.3	0.14	7-13	C	8°N 150°W	" "
1.0	0.60	10-2	C	37°N 46°W	North Atlantic Ocean
1.7	0.48	10-8	C	29°N 54°W	" " "
2.3	0.69	9-28	C	44°N 41°W	" " "
1.7	0.57	10-11	C	35°N 56°W	" " "

CH_3I Seawater Concentrations and Flux Calculations

C_l (pptv)	Date (1981)	P	T (°C)	H	C_g/H (pptv)	$-[Cg/H-C_l]$ (pptv)	Flux $x10^{12}$	Latitude-Longitude	Sine ϕ	Location
208	8-15	H	14	0.18	8	199	17		0.74	San Juan Islands, WA
245	8-15	H	14	0.18	8	236	21		"	" "
184	6-24	H	13	0.17	8	175	16		0.71	Bay Oyster House, Tillamook, OR
161	6-9	M	15	0.19	9	152	14	37°N 122°W	0.60	Cambria, CA, Boat
118	6-9	M	15	0.19	9	109	10	"	"	"
95	6-9	M	15	0.19	9	86	7.7	"	"	"
184	6-9	M	15	0.19	9	175	16	"	"	"
74	8-14	M	13	0.17	9	65	5.8		0.71	Newport Bay, OR
85	8-15	M	13	0.17	9	76	6.8		"	Depoe Bay, OR
82	8-15	M	13	0.17	9	73	6.5		"	"
65	4-26	M	13	0.17	9	56	5.0		"	Tillamook Bay, OR
47	5-29	L	13	0.17	9	38	3.4	46°N 125°W	"	Tillamook Boat
50	5-29	L	13	0.17	9	41	3.7	"	"	"
36	5-29	L	13	0.17	9	27	2.4	"	"	"

CH_3I Seawater Concentrations and Flux Calculations (continued)

C_l (pptv)	Date (1981)	P	T (°C)	H	C_g/H (pptv)	$-[C_g/H-C_l]$ (pptv)	Flux $x10^{12}$	Latitude-Longitude	Sine ϕ	Location
52	8-15	L	13	0.17	9	43	3.8	44°N 125°W	0.69	Waldport, OR, Boat
114	8-15	L	13	0.17	9	105	9.4	"	"	"
52	8-15	L	13	0.17	9	43	3.8	"	"	"
53	8-15	L	13	0.17	9	44	3.9	"	"	"
71	8-15	L	13	0.17	9	62	5.5	"	"	"
52	5-8	L	14	0.18	8	44	3.9	48°N 124°W	0.74	Pacific Coast Cruise
30	5-8	L	14	0.18	8	22	2.0	"	"	"
49	5-8	L	14	0.18	8	41	3.7	48°N 123°W	"	"
38	5-8	L	14	0.18	8	30	2.7	"	"	"
50	5-5	L	14	0.18	8	41	3.7	40°N 125°W	0.64	"
40	5-3	L	16	0.20	9	31	2.7	34°N 121°W	0.56	"
28	10-15	L	17	0.21	7	21	1.9	44°N 60°W	0.69	North Atlantic Ocean
34	10-18	L	14	0.18	9	25	2.2	41°N 68°W	0.66	"
41	10-18	L	14	0.18	9	32	2.9	"	"	"

CH_3I Seawater Concentrations and Flux Calculations (continued)

C_l (pptv)	Date (1981)	P	T (°C)	H	C_g/H (pptv)	$-[C_g/H-C_l]$ (pptv)	Flux $x10^{12}$	Latitude Longitude	Sine ϕ	Location
58	7-19	L	21	0.25	8	50	4.5	31°N 135°W	0.52	Pacific Ocean
59	7-19	L	21	0.25	8	51	4.5	"	"	"
74	7-18	L	22	0.26	8	66	5.8	26°N 137°W	0.44	"
63	7-18	L	22	0.26	8	55	4.9	"	"	"
64	7-15	L	26	0.30	9	55	4.9	15°N 140°W	0.26	"
72	7-15	L	26	0.30	9	63	5.6	"	"	"

Atmospheric $CHCl_3$ Measurements

C_g (pptv)	Sine ϕ	Date (1981)	Container	Latitude (ϕ)-Longitude	Location
20	0.57	6-24	C	35°N 150°W	Pacific Ocean
22	0.34	7-03	C	20°N 151°W	"
26	0.34	7-03	C	"	"
28	0.33	7-16	C	19°N 142°W	"
23	0.45	7-18	C	27°N 137°W	"
23	0.45	7-18	C	"	"
25	0.72	7-23	C	46°N 130°W	"
20	0.72	7-23	C	"	"
25	0.48	10-8	C	29°N 54°W	North Atlantic Ocean

$CHCl_3$ Seawater Concentrations and Flux Calculations

C_l (pptv)	Date (1981)	P	T (°C)	H	C_g/H (pptv)	$-[C_g/H-C_l]$ (pptv)	Flux $x10^7$	Latitude-Longitude	Sine ϕ	Location
576	7-19	L	21	0.19	126	450	2.6	31°N 135°W	0.51	Pacific Ocean
664	7-19	L	21	0.19	126	538	3.1	"	"	"
326	7-18	L	22	0.19	126	200	1.1	26°N 137°W	0.44	"
457	7-18	L	22	0.19	126	331	1.9	"	"	"
532	7-15	L	26	0.19	126	406	2.3	15°N 140°W	0.26	"
582	7-15	L	26	0.19	126	456	2.6	"	"	"
307	10-18	L	14	0.19	126	181	1.0	41°N 68°W	0.66	North Atlantic Ocean
375	10-18	L	14	0.19	126	249	1.4	"	"	"
225	10-15	L	17	0.19	126	99	0.56	44°N 60°W	0.68	"

Atmospheric F-11 Measurements

C_g (pptv)	Sine ϕ	Date (1981)	Container	Latitude (ϕ)- Longitude	Location
196	0.57	6-24	C	35°N 150°W	Pacific Ocean
199	0.34	7-03	C	20°N 151°W	"
199	0.34	7-03	C	"	"
198	0.33	7-16	C	19°N 142°W	"
---	0.45	7-18	C	27°N 137°W	"
200	0.45	7-18	C	"	"
203	0.72	7-23	C	46°N 130°W	"
201	0.72	7-23	C	"	"
192	0.48	10-8	C	29°N 54°W	North Atlantic Ocean

F-11 Seawater Concentrations and Flux Calculations

C_l (pptv)	Date (1981)	P	T (°C)	H	C_g/H (pptv)	$-[C_g/H-C_l]$ (pptv)	Flux $x10^8$	Latitude-Longitude	Sine ϕ	Location
27	7-19	L	21	4.2	47	-20	1.2	31°N 135°W	0.51	Pacific Ocean
26	7-19	L	21	4.2	47	-21	1.3	"	"	"
28	7-18	L	22	4.2	47	-19	1.2	26°N 137°W	0.44	"
27	7-18	L	22	4.2	47	-20	1.2	"	"	"
36	7-15	L	26	4.2	47	-11	0.55	15°N 140°W	0.26	"
26	7-15	L	26	4.2	47	-21	1.3	"	"	"
25	10-18	L	14	4.2	47	-22	1.9	41°N 68°W	0.66	North Atlantic Ocean
30	10-18	L	14	4.2	47	-17	1.6	"	"	"
20	10-15	L	17	4.2	47	-27	2.0	44°N 60°W	0.68	"

Atmospheric F-12 Measurements

C_g (pptv)	Sine ϕ	Date (1981)	Container	Latitude (ϕ)-Longitude	Location
330	0.57	6-24	C	35°N 150°W	Pacific Ocean
339	0.34	7-03	C	20°N 151°W	"
335	0.34	7-03	C	"	"
338	0.33	7-16	C	19°N 142°W	"
330	0.45	7-18	C	27°N 137°W	"
332	0.45	7-18	C	"	"
332	0.72	7-23	C	46°N 130°W	"
334	0.72	7-23	C	"	"
338	0.48	10-8	C	29°N 54°W	North Atlantic Ocean

F-12 Seawater Concentrations and Flux Calculations

C_l (pptv)	Date (1981)	P	T (°C)	H	C_g/H (pptv)	$-[C_g/H-C_l]$ (pptv)	Flux $x10^9$	Latitude-Longitude	Sine ϕ	Location
37	7-19	L	21	10	34	3	-1.7	31°N 135°W	0.51	Pacific Ocean
37	7-19	L	21	10	34	3	-1.7	"	"	"
48	7-18	L	22	10	34	14	-6.9	26°N 137°W	0.44	"
41	7-18	L	22	10	34	7	-3.5	"	"	"
63	7-15	L	26	10	34	29	-13.9	15°N 140°W	0.26	"
53	7-15	L	26	10	34	19	-9.2	"	"	"
30	10-18	L	14	10	34	4	1.7	41°N 68°W	0.66	North Atlantic Ocean
46	10-18	L	14	10	34	12	-5.9	"	"	"
22	10-15	L	17	10	34	12	5.9	44°N 60°W	0.68	"

Atmospheric CH_3CCl_3 Measurements

C_g (pptv)	Sine ϕ	Date (1981)	Container	Latitude (ϕ)-Longitude	Location
145	0.57	6-24	C	35°N 150°W	Pacific Ocean
157	0.34	7-03	C	20°N 151°W	"
153	0.34	7-03	C	"	"
157	0.33	7-16	C	19°N 142°W	"
---	0.45	7-18	C	27°N 137°W	"
156	0.45	7-18	C	"	"
153	0.72	7-23	C	46°N 130°W	"
154	0.72	7-23	C	"	"
149	0.48	10-8	C	29°N 54°W	North Atlantic Ocean

CH_3CCl_3 Seawater Concentrations and Flux Calculations

C_l (pptv)	Date (1981)	P	T (°C)	H	C_g/H (pptv)	$-[C_g/H-C_l]$ (pptv)	Flux $x10^9$	Latitude-Longitude	Sine ϕ	Location
91	7-19	L	21	1.4	110	19	-9.0	31°N 135°W	0.51	Pacific Ocean
87	7-19	L	21	1.4	110	23	-10.8	"	"	"
105	7-18	L	22	1.4	110	5	-2.4	26°N 137°W	0.44	"
105	7-18	L	22	1.4	110	5	-2.4	"	"	"
120	7-15	L	26	1.4	110	10	4.7	15°N 140°W	0.26	"
120	7-15	L	26	1.4	110	10	4.7	"	"	"
106	10-18	L	14	1.4	110	4	-1.9	41°N 68°W	0.66	North Atlantic Ocean
113	10-18	L	14	1.4	110	3	1.4	"	"	"
99	10-15	L	17	1.4	110	11	-5.2	44°N 60°W	0.68	"

Atmospheric CCl_4 Measurements

C_g (pptv)	Sine ϕ	Date (1981)	Container	Latitude (ϕ)-Longitude	Location
152	0.57	6-24	C	35°N 150°W	Pacific Ocean
151	0.34	7-03	C	20°N 151°W	"
156	0.34	7-03	C	"	"
158	0.33	7-16	C	19°N 142°W	"
---	0.45	7-18	C	27°N 137°W	"
154	0.45	7-18	C	"	"
154	0.72	7-23	C	46°N 130°W	"
155	0.72	7-23	C	"	"
154	0.48	10-8	C	29°N 54°W	North Atlantic Ocean

CCl_4 Seawater Concentrations and Flux Calculations

C_l (pptv)	Date (1981)	P	T (°C)	H	C_g/H (pptv)	$-[C_g/H-C_l]$ (pptv)	Flux $x10^8$	Latitude-Longitude	Sine ϕ	Location
68	7-19	L	21	1.0	153	85	-5.1	31°N 135°W	0.51	Pacific Ocean
70	7-19	L	21	1.0	153	83	-5.0	"	"	"
72	7-18	L	22	1.0	153	81	-4.9	26°N 137°W	0.44	"
78	7-18	L	22	1.0	153	75	-4.5	"	"	"
90	7-15	L	26	1.0	153	63	-3.8	15°N 140°W	0.26	"
90	7-15	L	26	1.0	153	63	-3.8	"	"	"
60	10-18	L	14	1.0	153	93	-5.6	41°N 68°W	0.66	North Atlantic Ocean
68	10-18	L	14	1.0	153	85	-5.1	"	"	"
52	10-18	L	17	1.0	153	101	-6.1	44°N 60°W	0.68	"

Atmospheric PCE Measurements

C_g (pptv)	Sine ϕ	Date (1981)	Container	Latitude (ϕ)-Longitude	Location
36	0.57	6-24	C	35°N 150°W	Pacific Ocean
44	0.34	7-03	C	20°N 151°W	"
45	0.34	7-03	C	"	"
41	0.33	7-16	C	19°N 142°W	"
42	0.45	7-18	C	27°N 137°W	"
43	0.45	7-18	C	"	"
33	0.72	7-23	C	46°N 130°W	"
40	0.72	7-23	C	"	"
39	0.48	10-8	C	29°N 54°W	North Atlantic Ocean

PCE Seawater Concentrations and Flux Calculations

C_l (pptv)	Date (1981)	P	T (°C)	H	C_g/H (pptv)	$-[C_g/H-C_l]$ (pptv)	Flux $x10^9$	Latitude-Longitude	Sine ϕ	Location
72	7-19	L	21	0.6	67	5	3.1	31°N 135°W	0.51	Pacific Ocean
64	7-19	L	21	0.6	67	3	-1.6	"	"	"
85	7-18	L	22	0.6	67	18	10.8	26°N 137°W	0.44	"
83	7-18	L	22	0.6	67	16	9.5	"	"	"
91	7-15	L	26	0.6	67	24	14.3	15°N 140°W	0.26	"
120	7-15	L	26	0.6	67	53	31.3	"	"	"
176	10-18	L	14	0.6	67	109	64.2	41°N 68°W	0.66	North Atlantic Ocean
211	10-18	L	14	0.6	67	144	86.7	"	"	"
---	10-15	L	17	---	--	---	----	44°N 60°W	0.68	"

APPENDIX B

RT as a Function of Temperature

Chlorinity-Salinity Conversions

Vapor Pressure of Water

Vapor Pressure of Seawater

RT as Function of Temperature

Temp °C	Temp °K	RT $L \cdot atm \cdot mole^{-1}$	RT $mmHg \cdot L \cdot mole^{-1}$
0	273.15	22.414	17035
5	278.15	22.824	17346
10	283.15	23.234	17658
15	288.15	23.645	17969
20	293.15	24.055	18282
25	298.15	24.465	18594
30	303.15	24.876	18905
40	313.15	25.696	19529
50	323.15	26.517	20153

Chlorinity - Salinity Conversions*

Salinity (o/oo)	Chlorinity (g kg^{-1})
10	5.527
15	8.290
20	11.054
25	13.817
30	16.581
31	17.133
32	17.685
33	18.239
34	18.791
35	19.344
36	19.897
37	20.449
38	21.002
39	21.555
40	22.107
41	22.660
42	23.213

*From Riley and Skirrow (1975)

Vapor Pressure of Water

T(°C)	T(°K)	Pvp(atm)	Pvp(mmHg)
0	273	0.0060	4.6
5	278	0.0086	6.5
10	283	0.0121	9.2
15	288	0.0168	12.8
20	293	0.0231	17.6
25	298	0.0313	23.8
30	303	0.0419	31.8
35	308	0.0555	42.2

Vapor Pressure of Seawater

Salinity 35o/oo

T(°C)	T(°K)	Pvp(atm)	Pvp(mmHg)
0	273	0.0059	4.5
5	278	0.0084	6.4
10	283	0.0118	9.0
15	288	0.0166	12.6
20	293	0.0228	17.3
25	298	0.0308	23.4
30	303	0.0411	31.2
35	308	0.0545	41.4

For other salinities:

$$\frac{\Delta Pvp}{p^\circ} = 0.0009206\ (o/oo\ Cl) + 0.00000236\ (o/oo\ Cl)^2$$

ΔPvp is the vapor pressure lowering.

p° is the vapor pressure of pure water at the temperature of interest.

From: Robinson (1954)

VITA

The author was born 30 September 1949 in Glen Ridge, New Jersey. He moved to California in 1952 where he attended Redlands Senior High School and graduated in 1968.

In 1972 the author graduated from the University of California at Irvine with a Bachelor of Arts degree in chemistry. He then attended graduate school at Northern Arizona University for one year where he studied organic chemistry. In 1973 he transferred to Oregon State University where he studied analytical chemistry and physical chemistry, and was awarded a Masters degree in analytical chemistry in 1976. While at Oregon State University he worked as a teaching assistant and also worked part-time at the Environmental Protection Agency, Corvallis.

After graduation, the author taught general and analytical chemistry at Victor Valley College and Crafton Hills College in California between 1975 and 1976. In 1976 he was hired by the California Water Quality Control Board in Palm Desert, California, where he set up and managed a complete water quality control laboratory until 1978.

In 1978 the author decided to attend the Oregon Graduate Center, Beaverton, Oregon, to study Environmental Science. While at The Graduate Center he worked on several projects involving the application of analytical chemistry to environmental science. These included the analysis of trace metals in river and geological samples,

development of analytical methods for trace organic analysis in air and water samples, and the application of mass spectrometry to trace organic analysis in environmental samples. In 1980 the author started working for Professor R. A. Rasmussen on analyzing trace gases produced in the ocean. This dissertation is the result of these studies. In July 1982 he completed the requirements for the degree of Doctor of Philosophy at the Oregon Graduate Center.

List of Publications

S. D. Hoyt & J. D. Ingle, Jr., "Simple Cooled Photomultiplier Housing." Anal. Chem. 48, 232 (1976).

S. D. Hoyt & J. D. Ingle, Jr., "A Chemiluminescence Analyzer and Its Application to Trace Cr(III) Analysis." Anal. Chem. Acta 84, 163 (1976).

R. A. Rasmussen, M. A. K. Khalil, & S. D. Hoyt, "Methane and Carbon Monoxide in Snow." J. Air Pollut. Control Assoc. 32, 176 (1982).

R. A. Rasmussen, M. A. K. Khalil, R. Gunawardena, & S. D. Hoyt, "Atmospheric Methyl Iodide (CH_3I)." J. Geophys. Res. 87, 3086 (1982).

R. A. Rasmussen, M. A. K. Khalil, & S. D. Hoyt, "Oceanic Source of Carbonyl Sulfide (OCS)." Atmos. Environ. 16, 1591 (1982).

R. A. Rasmussen, S. D. Hoyt, & M. A. K. Khalil, "Atmospheric Carbonyl Sulfide (OCS): Techniques for Measurement in Air and Water." Preprint Volume, 2nd Symposium on the Composition of the Nonurban Troposphere, American Meteorological Society, Boston, Massachusetts, 1982.